	Research and Development Program on Seismic Ground Motion	Ref : SIGMA2-2019-D3-027/1
		Version : 1

Methodology to identify reference rock sites

WORK PACKAGE 3 - GROUND MOTION




AUTHORS		REVIEW		APPROVAL	
Name	Date	Name	Date	Name	Date
<i>Chiara Felicetta</i> <i>Chiara Felicetta</i> Giovanni Lanzano <i>Giovanni Lanzano</i> Francesca Pacor <i>Francesca Pacor</i>	2019/04/16	John DOUGLAS Alain PECKER	2019/11/20 <i>J. Douglas</i> 2019/11/20 <i>Alain Pecker</i>	Emmanuel VIALLET <i>Emmanuel Viallet</i> Public access ✓ SIGMA-2 restricted	YYYY/MM/DD 2020/12/21

DISSEMINATION: This document must not be distributed to any person, institution or company other than members of SIGMA-2 steering and scientific committees, except under written formal permission of SIGMA-2 steering committee.

Document history

DATE	VERSION	COMMENTS
2019/04/16	0	
2019/10/01	1	

	<p>Research and Development Program on Seismic Ground Motion</p>	<p>Ref : SIGMA2-2019-D3-027/1</p>
		<p>Version : 1</p>

INDEX

Executive summary.....	3
Introduction.....	5
1. Training dataset.....	8
2. Residual and cluster analysis	13
3. Proxies and weighting scheme.....	19
3.1 Housing - HOU	22
3.2 Surface Geology - GEO	22
3.3 Topography - TOP	23
3.4 Shear-wave velocity - $V_{s,30}$	24
3.5 Horizontal-to-vertical spectral ratio from noise and earthquake recordings - HV	25
3.6 Horizontal-to-vertical spectral ratio from response spectra - HVRS	28
3.7 Site-to-site term of horizontal component - $\delta S2S-H$	29
3.9 Station scoring.....	30
3.10 High-frequency attenuation parameter k for reference rock sites	33
4. GMMs calibration.....	35
5. Conclusions.....	40
6. Reference	41
APPENDIX I	47
APPENDIX II	50
APPENDIX II	56

	<p style="text-align: center;">Research and Development Program on Seismic Ground Motion</p>	<p>Ref : SIGMA2-2019-D3-027/1</p>
		<p>Version : 1</p>

Executive summary

This work is part of the collaboration between the EDF (*Electricité DE France*) company and the INGV (*Istituto Nazionale di Geofisica e Vulcanologia*) of Milan in the framework of Sigma2 project, with the aim to improve the strategy for reference rock sites identification and for reference ground motion prediction.

To assess site-specific ground-motion, it is common practice to calculate seismic hazard at bedrock and then apply a deterministic site-specific amplification factor, computed using 1D/2D numerical site response analyses. For this reason, the ground motion at bedrock should be free from amplification phenomena and its site response flat. This can then be considered “reference rock motion”. Ground Motion Models (GMMs) are generally calibrated using records at stations classified as rock that, however, can be affected by site-effects. The assumption currently made that GMM based rock site predictions are unaffected by amplification phenomena may cause inaccurate prediction of the expected motion when the hazard is evaluated including site effects, due to the amplified response of rock motion.

To address this issue, following Felicetta et al. (2018), we propose a strategy for the identification of reference rock sites based on seven proxies, inferred from geophysical and geological data and from seismological analysis.

The deliverable is developed as follows:

1. Identification and qualification of a training dataset on which computing and testing the proposed proxies. We select a dataset composed by earthquakes and stations located in central Italy, where a huge quantity of data are available after the recent seismic sequences that have occurred in this area (2009 M 6, L’Aquila and 2016-2017 M 6.5, Central Italy). The stations are characterized collecting information about: i) installation, ii) local geology, iii) geophysical and geotechnical data; iv) seismological analyses (residual analysis, horizontal-to-vertical spectral ratio on earthquakes and noise signals), and v) Eurocode 8 soil category.
2. Given the large number of stations included in the training dataset, a preselection to identify candidate stations to be references-rock sites is performed. These stations are selected executing a residual analysis with respect to ITA10 (Bindi et al., 2011) predictions for generic rock (EC8-A) and estimating the horizontal site-to-site term (δS_2S) and the associated variability. Since these terms quantify the systematic amplification/deamplification of the observed ground motion at a given station, we consider as possible reference sites only those having the site-to-site terms close or lower than zero;

	<p style="text-align: center;">Research and Development Program on Seismic Ground Motion</p>	<p>Ref : SIGMA2-2019-D3-027/1</p>
		<p>Version : 1</p>

3. In addition to the horizontal site-to-site term (δS_{2S-H}), additional indicators, that may affect the seismic response of a site, are selected as proxies:
 - Housing (HOU)
 - Topography (TOP)
 - Average shear wave velocity in the first 30 m ($V_{S,30}$);
 - Surface geology from cartography (GEO);
 - Resonant frequency and shape of the curve obtained from H/V of Fourier spectra of noise records (HVNSR) or from H/V of coda or S-waves of earthquake records (HVSR-C or HVSR-S);
 - Resonant frequency and shape of the curve obtained from H/V of acceleration response spectra (HVRS);
 - With the aim of handling the relevance, the data quality and the lack of these indicators, a weighting scheme is also introduced to award a score to each proxy and establish a ranking of the candidate reference rock stations.
4. To evaluate the impact on the ground motion median values and associated variabilities, a set of GMMs for generic rock and reference rock sites are calibrated.

	<p style="text-align: center;">Research and Development Program on Seismic Ground Motion</p>	<p>Ref : SIGMA2-2019-D3-027/1</p>
		<p>Version : 1</p>

Introduction

The identification of reference sites, i.e., sites where no seismic amplification effects may occur as the results of local morphologic/stratigraphic configuration, is of paramount importance in the seismic engineering practice.

Traditionally, the site-specific hazard assessments rely on the estimates performed for rock conditions, properly modified for deterministic amplification factors. In seismic hazard assessment for nuclear installation, it is common practice to assess seismic hazard at the seismological bedrock beneath the site, and to apply site-specific amplification factors assessed by numerical 1D-2D site response analyses. Furthermore, to evaluate the response of different soils, empirical approaches, based on Ground Motion Models (GMMs), also need to define the reference ground motion, i.e. the ground motion recorded at stations unaffected by site-effects.

It is common practice to assume that sites, where rocks or stiff soils outcrop and the average shear-wave velocity in the uppermost 30 m ($V_{s,30}$) exceeds a given value, represent an example of reference sites. This is the case of the seismic actions defined in the European provisions (Eurocode 8 - EC8), that adopt a soil classification scheme based on $V_{s,30}$ and identify the rock sites as those with $V_{s,30}$ equal or larger than 800 m/s (soil category EC8-A); another example is the calibration of GMMs where the site amplifications at the different stations are evaluated with respect to the predictions of sites with $V_{s,30}$ exceeding or corresponding to a given value (i.e. 760 m/s for Boore et al. 2014; 800 m/s for Lanzano et al. 2019).

However, the simple definition of reference rock sites, based only on geological features and measurements of the shear wave profiles, does not ensure the identification of sites where the amplification is expected to be negligible. It is well known that alteration or intensive fracturing of rock bodies may significantly modify their mechanical behavior and, in particular, may be responsible of energy trapping phenomena that can change the amplitude of impinging waves. Similarly, there are several cases in literature that describe local amplification at sites having $V_{s,30}$ larger than 800 m/s, such as intermediate and high-frequency resonance peaks (Steidl et al., 1996; Bindi et al., 2009; Rovelli et al., 2002; Marzorati et al., 2011) and effects of wave polarization (Pischiutta et al., 2011; Pacor et al., 2011; Burjanek et al., 2014). As a consequence, an inappropriate selection of reference sites may cause inaccurate prediction of the expected motion when hazard is evaluated including site effects, due to the amplified response of the rock motion. For instance, Figure 1 shows the horizontal-to-vertical spectral ratio analysis performed on noise measurements (Figure 1) at SRT-Sortino station that is classified as EC8-A in the ITACA archive (Luzi et al., 2019) on the base of shear-wave velocity profile with $V_{s,30}$

C. FELICETTA/ G. LANZANO/ F. PACOR- Methodology to identify reference rock sites- SIGMA2-2019-D3-027/1

value equal to 871 m/s (Figure 2). We can observe that, despite the rock site class, SRT exhibits a high amplitude peak (about 8.0) at 5.6 Hz.

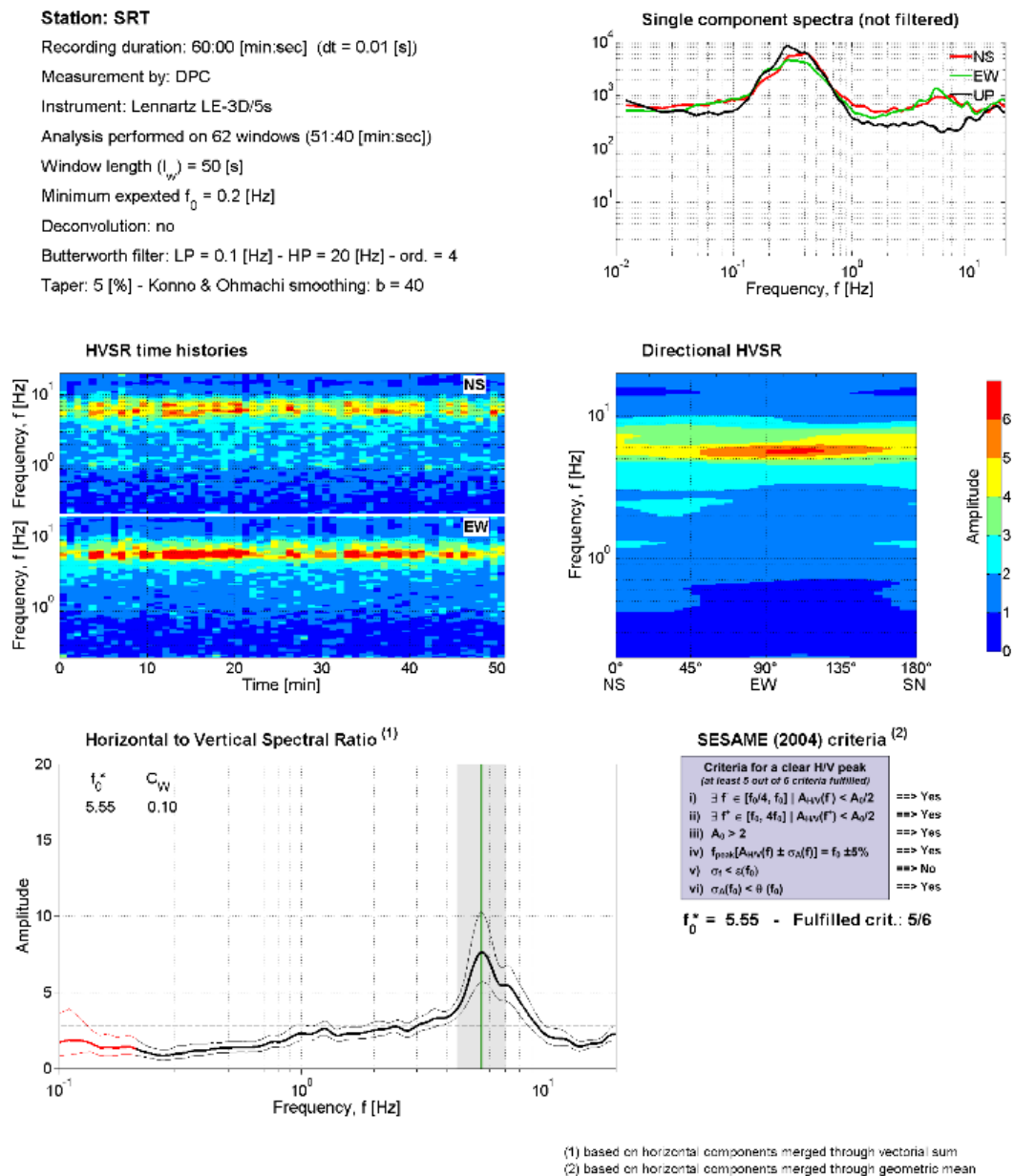


Figure 1. Horizontal-to-vertical spectral ratio analysis performed on noise measurements at IT.SRT (Sortino) station (from ITACA, Luzi et al., 2019).

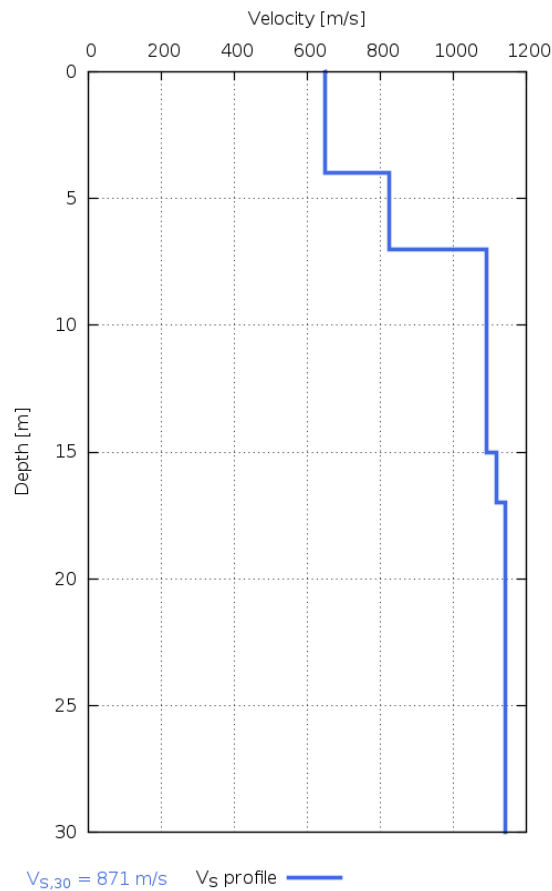


Figure 2. Shear-wave velocity profile at IT.SRT (Sortino) station (from ITACA, Luzi et al., 2019).

This issue was tackled by Felicetta et al. (2018), that proposed a procedure to recognize reference rock sites among the recording stations of the Italian ACcelerometric Archive (ITACA, <http://itaca.mi.ingv.it>, Luzi et al., 2019) using six proxies, based on geological, topographical and geophysical indicators. Three proxies out of six are based on geophysical and seismological data ($V_{s,30}$, Horizontal to Vertical spectral ratio of noise measurements, *HVNRS*, and Horizontal to Vertical spectral ratio of response spectra, *HVSR*), whereas the remaining on geologic and geomorphological features (outcropping rocks, flat topography and absence of interaction with structures). These proxies were applied to the set of stations classified as EC8-A, formerly used for the calibration of the reference GMMs for Italy (ITA10, Bindi et al., 2011). The authors showed that GMMs calibrated for reference rock sites provide significantly lower median values and associated standard deviations with respect to the ITA10 values, estimated for generic rock sites (EC8-A).

Following the approach proposed by Felicetta et al. (2018), the aim of this study is to propose and test a set of proxies to identify recording stations installed on reference rock sites. The idea is to exploit the

seismic records to enlarge the number of significant parameters useful to characterize the response site at the recording stations. Furthermore, since information on site response may be limited for large seismic datasets, a weight scheme is proposed to take into account the epistemic uncertainty associated to poor data quality or missing information of proxies selected to identify reference rock sites.

1. Training dataset

The dataset used for the analysis was assembled in cooperation with the working group involved in the microzonation study carried out in Central Italy after the 2016-2017 seismic sequence (Priolo et al., 2019). The collection of records is composed by accelerometric and velocimetric earthquake signals, recorded by stations and events located in Central Italy since 2008 and mainly includes data of the 2009 L'Aquila and the 2016-2017 Central Italy sequences (Figure 3 and Figure 4).

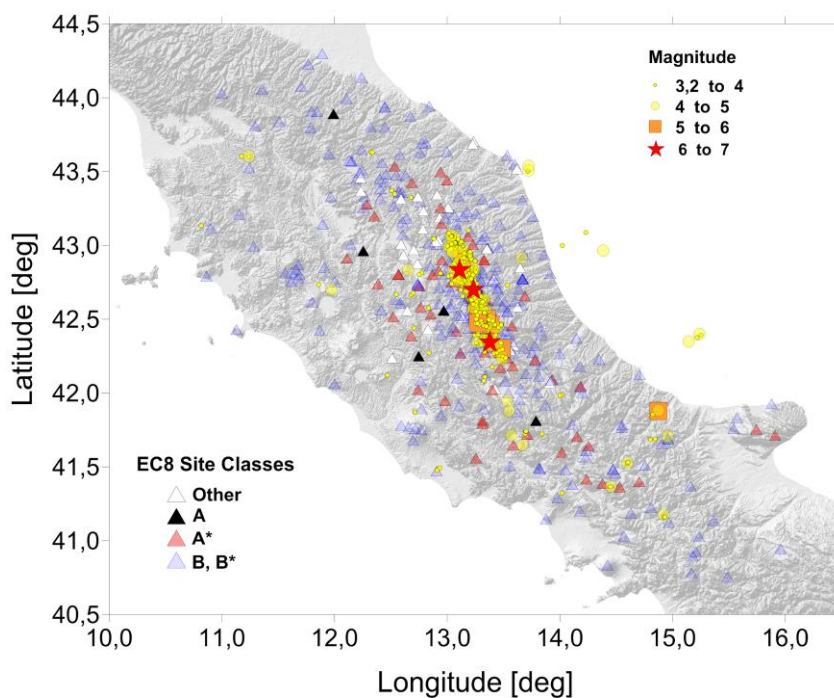


Figure 3: Geographical distribution of stations and epicenters of the events included in the training dataset

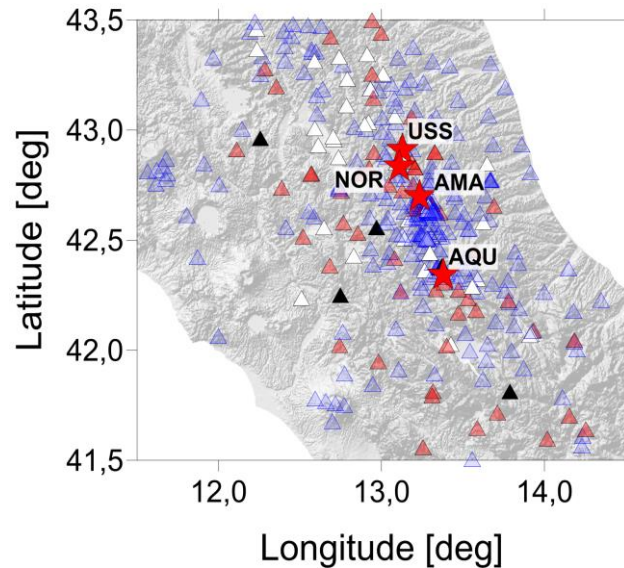


Figure 4: Zoom of the station distributions around the epicentral area of 2009 L'Aquila and 2016-2017 Central Italy seismic sequences

The epicentral distribution of events is spatially coherent with the extensional system of the active faults along the Apennine chain (Boncio et al., 2004 and references therein; Chiaraluce et al., 2017; Porreca et al., 2018), where most of the historical and instrumental seismicity is located. The Time Domain Moment Tensor focal mechanisms of the strongest events are normal dip-slip with NNW-SSE striking focal planes (<http://cnt.rm.ingv.it/tdmt>; Pondrelli et al., 2016), compatible with both the kinematics of the main faults and the SW-NE trending tensional stress regime characterizing the regions of Central Italy (Ferrarini et al., 2015).

The recording stations installed in the area belong to national networks (RAN-*Rete Accelerometrica Nazionale* and RSN-*Rete Sismica Nazionale*, network codes IT and IV, respectively) and temporary networks installed to monitor the seismic sequences and to investigate the site effects in Central Italy, after the main events of 2009 and 2016 (network codes: IV, 4A, XO and 3A). The waveforms and associated information on earthquakes and stations were extracted from different archives, listed in Table 1.

Several tests on data quality and consistency (Pacor et al., 2016) were performed to build a dataset representative of the ground motion characteristics in Central Italy. These tests include: i) visual inspection of waveforms, instrumental correction, analysis of the signal-to-noise ratio (SNR), automatic picks of P- and S-wave onset (Spallarossa et al., 2014), and manual validation; ii) local magnitude (M_L) estimation using the model proposed by Di Bona (2016); iii) residual analysis of peak ground acceleration

	<p style="text-align: center;">Research and Development Program on Seismic Ground Motion</p>	Ref : SIGMA2-2019-D3-027/1
		Version : 1

(PGA) and peak ground velocity (PGV) to identify unreliable recordings, using the Italian ground motion prediction equation of Bindi et al. (ITA10) as a reference model.

Table 1. List of the networks (T, temporary; P, permanent) and archives populating the training dataset. The column marked “Name” reports the full name of the networks, with a short description in some cases.

Network Code (T/P)	Owner	Data Sources	Name
4A (T)	INGV	Eida [^] , ITACA*, ESM [°]	Emersito Seismic Network for Site Effect Studies in L'Aquila, Central Italy (http://cnt.rm.ingv.it/instruments/network/4A)
IT (T/P)	DPC	RANdownload [§] , ITACA*, ESM [°]	RAN, Italian Strong Motion Network (DOI: https://doi.org/10.7914/SN/IT)
IV (T/P)	INGV	Eida [^] , ITACA*, ESM [°]	RSN, Italian Seismic Network (DOI: https://doi.org/10.13127/SD/X0FXnH7QfY)
MZ (T)	OGS	OASIS [§]	Rete Sismica Temporanea di Arquata/Montegalfo
SP (T)	OGS	OASIS [§]	Rete Sismica Temporanea di Spoleto
XJ-2009 (T)	RESIF	Eida [^]	French part of L'Aquila (Italy) aftershock experiment (RESIF-SISMOB). (DOI: https://doi.org/10.15778/RESIF.XJ2009)
XO (T)	INGV	Eida [^] , ITACA*, ESM [°]	Emersito Seismic Network, 2016 Central Italy (DOI: 10.13127/SD/7TXeGdo5X8)
3A (T)	INGV IDPA-CNR IMAA-CNR ENEA	Eida [^] , ITACA*, ESM [°]	Seismic Microzonation Network, 2016 Central Italy (DOI: 10.13127/SD/ku7Xm12Yy9)
[^] Eida: http://www.orfeus-eu.org/data/eida/ [*] ITACA: http://itaca.mi.ingv.it [°] ESM: http://esm.mi.ingv.it [§] OASIS: http://oasis.crs.inogs.it [§] RANdownload: http://ran.protezionecivile.it/IT/			

To carry out the analysis, a subset of waveforms is selected by applying the following criteria: i) hypocentral depth < 20 km and hypocentral distance up 250 km; ii) Magnitude $M > 3.0$; iii) Fourier amplitude spectra composed of at least 70% of spectral ordinates with $SNR \geq 3$ in the frequency range [0.2-40] Hz. The Fourier spectra are computed on time windows starting 0.1s before the S-wave onset and ending when different percentages of the total energy are reached, as a function of the source-to-site distance (Pacor et al., 2016). The extracted signals are tapered with Hanning windows of variable length depending on the selected S-waves portion.

The final subset is composed of approximately 30,000 velocimetric and accelerometric time histories and the corresponding Fourier and acceleration response spectra (5% damping) relative to about 450 earthquakes in the magnitude range 3.2 - 6.5 (local magnitude for $M < 4.5$ and moment magnitude for $M \geq 4.5$) and more than 460 stations within 250 km from the epicentres (Figure 4 and Figure 5).

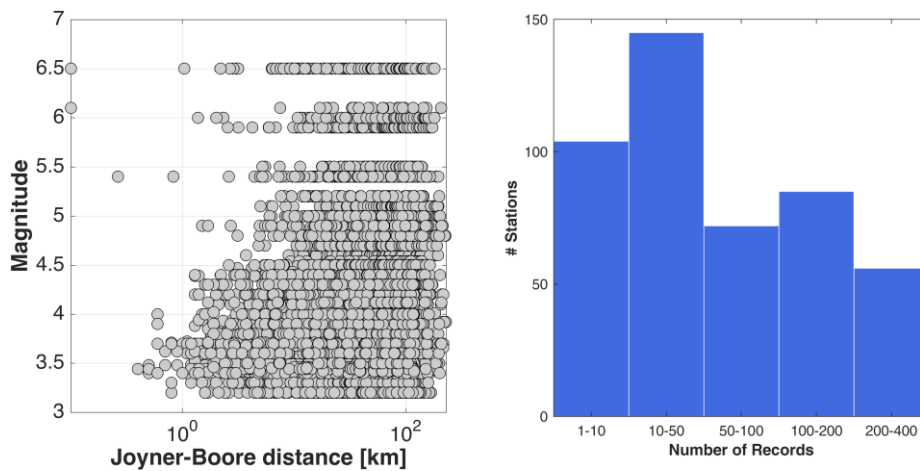


Figure 5. Left: Magnitude-distance scatter plot of the training dataset. Right: Records sampling for station

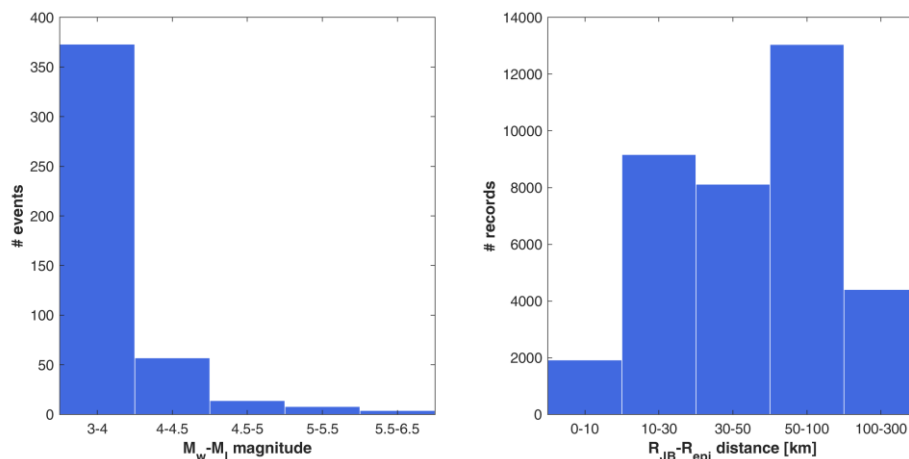


Figure 6. Magnitude (left) and distance (right) distributions of the training dataset.

For the strongest events, the Joyner and Boore distance, R_{JB} , is computed adopting the fault geometry, if available in the ITACA database, for the others the epicentral distance is used. The dataset is very well sampled in the distance and magnitude ranges R [10 - 100] km and M [3.2 - 4.5]. The large quantity of records at short distances and for small events is due to the stations of the temporary networks (Figure 4). More than 75% of the stations are densely sampled and the majority of them recorded more than 10 events and in some cases, more than 100 (Figure 5).

Due to the complex setting and evolution of the area under the study, the local conditions at the instrumented sites are highly heterogeneous, with large and narrow alluvial valleys, sedimentary basins, slopes and mountain peaks (Cacciuni et al. 1995). The continental units are mainly constituted by gravel

and sand deposits in the valley floors, alluvial terraces, and fan, while thick debris covers are often found along the slopes, which are characterized by intense and widespread gravitational processes. Such conditions are prone to seismic site-effects, also in case of rock and stiff sites (Priolo et al., 2019).

The site information available to the recording stations is quite poor, especially for the temporary stations. However, the microzonation studies carried out in the region allowed to collect several geological and geophysical data that can be exploited to characterize the stations. As an example, for about half of the recording stations of the 3A network (Cara et al. submitted), installed to monitor 50 sites in the epicentral area of the 2016, M 6.0, Amatrice earthquake, detailed site characterization was undertaken, including geological maps, single-station noise measurements and S-wave velocity profiles (Pacor et al., 2019). For about 10% of the recording stations included in the training dataset, the S-wave profile is available and the EC8 soil category is assigned according to the $V_{S,30}$ value. For the remaining stations, the EC8 class is attributed on the base of the surface geology, inferred from the existing cartography (Figure 7).

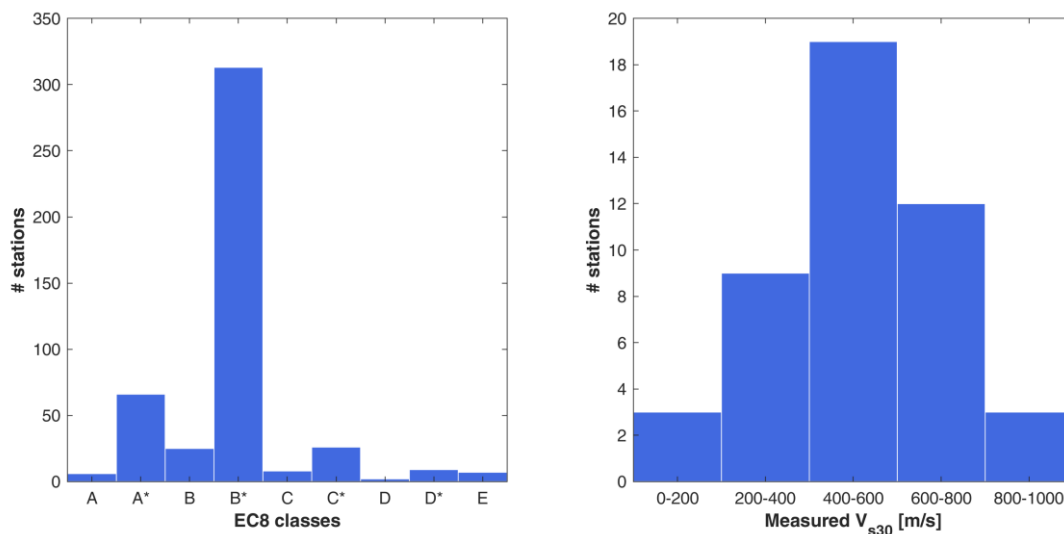



Figure 7. EC8 soil categories (left) and measured $V_{S,30}$ (right) distributions of the training dataset. The asterisk indicates soil categories inferred from surface geology.

As expected, the majority of the recording stations are classified as EC8-B sites (*deposits of very dense sand, gravel, or very stiff clay at least several in thickness, characterized by a gradual increase of the mechanical properties with depth; $V_{S,30}$ in the range 360-800 m/s*). The EC8-A rock sites, corresponding to $V_{S,30} \geq 800$ m/s or located to rock-like geological formation, are about 15% of the selected stations. Not all the EC8-A sites can be assumed free of amplifications: the empirical analysis carried out in Central

	<p style="text-align: center;">Research and Development Program on Seismic Ground Motion</p>	<p>Ref : SIGMA2-2019-D3-027/1</p>
		<p>Version : 1</p>

Italy show that sites located on stable zone (geological bedrock) may have amplifications, especially in the short-period band, probably related to the local weathered and jointed condition of the outcropping bedrock, which results in a reduction of the rock stiffness at shallow depths (Priolo et al., 2019).

2. Residual and cluster analysis

The preliminary selection of the stations candidate to be reference rock sites is carried out via a residual analysis. The residuals of the training dataset are calculated as the (natural) logarithmic difference between observation and predictions, i.e. positive values correspond to model underestimations and negative values to overestimations. The GMM, used as reference predictive equation in this analysis, is that proposed by Bindi et al. (2011) for shallow active crustal earthquakes in Italy (ITA10). It was basically derived from the dataset of ITACA up to the 2009 L’Aquila seismic sequence, composed by 769 records of 99 events (M_w range 4.1-6.9) and 150 stations. ITA10 adopts the site classification of the EC8 to describe the site effects in the functional form. The analysis is carried out on the geometric mean of the horizontal components of the peak ground acceleration and 69 ordinates of the acceleration response spectra (5% damping) in the period interval $T=0.04-2s$.

The total residuals, R_{es} , are decomposed by means of the well-known procedure to move from ergodic to partially non-ergodic assumption (Al-Atik et al. 2010; Luzi et al. 2014). Sources of the variability of ground motion are recognized, then, they are separated from the total residual and accounted as epistemic uncertainties, thus reducing the aleatory component. Practically, R_{es} is splitted in between-event, δB_e , and within-event, δW_{es} , terms. δB_e is calculated as the mean of the total residuals of each earthquake in the dataset and represents the average misfit of recordings of one particular earthquake with respect to the median ground-motion model (Lanzano et al., 2017a). The bias of this term with respect to the median is generally related to source parameters, such as the stress drop, that can scale up or down the ground motion level of the earthquake (Bindi et al. 2019). τ and ϕ are the standard deviations of δB_e and δW_{es} , respectively. Figure 8 shows R_{es} and δW_{es} as a function of distance and δB_e as a function of magnitude for PGA, and SA at 0.1, 1 and 2s.

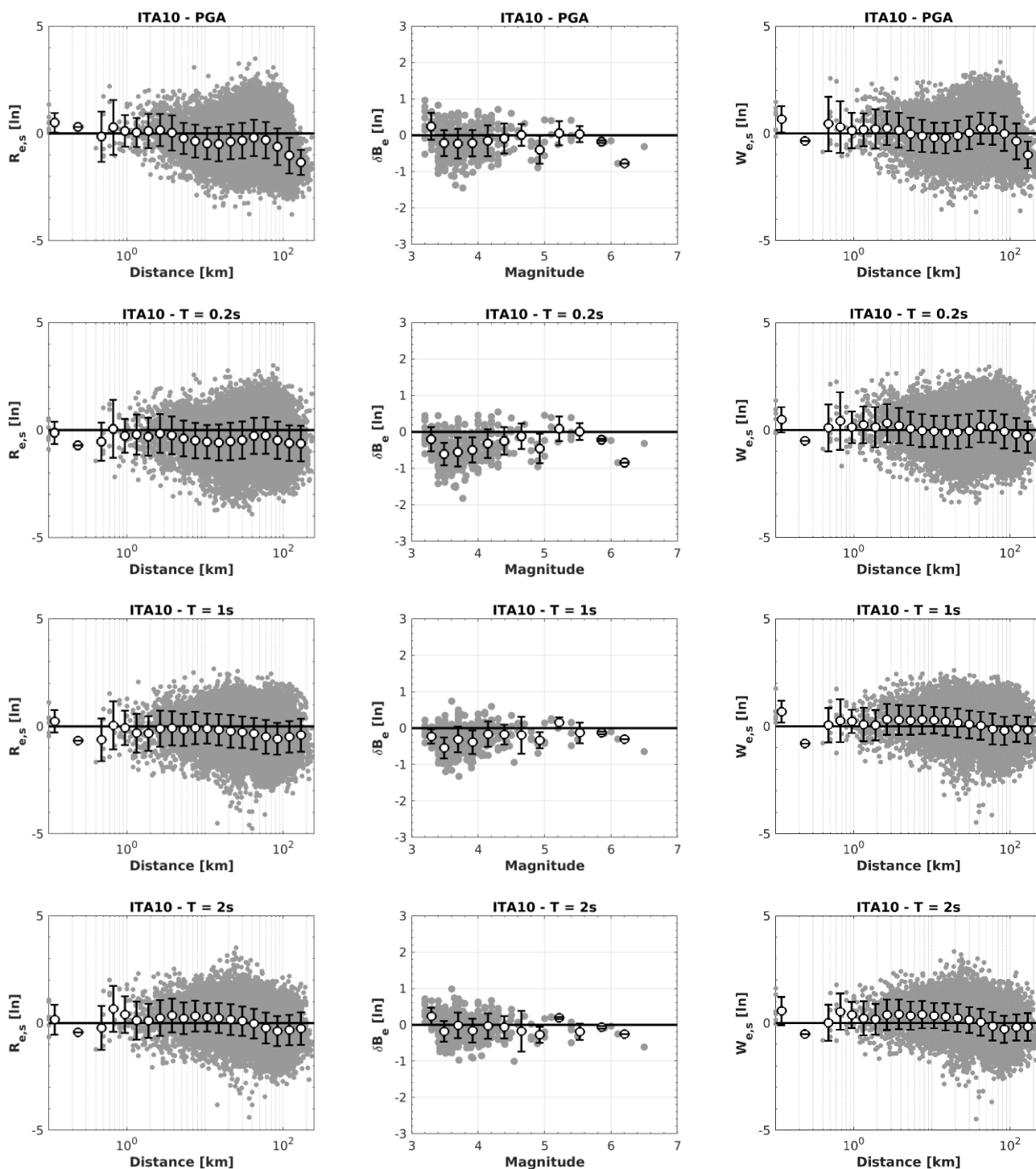



Figure 8. Total residuals $R_{e,s}$ vs. distance (left), between-event residuals δB_e vs. magnitude (centre) and within-event residuals $\delta W_{e,s}$ vs. distance (right) for PGA (top) and SA at $T=0.2$ (middle top), 1 (middle bottom) and 2s (bottom).

	<p>Research and Development Program on Seismic Ground Motion</p>	<p>Ref : SIGMA2-2019-D3-027/1</p> <hr/> <p>Version : 1</p>
---	--	--

According to the trend of total residuals with distance, the attenuation at short periods (e.g. PGA) for distances larger than 70 km is not well captured by ITA10, as already showed by Luzi et al. (2017) and corrected by Lanzano et al. (2019) in the recently published GMM for Italy. Since ITA10 is valid for events with magnitude larger than 4.0, the values of δB_e are found to be negative for smaller events, i.e. the model predictions are overestimated w.r.t the observations. After the event correction, the bias of the within-event residuals is reduced and the over-estimations are clear only at distances longer than 100km. At longer periods the variability is generally smaller and the residuals are less biased.

The δW_{es} is further decomposed into site-to-site term, $\delta S2S_s$, and event- and site- corrected residual, $\delta W_{0,es}$. $\delta S2S_s$ is calculated as:

$$\delta S2S_s = \frac{1}{NE_s} \sum_{e=1}^{NE_s} \delta W_{es} \quad (1)$$

where NE_s is the number of events recorded at the station s and quantifies the average misfit of recordings from one particular site with respect to the event-corrected median ground-motion. The event-corrected single-station standard deviation for an individual site, $\phi_{ss,s}$, is computed as:

$$\phi_{ss,s} = \sqrt{\frac{\sum_{e=1}^{NE_s} (\delta W_{es} - \delta S2S_s)^2}{NE_s - 1}} \quad (2)$$

In order to be sure that the within-event residuals truly reflect the site response of the recording stations, we limited the dataset for the subsequent analyses to a maximum distance of 120km for the computation of $\delta S2S_s$.

For the purpose of this study, we decide to compute the site-to-site term with respect to reference site category of ITA10, i.e. the EC8-A class. In this way, the site-to-site term, named $\delta S2S_{EC8-A}$, represents the empirical amplification function of the station, with respect to the generic rock prediction. We expect that the candidates for reference rock sites exhibit negative or almost zero values of $\delta S2S_{EC8-A}$ at all periods, since the ITA10 gives a mean prediction of the EC8-A category, which includes both reference sites and stations affected by amplifications (Felicetta et al. 2018).

Our strategy to identify the candidate reference rock sites is to perform a cluster analysis on the $\delta S2S_{EC8-A}$ curves ($\delta S2S_{EC8-A}$ as a function of period) with the aim of detecting the sites belonging to the class with the lowest values and flat trend. This approach to describe the site effects on the basis of the empirical recordings is becoming popular recently (Puglia et al. 2015; Kotha et al. 2018).

A preliminary selection among the 462 sites of the training dataset is carried out. The acceptance criteria are:

C. FELICETTA/ G. LANZANO/ F. PACOR- Methodology to identify reference rock sites- SIGMA2-2019-D3-027/1

- the vectors of $\delta S2S_{EC8-A}$ must have the same length to perform the cluster analysis; in particular, we decide to exclude PGA and perform the analysis in the period interval $T=0.04-2s$ (69 parameters);
- the single station variability ($\phi_{ss,s}$) must be lower than the within-event variability of ITA10 (ϕ_{ITA10}) for the 75% of the ground motion parameters considered (52 periods out of the 69);
- the $\delta S2S_{EC8-A}$ must be calculated on, at least, 10 records (Lanzano et al. 2017).

Some examples of $\delta S2S_{EC8-A}$ curves are reported in Figure 9.

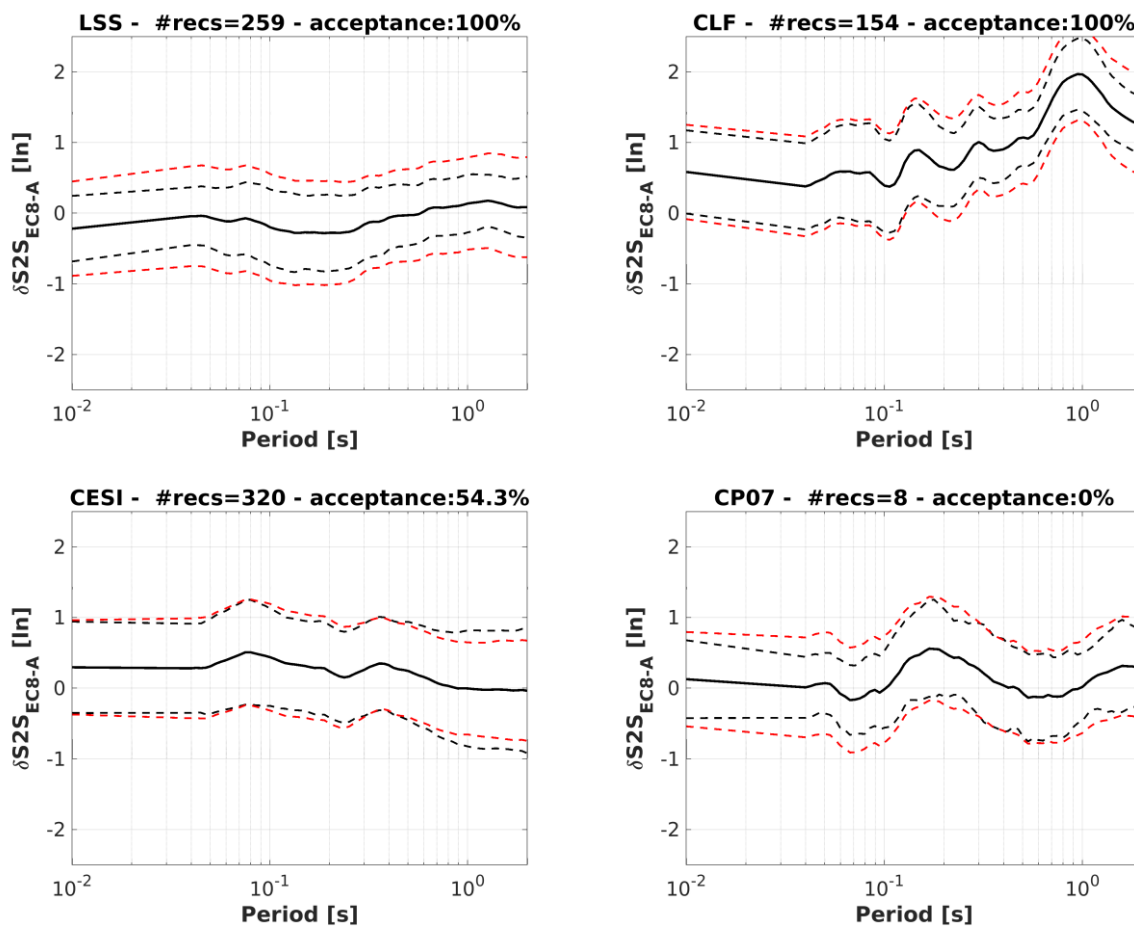


Figure 9. Examples of $\delta S2S_{EC8-A}$ as a function of period for four recording stations: LSS-Leonessa (a); CLF-Colfiorito (b); CESI-Cesi (c); CP07-San Giovanni Paganica (d).

Two stations that pass the acceptance criteria are IT.LSS and IT.CLF: LSS (Leonessa) is a rock site that exhibits a flat site-to-site term, slightly negative for the majority of periods, and can be considered as a potential reference site; CLF (Colfiorito) is classified as EC8-D on the basis of geophysical measurements and shows amplifications of multiple peaks, with the largest around 1s, typical of sites located in alluvial

basins. Other stations, such as IV.CESI and XO.CP07 (Figure 3), are rejected for two different reasons: CESI (Cesi) exhibits a single-station variability ($\phi_{ss,s}$) larger than the within-event variability of ITA10 at the majority of periods, probably due to directional effects; the $\delta S2S_{EC8-A}$ of CP07 (San Giovanni Paganica) is computed only on 8 records and could be roughly estimated.

The map of the stations is reported in Figure 10: the total number of selected stations is 343, while 119 (25%) sites mainly located at the border of the investigated area, are disregarded. This evidence is mainly related to the fact that most of the stations (about 90%), excluded from the analysis, are disregarded because of the limited amount of records.

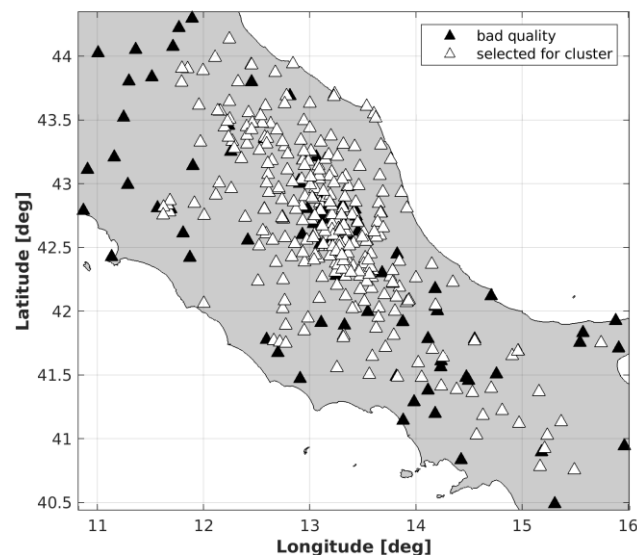


Figure 10. Stations selected for the cluster analysis.

Among several techniques for data aggregation available in literature, we use the *k-means* clustering (David and Vassilvitskii, 2007) to partition the observations of the n -by- p $\delta S2S_{EC8-A}$ matrix into k clusters, where n is the number of sites and p is the number of parameters. The main advantage of this method is that it converges very quickly, but the clusters number must be assigned *a-priori*.

The clusterization is carried out on the amplification factors ($e^{\delta S2S}$), through the **kmeans** function, available in the Matlab Package 2019b. After some trials, we set the number of $k = 9$, despite the fact that it is not the optimal number of clusters (Tibshirani et al. 2001): in this way, the clusters of stations with ground motion level lower or similar to the EC8-A prediction of ITA10 are clearly represented and distinguished. Few stations (19) are found to be not clustered in any of the 9 classes. Figure 11 reports the

mean amplification curves $e^{\delta S_{2S}}$ as a function of period for the 9 clusters, identified by the k-means algorithm.

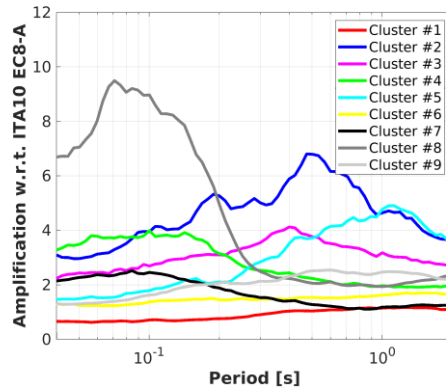


Figure 11. Mean amplification ($e^{\delta S_{2S}}$) of the classes after the k-means clusterization.

The *cluster #1* contains the candidate reference rock sites, since the average value of $e^{\delta S_{2S}}$ for this cluster is characterized by a deamplification ($e^{\delta S_{2S}} < 1$) and a quite flat response above all periods with factors close to 1 at longest period. The *cluster #6* exhibits, on average, a zero amplification at all periods, i.e. it includes sites having a mean ground motion response very similar to those predicted by the EC8-A of ITA10. All other classes are amplified ($e^{\delta S_{2S}} > 1$). In particular:

- *cluster #9* has a broadband response with a mean amplification around 2;
- *cluster #4* and *cluster #7* have similar shape, characterized by short periods amplification, but different levels (around 2 for *cluster #7* and around 4 for *cluster #4*);
- *cluster #5* is characterized by long period amplification, with maximum value of 5 at 1s;
- *cluster #2* and *cluster #3* have a peak at intermediate periods (0.4-0.5s) with different amplification levels (about 7 for *cluster #2* and 4 for *cluster #3*);
- *cluster #8* has a very large amplification at short period, typical of the ITA10 EC8-E sites.

The initial list of sites, candidate to be reference rock stations, is composed by the stations of *cluster #1* and *cluster #6*.

In order to provide additional information on the clustering results, we add a flag to each station, that indicates if the amplification is close to the median of each cluster. In particular, it indicates if the curve is between the 5th and 95th percentile of the data distribution at each period.

The results for *cluster #1* and *#6* are also reported in Figure 12.

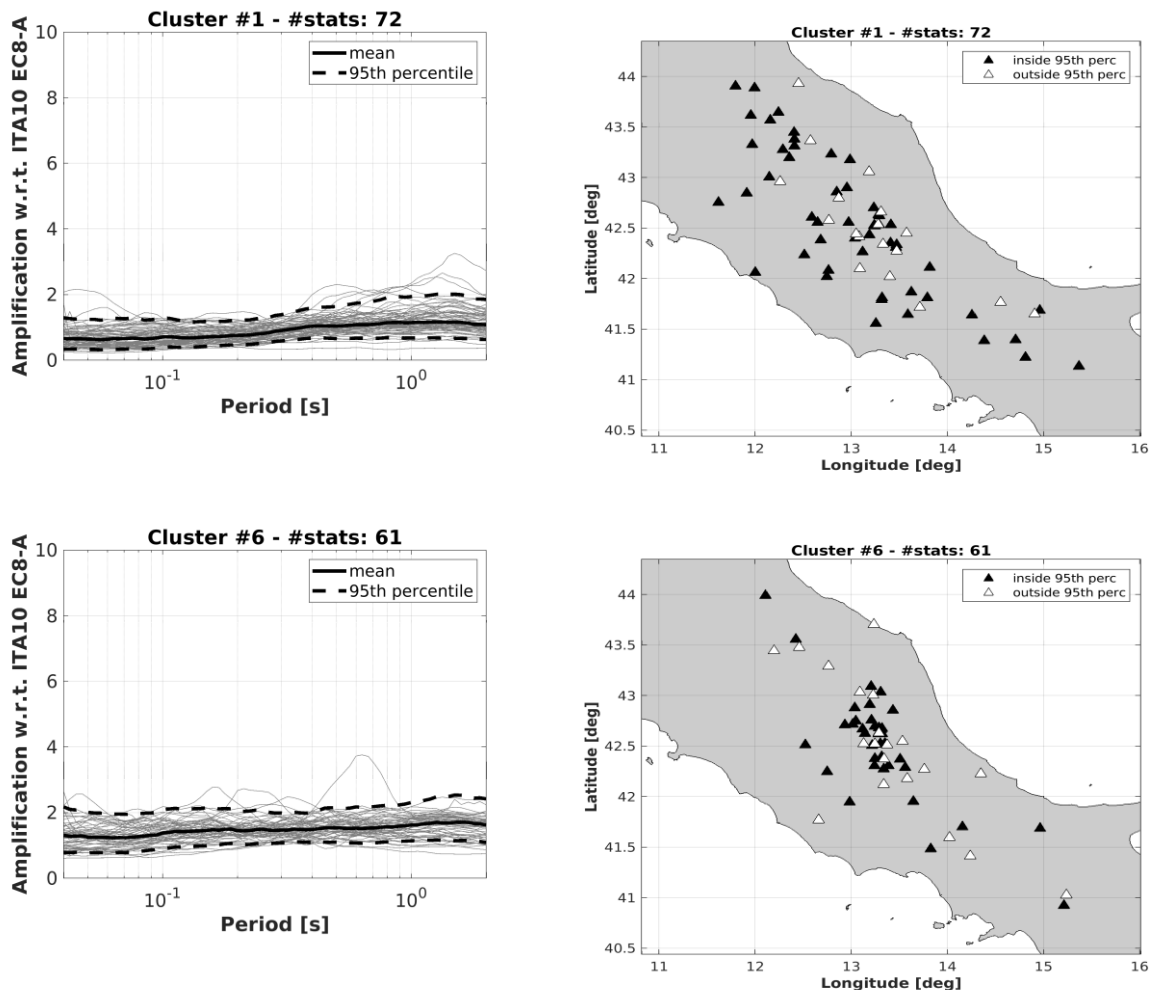


Figure 12. Left: Amplification (e^{8S2S}) versus period; right: maps of the stations. Top: cluster #1; bottom: cluster #6. White triangles indicate the stations for which more than 90% of spectral ordinates are outside the confidence interval.

The *cluster #1* is composed by 72 stations, quite well distributed in the investigated area, especially along the Apennine chain and towards the Tyrrhenian sea. 54 stations of *cluster #1* are within the confidence interval, corresponding to 75% of the total number of station in the cluster. The *cluster #6* is composed by 61 stations, mainly concentrated in the epicentral area of 2016-2017 Central Italy seismic sequence.

3. Proxies and weighting scheme

This chapter is focused on the description of the proxies selected to identify the references sites. In addition of the horizontal site-to-site terms, we propose further six proxies, based on geological,

	Research and Development Program on Seismic Ground Motion	Ref : SIGMA2-2019-D3-027/1
		Version : 1

topographical, geophysical and seismological indicators. With the aim of handling the relevance, the data quality and the lacking of these indicators, we also introduce a weights scheme. This will be applied to award a scoring and establish a ranking of stations belonging to cluster #1 and cluster #6. The proposed proxies and the acceptance criteria are listed in Table 2, while the assigned weights are listed in Table 3.

Table 2. List of the proxies used to identify reference rock stations.

	PROXY	CRITERION
1	Housing (HOU)	absence, or limited, of interaction with structures (free-field condition)
2	Topographic condition (TOP)	flat or smooth topographic surface
3	Surface geology (GEO)	rock or stiff conditions from geological/lithological map
4	Average shear wave velocity in the first 30 m ($V_{s,30}$)	$V_{s,30} \geq 750$ m/s
5	Horizontal-to-Vertical spectral ratio (H/V) of Fourier spectra of noise measurements (HVNSR) or coda-waves (HVSR-C) or S-waves (HVSR-S) of earthquake records	flat or moderately broad-band curve
6	Horizontal-to-Vertical spectral ratio (H/V) of acceleration response spectra (HVRS)	flat or moderately broad-band curve
7	Site-to-Site term of the horizontal components ($\delta S2S-H$)	negative or close to 0 on the entire period range


Four proxies out of seven are based on seismological data (HVNSR, HVRS, $\delta S2S-H$), whereas the remaining ones rely on geophysical, geological and geomorphological features (HOU, TOP, GEO, $V_{s,30}$).

The majority of information, necessary to evaluate the proxies are extracted from ITACA and ESM databases; the CRISP (Bordoni et al., 2017) repository is consulted to integrate data for the RSN stations.

When assigning the weights (Table 3) to the proxy values, we use these general rules:

- If the criterion is largely met, the weight is set equal to 1;
 - If the proxy value does not fulfil the requirement, the weight is set equal to 0;
 - If no information is available for the proxy, the weight is set equal to 0.5;
- If the criteria are partially met, the weights may range from 0.25 to 0.75;


Furthermore, in the set of the proposed proxies, we assume that the most important parameters for site-effect characterization are the surface geology (GEO), the $V_{s,30}$ and the HV from Fourier spectra. As a

	Research and Development Program on Seismic Ground Motion	Ref : SIGMA2-2019-D3-027/1
		Version : 1

consequence, we introduce a hierarchical index (Table 3): GEO, VS,30 and HV (HVNSR, HVSR-C or HVSR-S) are equal to 2, the results of seismological analyses on response spectra (HVRS and $\delta S2S-H$) have a maximum score of 1, while to the housing (HOU) and topography (TOP) a value of 0.5. The final score assigned for each proxy is given by the product of the hierarchical index and the weight value of the proxy. In the following, a brief description of the proxies and their score is given.

Table 3. Assigned weights to the proxies.

Proxy	Hierarchical index	Criterion	Proxy value weight
HOU	0.5	Free-field condition	1
		Electrical transformation cabin	0.75
VS,30	2	> 1500 m/s	1
		> 750 m/s	0.75
		\leq 750 m/s	0
GEO	2	EC8-A (scale-map \geq 1:10,000)	1
		EC8-A (scale-map < 1:10,000)	0.75
		EC8-B (scale-map \geq 1:10,000)	0.5
		EC8-B (scale-map < 1:10,000)	0.25
TOP	0.5	slope \leq 15°	1
		slope > 15°	0.5
HVNSR HVSR-C HVSR-S	2	Flat	1 1 0.5
		Broad-band	0.5 0.5 0.25
HVRS	1	Flat	1
		Broad-band	0.5
$\delta S2S-H$	1	cluster #1 within the 95th percentile	1
		cluster #1 beyond the 95th percentile	0.5
		cluster #6 within the 95th percentile	0.75
		cluster #6 beyond the 95th percentile	0.25

	<p style="text-align: center;">Research and Development Program on Seismic Ground Motion</p>	<p>Ref : SIGMA2-2019-D3-027/1</p>
		<p>Version : 1</p>

3.1 Housing - HOU

Many studies (Gallipoli et al., 2004; Stewart et al., 1999; Stewart 2000) evidenced the influence of building vibration on free-field ground motion measurements recorded inside or nearby buildings. This issue may be relevant in Italy, since several accelerometric stations of the National Accelerometric Network (RAN, <https://doi.org/10.7914/SN/IT>) are located in electrical transformation cabins (Gorini et al., 2010), while others are installed nearby or inside buildings. As an example, Figure 13 shows different installations of the accelerometric stations in Italy: a) San Demetrio nei Vestini mounted inside an electrical transformation cabin (Central Italy); b) Macchia Romana Campus of Basilicata University at Potenza installed in a small masonry building (Southern Italy); c) Sarnano in a fiberglass box (Central Italy). For the first two, Ditommaso et al. (2010) and Ditommaso and Mucciarelli (2010) demonstrated that the recorded ground motion may be affected by resonance frequency of the host building (around 7 and 12 Hz, respectively). The third one, instead, shows a typical fiberglass box hosting the accelerometric station that can be considered in free-field condition thanks to sufficient distance from big building and the absence seismic soil-structure interaction (Stewart, 2000).

To remove stations with possible dynamic interaction effects, we introduce the proxy housing (HOU), that denotes the place where the recording stations is located. Its weight is 1 for free-field stations, 0.75 for sites installed inside electrical cabin or small building and 0 otherwise.

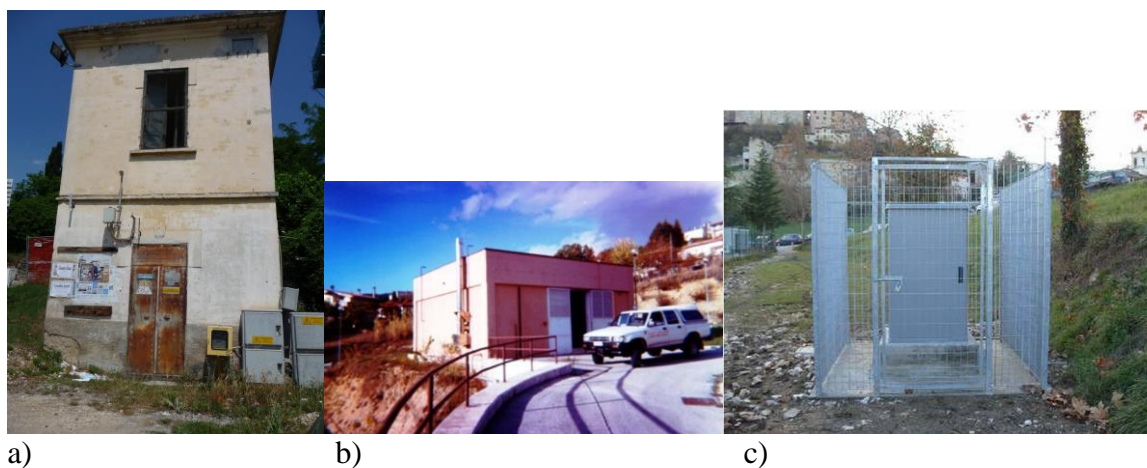


Figure 13. Outside view of the stations (a) IT.SDM-San Demetrio nei Vestini, (b) IT.PTZ-Potenza and (c) IT.SNO-Sarnano (from ITACA, Luzi et al., 2019).

3.2 Surface Geology - GEO

	<p style="text-align: center;">Research and Development Program on Seismic Ground Motion</p>	<p>Ref : SIGMA2-2019-D3-027/1</p>
		<p>Version : 1</p>

The surface geology proxy (GEO) implies the availability of geological/lithological maps. Detailed scale ($\geq 1:10,000$) surveys, typically realized for specific studies such as seismic microzonation or urban planning, are, always, preferred over maps at small scale ($<1:10,000$). We include this proxy to partially compensate for the lack of direct geophysical and geotechnical measurements to the accelerometric stations and to collect information on surface geology, morphology and on lateral heterogeneity in the lithological structure. The criterion is fully met when the station is installed on rock or other rock-like geological formation corresponding to the EC8-A ground type, as inferred from maps at detailed scale. Figure 13 shows the geologic map (scale 1:5,000) for IT.MTR (Montereale) station located on sandstone, that fulfills the shallow geological criterion. To enlarge our dataset, we, also, select stations classify as EC8-B, based on surface geology. An example of stiff site is given in Figure 13b where the lithological map (1:5,000) of IT.FMG (Fiamignano, central Italy) is shown. Different weights (Table 3) are assigned to take into account the EC8 classes inferred from geology surface: 1 and 0.75 for EC8-A rock sites inferred from map with scale greater and lower than 1:10,000, respectively; 0.5 and 0.25 for EC8-B soil category inferred from map scale greater and lower than 1:10,000.

3.3 Topography - TOP

To fulfill the topographic proxy, the site has to be located on either a flat surface or isolated slopes and reliefs with average ground inclination (i) from the horizontal plane less than 15° (NTC18, 2018), for which the topography effects can be, typically, neglected. This proxy is introduced to exclude sites with possible amplifications due to particular topographic settings (Massa et al., 2014; Paolucci 2002). Its weight (Table 3) is 1 for sites with slope less than 15° (T1 class) and 0.5 in case of slope greater than 15° (T2 class). Examples of flat topography (slope $\leq 15^\circ$) and smooth topography (slope $> 15^\circ$) are shown in Figure 14 (geological cross section of MRT and FMG, respectively).

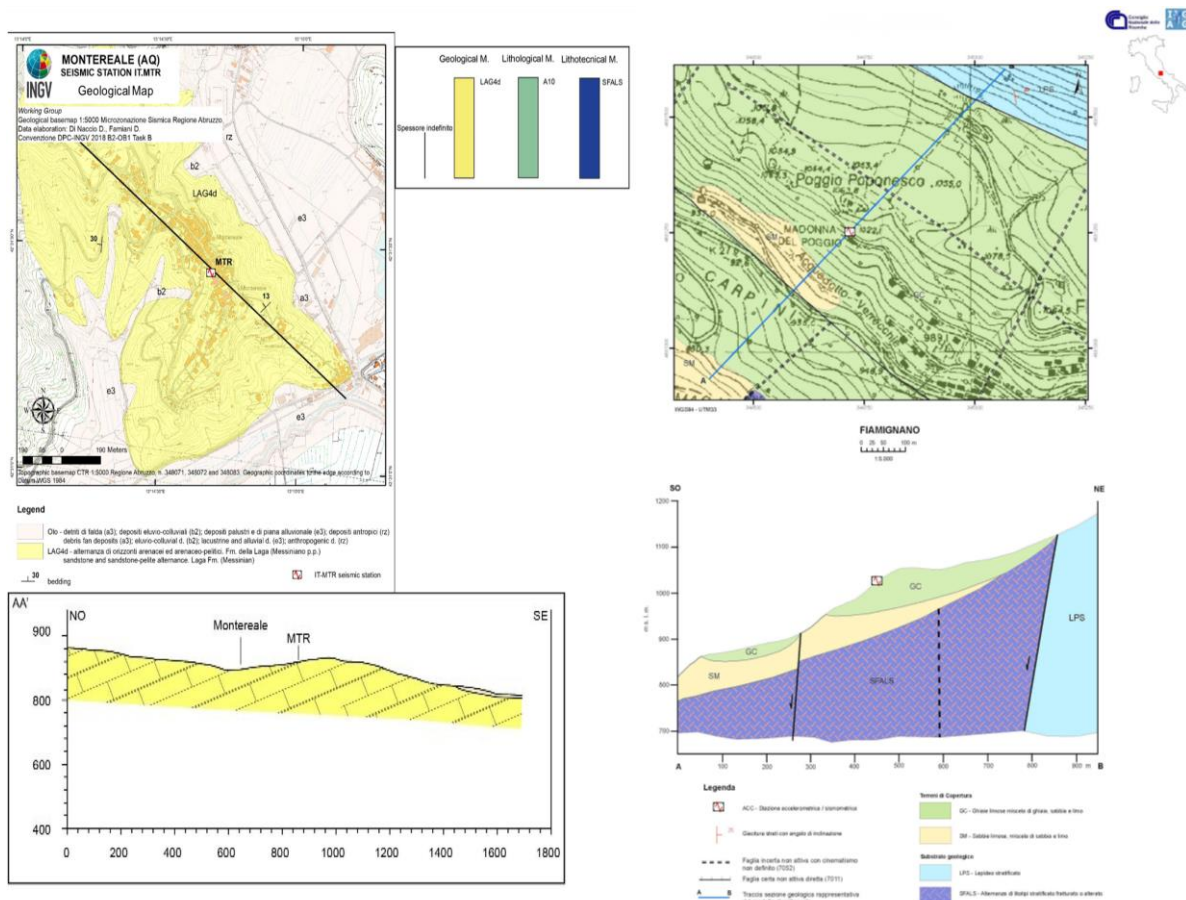


Figure 14. Detailed geological maps (1:5,000) and cross-sections for IT.MTR-Montereale (left) and IT.FMG-Fiamignano (right) stations (from ITACA, Luzi et al., 2019).

3.4 Shear-wave velocity - $V_{s,30}$

Due to the relation between shear wave velocity and stiffness of the material, the $V_{s,30}$ is the most common parameter used to recognize soils with similar response site. This proxy, introduced by Borchardt and Glassmoyer (1992) and Borchardt (1994), requires that geophysical tests have been conducted in order to evaluate the shear wave velocity profile, at least in the uppermost 30 m.

The majority of seismic codes (Eurocode 8-EC8, CEN 2004; Norme Tecniche per le Costruzioni-NTC18, CS.LL.PP 2008; National Earthquake Hazard Reduction Program-NEHRP, BSSC 2003) uses the $V_{s,30}$ to classify the soils in categories and to associate the corresponding site amplification factor. Moreover, the most recent GMMs parametrize the site responses by means of continuous functions of $V_{s,30}$. In both cases, the generic rock conditions correspond to site amplification equal to 1 over the entire range of periods and are identified when the measured $V_{s,30}$ exceeds a given threshold. In European codes, this value is set to 800 m/s (soil category EC8-A), while in the NEHRP provision, a distinction is introduced

C. FELICETTA/ G. LANZANO/ F. PACOR- Methodology to identify reference rock sites- SIGMA2-2019-D3-027/1

	<p style="text-align: center;">Research and Development Program on Seismic Ground Motion</p>	<p>Ref : SIGMA2-2019-D3-027/1</p>
		<p>Version : 1</p>

between hard rock, corresponding to $V_{s,30} > 1500$ m/s, and firm to hard rock, for $V_{s,30}$ in the range [760-1500] m/s.

In this study, we adopted a scheme similar to that of the NEHRP code assigning a score equal to 1 if $V_{s,30} > 1500$ m/s as and 0.75 for $750 \text{ m/s} < V_{s,30} \leq 1500$ m/s. We selected the value 750 m/s since in the investigated area the geological bedrock is associated with soft rocks characterized by shear-wave velocity in the range 700-800 m/s.

3.5 Horizontal-to-vertical spectral ratio from noise and earthquake recordings - HV

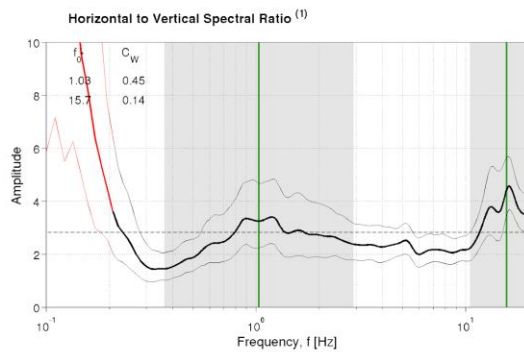
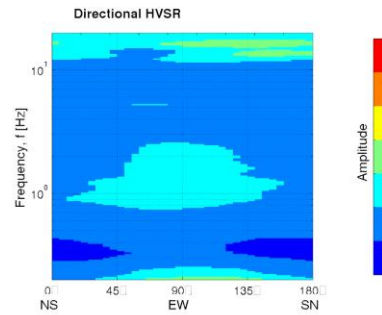
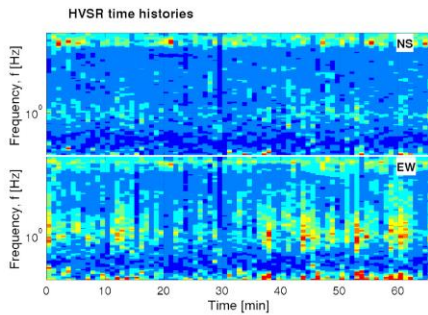
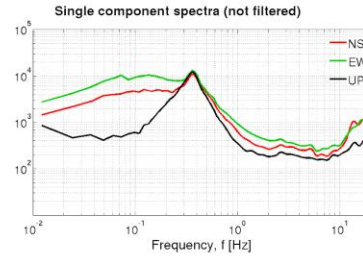
The horizontal-to-vertical spectral ratios of noise measurements (Nakamura, 1989; Bonnefoy-Claudet et al., 2006 and references listed therein) and earthquakes (Lermo and Chavez-Garcia, 1993; Puglia et al., 2011a) represent well-established non-reference site techniques to detect the fundamental resonance frequency of the site (f_0). Furthermore, they have low execution costs and can be easily calculated.

In order to obtain comparable results, the computation of H/V from noise (HVNSR) and the estimate of the fundamental frequencies were performed using the same procedure, proposed by Puglia et al. (2011). The noise signals of the IV, 4A and XO stations were extracted from the continuous waveforms stored in Eida repository (<http://www.orfeus-eu.org/data/eida/>); in situ measurements performed by DPC and the Microzonation Working Group (EmerTer Project, 2017-2018) were used for IT and 3A stations, respectively.

In order to assign the weights to the HV proxy, we define three possible shapes of the HV curves: flat, broad-band and peaked. In the first case, the HV curve does not present any clear peak and amplitude does not exceed the threshold $2\sqrt{2}$ (vectorial sum of horizontal components) across frequencies (Puglia et al., 2011). In case of broad-band curve, the amplitude exceeds the threshold $2\sqrt{2}$ over a wide range of frequency. In the last case, the HV curve presents at least one clear peak.

Figure 15 and 16 report HVNSR analysis at IT.MTR (Montereale) and IT.LSS (Leonessa) stations, respectively, both classified as EC8-A: MTR ($V_{s,30} = 1024$ m/s) has peaked curve (resonance frequencies at around 1 and 16 Hz), while LSS station ($V_{s,30} = 1090$ m/s) has a flat curve.

Station: MTR
 Recording duration: 71:02 [min:sec] (dt = 0.005 [s])
 Measurement by: DPC
 Instrument: Lennartz LE-3D/5s
 Analysis performed on 80 windows (66.40 [min:sec])
 Window length (t_w) = 50 [s]
 Minimum expected $f_0 = 0.2$ [Hz]
 Deconvolution: no
 Butterworth filter: LP = 0.1 [Hz] - HP = 20 [Hz] - ord. = 4
 Taper: 5 [%] - Konno & Ohmachi smoothing: b = 40



SESAME (2004) criteria (2)

Criteria for a clear HV peak (at least 5 out of 6 criteria fulfilled)

- i) $\exists f \in [f_0/4, f_0] | A_{HV}(f) < A_0/2$ Yes
- ii) $\exists f' \in [f_0, 4f_0] | A_{HV}(f') < A_0/2$ Yes
- iii) $A_0 > 2$ Yes
- iv) $f_{peak}[A_{HV}(f)] \pm \sigma_A(f) = f_0 \pm 5\%$ Yes
- v) $\sigma_f < \alpha(f_0)$ Yes
- vi) $\sigma_A(f_0) < \theta(f_0)$ Yes

$f_{01} = 1.03$ - Fulfilled crit.: 4/6

Criteria for a clear HV peak (at least 5 out of 6 criteria fulfilled)

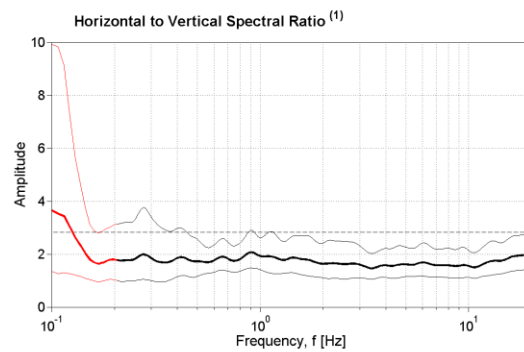
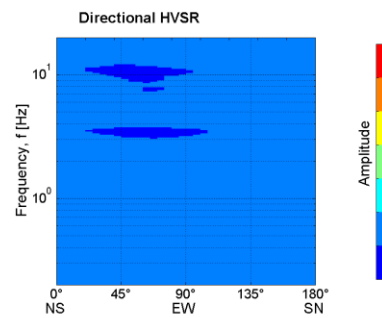
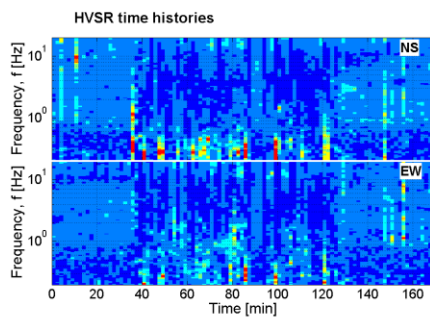
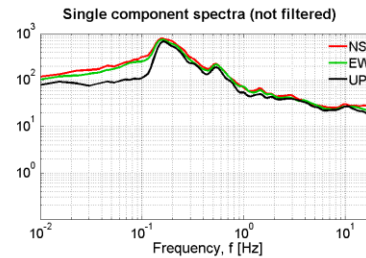
- i) $\exists f \in [f_0/4, f_0] | A_{HV}(f) < A_0/2$ Yes
- ii) $\exists f' \in [f_0, 4f_0] | A_{HV}(f') < A_0/2$ Yes
- iii) $A_0 > 2$ Yes
- iv) $f_{peak}[A_{HV}(f)] \pm \sigma_A(f) = f_0 \pm 5\%$ Yes
- v) $\sigma_f < \alpha(f_0)$ No
- vi) $\sigma_A(f_0) < \theta(f_0)$ No

$f_{02} = 15.70$ - Fulfilled crit.: 4/6

(1) based on horizontal components merged through vectorial sum
(2) based on horizontal components merged through geometric mean

Figure 15. Horizontal-to-vertical spectral ratio analysis from noise measurements at IT.MTR-Montereale station (from ITACA, Luzi et al., 2019).

Station: LSS
Recording duration: 180:52 [min:sec] (dt = 0.008 [s])
Measurement by: DPC
Instrument: Lennartz LE-3D/5s
Analysis performed on 103 windows (171:40 [min:sec])
Window length (t_w) = 100 [s]
Minimum expected $f_0 = 0.2$ [Hz]
Deconvolution: no
Butterworth filter: LP = 0.1 [Hz] - HP = 20 [Hz] - ord. = 4
Taper: 5 [%] - Konno & Ohmachi smoothing: b = 40



(1) based on horizontal components merged through vectorial sum

Figure 16. Horizontal-to-vertical spectral ratio analysis from IT.LSS-Leonessa station (from ITACA, Luzi et al., 2019).

When noise measurements are not available, we evaluate the proxy based on the Horizontal-to-Vertical spectral ratio using the Fourier spectra of coda-waves of earthquake records (HVSr-C), or, if these analyses are missing, the Fourier spectra of S-waves (HVSr-S). After some preliminary test, the curves obtained from coda-waves are generally similar to those calculated from noise measurements as already observed in previous studies (Stehly et al., 2006). The mean HV curves obtained from S-wave window are comparable to those of coda-wave but the dispersion is generally larger, especially when directional effects are present (Puglia et al., 2011).

The results of HVSR-C and HVSR-S analyses at BGR (Bagno di Romagna) station are shown in Figure 17. The HV curves are almost flat in accordance with the EC8-A subsoil category associated to the station ($V_{S,30} = 830$ m/s).

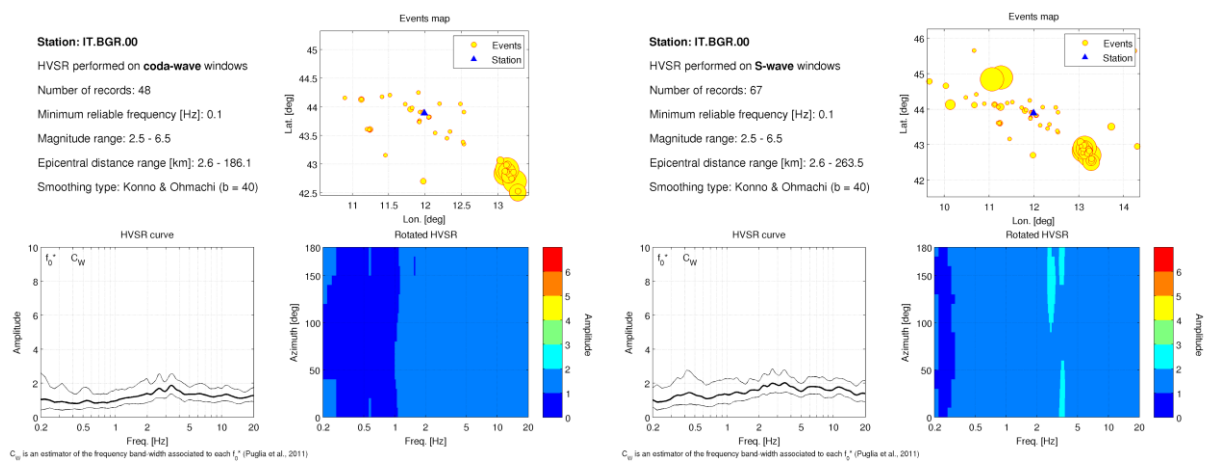


Figure 17. Horizontal-to-vertical spectral ratio from earthquake recording on coda (left) and S-waves (right) for the IT.BGR (Bagno di Romagna) station.

Different weights (Table 3) are assigned to consider the three different types of analyses and the shape of the HV curves: 1 and 0.75 for HV flat or broad-band, respectively, derived from HVNRS and HVSR-C; HVSR-S analysis is weighted 0.5 and 0.25 for flat and broad-band curve, respectively. In case of picked curves the weight is, always, set to 0. [Appendix I](#) reports the description of the methods used to calculate the HV mean curves from noise measurements, coda- and S-waves of earthquake recordings.

3.6 Horizontal-to-vertical spectral ratio from response spectra - HVRS

HVRS proxy consists of horizontal-to-vertical spectral ratio computed on 5% damped acceleration response spectra of earthquake recordings. The main advantages of using HVRS are: i) no smoothing is required; ii) the absence of sharp peaks leading to large variability of the average Fourier H/V curves (Zhao et al., 2006); iii) a reduction of the computational cost in calculating spectral ratios.

Even though the use of damped response spectra does not guarantee that only the S-wave portion of a record contributes to the spectral analysis, they can be efficiently employed to characterize the site response of a large number of station using all available records (Zhao et al., 2006).

C. FELICETTA/ G. LANZANO/ F. PACOR- Methodology to identify reference rock sites- SIGMA2-2019-D3-027/1

As observed by Puglia et al. (2011), in case of clear resonance frequencies, the outcomes from microtremor measurements and HVRS analysis generally agree. We perform some tests and find similar agreement also in case of absence of resonance.

As an example, Figure 18 shows the results of HVRS (left) and HVNSR (right) analyses for the IV.SACS-San Casciano dei Bagni station: curves are flat and the shape is similar between the two types of analysis. We adopt the same weight scheme both for HVRS and HVNSR proxies.

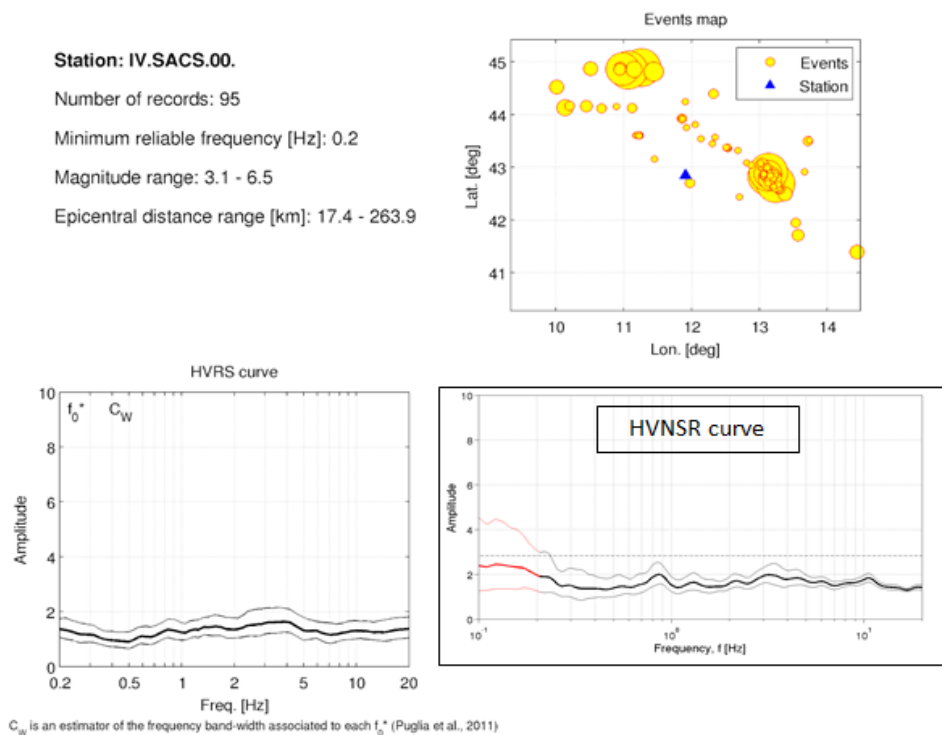


Figure 18. Horizontal-to-vertical spectral ratio from 5% damped acceleration response spectra of earthquake recordings (left) and from noise measurement (right) for the IV.SACS (San Casciano dei Bagni) station.

3.7 Site-to-site term of horizontal component - $\delta S2S-H$

In addition to the preliminary pre-selection of the stations from the cluster analysis of horizontal $\delta S2S_{EC8-A}$, we also evaluate the membership of stations, attributing different weights at clusters #1 and #6 and if the stations are or not within the confidence interval of each cluster (section 2.0). The proposed weights for horizontal $\delta S2S_{EC8-A}$ is reported in Table 4.


	Research and Development Program on Seismic Ground Motion	Ref : SIGMA2-2019-D3-027/1 Version : 1
---	--	---

Table 4. Proposed weights for stations in cluster #1 and #6.

$\delta S2S-H/\delta S2S-V$	cluster #1 within the 95th percentile	1
	cluster #1 beyond the 95th percentile	0.5
	cluster #6 within the 95th percentile	0.75
	cluster #6 beyond the 95th percentile	0.25

3.9 Station scoring

Before applying the weighting scheme of Table 3 to the candidate stations we checked that, at least, one of the three most important proxies (GEO, VS30 and HV) is available, in order to constrain the results to some geological and/or geophysical observations. Then, we assume that a station is a reference site if it reaches a minimum score of 5.5 out of 9, summing the results of the products between the weights and the hierarchical index in Table 3. Adopting this criterion, almost 60% of the required criteria are met.

Furthermore, considering the hierarchy of the proposed proxies, if a site completely satisfies the acceptance criteria of the most important proxies (GEO, $V_{S,30}$, HVNSR), it will be classified as a reference, with a minimum score of 6 if the $V_{S,30} > 1500$ m/s and 5.5 if $V_{S,30}$ is between 750 and 1500 m/s.

First, we verify the existences of at least other one of the three most important proxies for the memberships of cluster #1 (71 out to 72) and cluster #6 (55 out to 61) and then we apply the weight scheme of Table 3. The list of the candidate stations and the corresponding ranking are reported in Appendix II.

After the application of the seven proxies, 28 stations out of 71 of cluster #1 and 13 out of 55 of cluster #6 can be considered as reference rock-sites. Any selected stations reach the maximum awardable score (9) because the $V_{S,30}$ value greater than 1500 m/s is not represented in the training dataset.

These stations are listed in Table 5 and Table 6 for *cluster #1* and *#6*, respectively. Figure 19 shows the distribution of the 41 selected reference rock-sites in terms topographic classification, EC8 class on surface geology, shape of Fourier H/V and HVRS curves.

In Figure 20, we show the mean shear-wave velocity profile (up to 30 m) obtained from the V_S profiles available for the selected reference rock-sites.


	Research and Development Program on Seismic Ground Motion	Ref : SIGMA2-2019-D3-027/1 Version : 1
---	--	---

Table 5. List of the cluster #1 stations with score (SUM_W) ≥ 5.5 . For each station, the table reports: network code (NET CODE); station code (STA CODE); housing condition (HOU); housing weight (W_H); HV analysis (HVtype); shape of HV curve (HV); weight for the HV proxy (W_HV); shape of HVRS curve (HVRS); weight HVRS weight (W_HVRS); slope range (TOP); topographic weight (W_T); scale of the geological/lithological/litotechnical map; EC8 subsoil classification from surface geology (EC8); weight for the geological proxy (W_GEO); weight for cluster #1 (W_CL#1); number of available proxies (AV PROXIES).
 FF = free-field condition; CAB = Electrical transformation cabin; NO-FF = no free-field condition
 F = flat curve; BB = broad-band curve; P = picked curve

NET CODE	STA CODE	HOU	W_H	HVtype	HV	W_HV	HVRS	W_HVRS	TOP	W_T	VS,30	W_Vs	GEO scale	EC8	W_GEO	W_CL#1	AV.PROXIES	SUM_W
IT	BGR	FF	0.5	HVNSR	F	2	F	1	slope $\leq 15^\circ$	0.5	A	1.5	5000	A	2	1	7	8.5
IT	MVB	FF	0.5	HVNSR	F	2	F	1	slope $\leq 15^\circ$	0.5	A	1.5	5000	A	2	0.75	7	8.25
IT	LSS	FF	0.5	HVNSR	F	2	F	1	slope $> 15^\circ$	0.25	A	1.5	10000	A	2	1	6	8.25
IT	GRN	CAB	0.375	HVNSR	F	2	F	1	slope $> 15^\circ$	0.25	1	5000	A	2	1	4	7.625	
IV	SACS	FF	0.5	HVNSR	F	2	F	1	slope $\leq 15^\circ$	0.5	1	100000	A	1.5	1	6	7.5	
3A	MZ102	FF	0.5	HVNSR	F	2	BB	0.5	slope $\leq 15^\circ$	0.5	1	5000	A	2	1	6	7.5	
IV	POFI	FF	0.5	HVNSR	F	2	F	1	slope $\leq 15^\circ$	0.5	1	100000	A	1.5	0.75	6	7.25	
IV	CAFI	FF	0.5	HVNSR	F	2	F	1	slope $> 15^\circ$	0.25	1	100000	A	1.5	1	5	7.25	
IV	FIAM	FF	0.5	HVNSR	F	2	F	1	slope $> 15^\circ$	0.25	1	100000	A	1.5	1	5	7.25	
IV	SACR	0.25	0.25	HVNSR	F	2	F	1	slope $\leq 15^\circ$	0.5	1	100000	A	1.5	1	5	7.25	
IV	SGTA	0.25	0.25	HVNSR	F	2	F	1	slope $\leq 15^\circ$	0.5	1	100000	A	1.5	1	5	7.25	
3A	MZ31	FF	0.5	HVNSR	F	2	F	1	slope $\leq 15^\circ$	0.5	1	5000	B	1	1	6	7	
IT	CSO1	FF	0.5	HVNSR	F	2	F	1	slope $> 15^\circ$	0.25	1	25000	A	1.5	0.75	5	7	
IV	ATLO	FF	0.5	HVNSR	F	2	F	0.5	slope $\leq 15^\circ$	0.5	1	100000	A	1.5	1	5	7	
IV	TRIV	0.25	0.25	HVNSR	F	2	F	1	slope $\leq 15^\circ$	0.5	1	100000	A	1.5	0.75	5	7	
IT	FMG	NO-FF	0	HVNSR	F	2	F	1	slope $> 15^\circ$	0.25	B	1.5	5000	B	1	1	5	6.75
IT	PAN	FF	0.5	HVSR-S	F	1	F	1	slope $\leq 15^\circ$	0.5	1	20000	A	1.5	1	6	6.5	
IT	SLO	FF	0.5	HVSR-C	BB	1	BB	0.5	slope $\leq 15^\circ$	0.5	1	10000	A	2	1	6	6.5	
IV	ATVO	FF	0.5	HVNSR	F	2	BB	0.5	relief	0	1	100000	A	1.5	1	5	6.5	
IT	MNF	HOU	0	HVNSR	F	2	F	1	slope $> 15^\circ$	0.25	1	50000	A	1.5	0.75	4	6.5	
IV	RM03	0.25	0.25	HVSR-C	F	2	BB	0.5	slope $\leq 15^\circ$	0.5	1	100000	A	1.5	0.75	5	6.5	
IT	PSC	FF	0.5	HVNSR	P	0	F	1	slope $> 15^\circ$	0.25	A	1.5	5000	A	2	1	5	6.25
IV	ATPI	FF	0.5	HVSR-S	F	1	F	0.5	slope $\leq 15^\circ$	0.5	1	100000	A	1.5	1	5	6	
IV	GUAR	FF	0.5	HVSR-S	F	1	F	0.5	slope $\leq 15^\circ$	0.5	1	100000	A	1.5	1	5	6	
IV	T1215	0.25	0.25	HVSR-S	F	1	F	1	slope $\leq 15^\circ$	0.5	1	100000	A	1.5	0.75	5	6	
IV	CIGN	FF	0.5	HVSR-S	F	1	F	0.5	slope $\leq 15^\circ$	0.5	1	100000	A	1.5	0.75	5	5.75	
IV	MNS	0.25	0.25	HVSR-C	BB	1	BB	0.5	slope $\leq 15^\circ$	0.5	1	100000	A	1.5	1	5	5.75	
IV	ATVA	0.25	0.25	HVSR-S	F	1	BB	0.5	slope $\leq 15^\circ$	0.5	1	100000	A	1.5	1	4	5.75	

Table 6. List of the cluster #6 stations for which the score is equal to or greater than 5.5. For each station, the table reports the same information described in Table 5 caption.

NET CODE	STA CODE	HOU	W_H	HVtype	HV	W_HV	HVRS	W_HVRS	TOP	W_T	VS,30	W_Vs	GEO scale	EC8	W_GEO	W_CL#1	AV.PROXIES	SUM_W
IT	SNO	FF	0.5	HVNSR	F	2	F	1	slope $\leq 15^\circ$	0.5	1	10000	A	2	0.75	7	7.75	
IV	APEC	NO-FF	0	HVNSR	F	2	F	1	slope $\leq 15^\circ$	0.5	1	100000	A	1.5	0.75	6	6.75	
IV	SNAL	0.25	0.25	HVNSR	F	2	F	1	slope $> 15^\circ$	0.25	1	100000	A	1.5	0.75	5	6.75	
IV	CAFR	FF	0.5	HVNSR	F	2	F	0.5	slope $\leq 15^\circ$	0.5	1	100000	A	1.5	0.5	6	6.5	
IT	ORC	NO-FF	0	HVSR-C	BB	1	BB	0.5	slope $\leq 15^\circ$	0.5	767	1.5	5000	A	2	0.75	7	6.25
IT	SDM	CAB	0.375	HVNSR	F	2	F	1	slope $\leq 15^\circ$	0.5	752	1.5	5000	C	0	0.75	6	6.125
3A	MZ25	0.25	0.25	HVNSR	F	2	F	0.5	slope $\leq 15^\circ$	0.5	1	5000	B	1	0.75	5	6	
IT	MMP1	FF	0.5	HVNSR	P	0	BB	0.5	slope $\leq 15^\circ$	0.5	800	1.5	5000	A	2	0.75	7	5.75
IT	CSC	NO-FF	0	HVNSR	F	2	F	1	relief	0	698	0	10000	A	2	0.75	5	5.75
IT	NRN	CAB	0.375	HVNSR	BB	1	BB	0.5	slope $\leq 15^\circ$	0.5	1	50000	A	1.5	0.75	6	5.625	
3A	MZ05	0.25	0.25	HVNSR	P	0	F	1	slope $\leq 15^\circ$	0.5	1	5000	A	2	0.75	5	5.5	
IV	CSP1	0.25	0.25	HVSR-S	F	1	F	0.5	slope $\leq 15^\circ$	0.5	1	100000	A	1.5	0.75	5	5.5	
IV	RM01	0.25	0.25	HVSR-C	BB	1	BB	0.5	slope $\leq 15^\circ$	0.5	1	A	1.5	0.75	6	5.5		

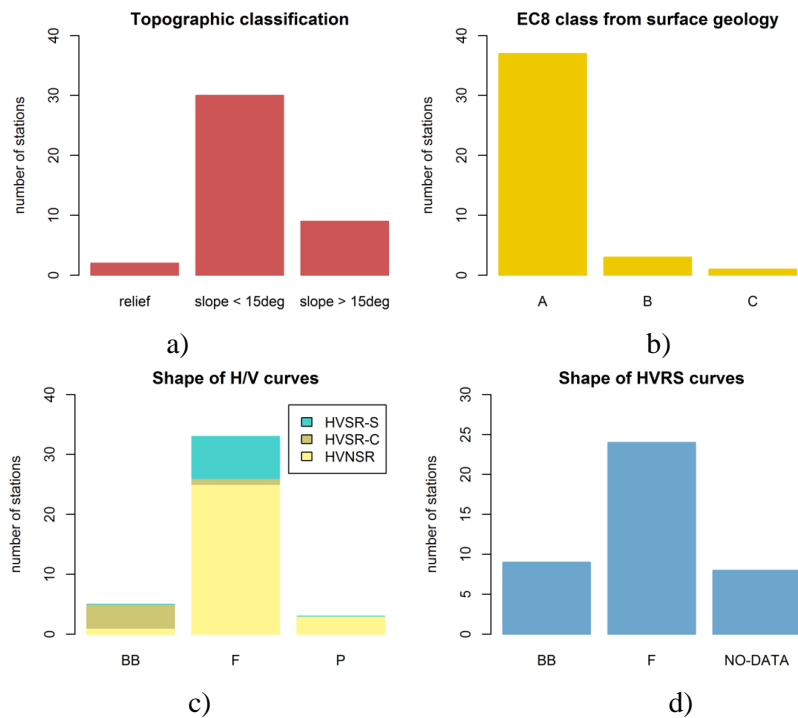


Figure 19. Distribution of the 52 selected reference rock-sites in terms of: a) Topographic classification (TOP proxy); b) EC8 class evaluated on surface geology (GEO proxy); c) shape of HV curves colored as function of the analysis type (HVNSR in yellow, HVSR-C in light brown, HVSR-S in teal); d) shape of HVRS curves.

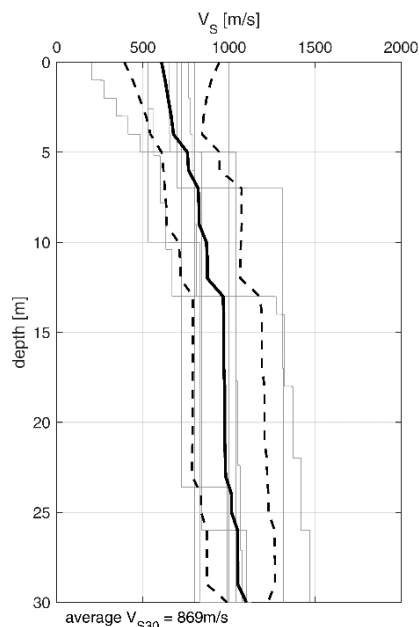


Figure 20. Mean shear-wave velocity profile (black line) and its standard deviation (dotted lines), up to 30 m, obtained from VS profiles available for the selected reference rock-sites (grey lines). The average value of $V_{s,30}$ (869 m/s) is, also, reported.

3.10 High-frequency attenuation parameter k for reference rock sites

The aim of this section is the computation of the high-frequency attenuation parameter k for the reference rock sites to provide its range of variability and, in case, propose it as further possible proxy.

The parameter k (kappa) was introduced by Anderson and Hough (1984) to describe the high frequency attenuation of the Fourier spectra of observed ground motion. Although its origin is largely debated (Ktenidou et al., 2015), this parameter is widely adopted in various fields of the engineering seismology, spanning from stochastic ground motion simulation to adjustment factors for different rock conditions (standard versus hard rock). Many approaches are proposed to estimate k ; a detailed review can be found in Ktenidou et al. (2014).

In this paragraph, we adopt the classical approach (Anderson and Hough, 1994) to compute the k at the selected reference rock sites, estimating the frequency decay of the semi-logarithm acceleration Fourier spectra ([Appendix I](#)).

The average frequency band used for evaluating the high frequency falloff is 15–25 Hz, although it varies site by site and record by record depending on magnitude and distance.

We estimate the site-specific component k_0 , representing the attenuation due to propagation in the shallower layers, using a linear model with distance for each station:

$$k_s = k_{0,s} + k_r \times R \quad (3)$$

where R is the epicentral distance (Figure 21). Although non parametric approach are often adopted to better represent the regional contribution to the high-frequency attenuation, the linear model is often proven to be a good approximation (Ktenidou et al., 2015 and references listed therein).

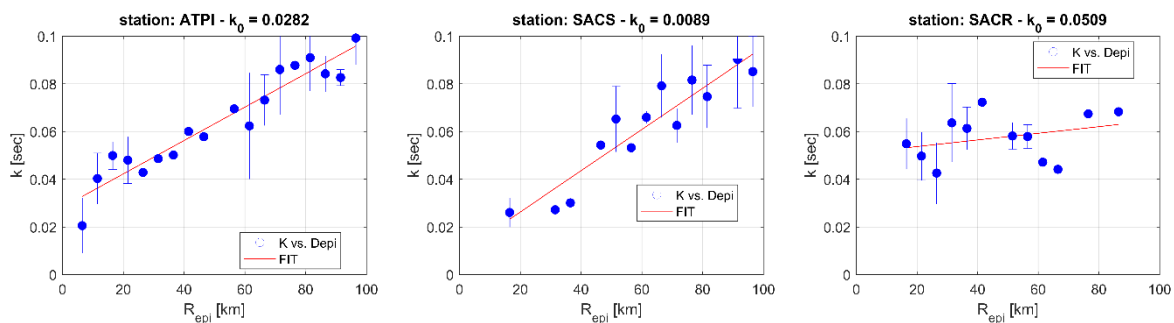


Figure 21. Distribution of k values for IV.ATPI, IV.SACS and IV.SACR, averaged on distance bin of 5 km. Regressed line is shown in red. The maximum distance is 100km

A total of 36 out 41 k_0 values are estimated for the stations of Table 5 and 6, using records within 100km from the epicentre. Figure 22 and Figure 23 report the k distribution obtained from this analysis: the values range from 0.0064 (SLO) and 0.051s (SACR), with a mean value equal to $k_0=0.245s$. Although our results C. FELICETTA/ G. LANZANO/ F. PACOR- Methodology to identify reference rock sites- SIGMA2-2019-D3-027/1

are preliminary, the range of variability is in agreement with the estimates obtained in other studies for rock sites (Ktenidou and Abrahamson, 2016; Bard et al. 2018).

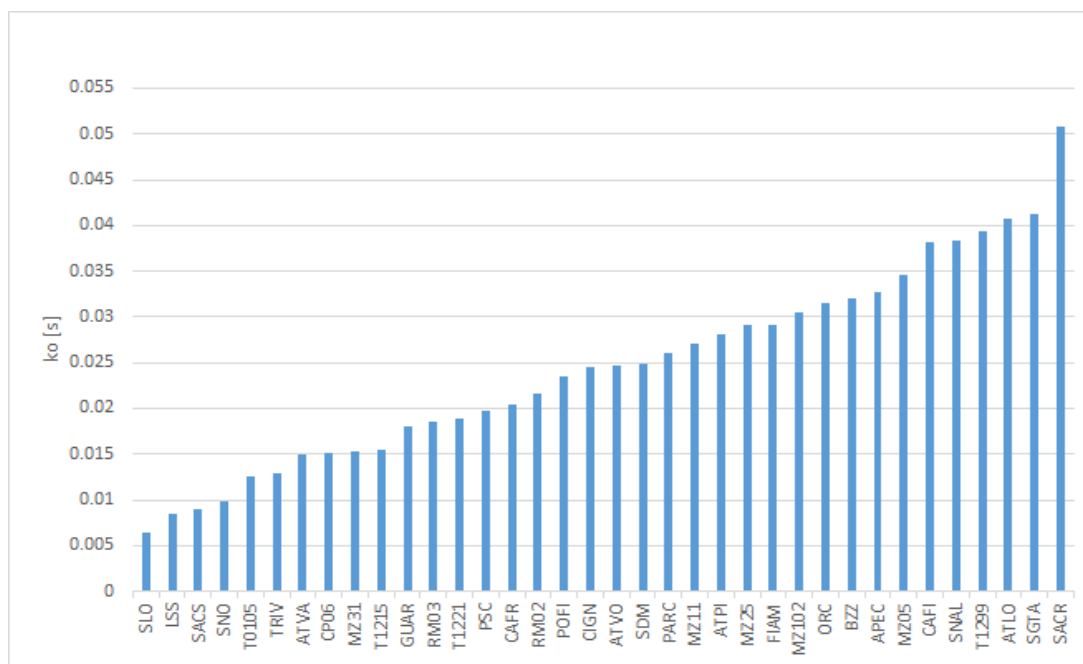


Figure 22. k_0 values for 36 reference sites.

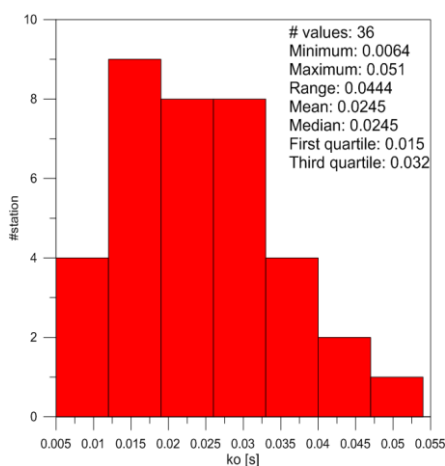



Figure 23. Histograms of k_0 values for 36 reference sites.

	<p style="text-align: center;">Research and Development Program on Seismic Ground Motion</p>	<p>Ref : SIGMA2-2019-D3-027/1</p>
		<p>Version : 1</p>

4. GMMs calibration

Once the reference rock sites are detected, a set of GMMs is calibrated to test the efficiency of this selection. The functional form is:

$$\log Y = a + F_M(M) + F_R(M, R) + F_S + \delta B_e + \delta S_2 S_s + \varepsilon_{es} \quad (4)$$

where the fixed-effects are the offset a , the magnitude term F_M , the distance term F_R and the site effect term F_S . The random-effects are performed on events (δB_e) and stations ($\delta S_2 S_s$) and ε_{es} is the residual variability (corrected by site and event).

The magnitude term F_M is:

$$F_M(M) = \begin{cases} b_1(M_w - M_h) & \text{for } M_w \leq M_h \\ b_2(M_w - M_h) & \text{otherwise} \end{cases} \quad (5)$$

where b_1 and b_2 are coefficients obtained from the regression, M_h is the hinge magnitude and the magnitude M is the moment magnitude M_w . After some trial tests, the magnitude scaling is assumed to be a bi-linear function with a fixed hinge magnitude $M_h=5.0$.

The distance term F_R is:

$$F_R(M, R) = [c_1(M_w - M_{ref}) + c_2] \log_{10} \frac{\sqrt{R_{JB}^2 + h^2}}{R_{ref}} + c_3 \left(\sqrt{R_{JB}^2 + h^2} - R_{ref} \right) \quad (6)$$

where the c_1 , c_2 and c_3 are the calibration coefficients, M_{ref} is the reference magnitude, h is the pseudo-depth and R_{ref} is the reference distance ($R_{ref}=1\text{km}$). The model is calibrated for the Joyner-Boore distance, R_{JB} , and the maximum value is 120km.

We calibrate three models, accounting for site effects (F_S) in different ways, all expressed in terms of site categories (dummy variables):

- **EC8:** Eurocode 8 site classification, where the coefficients of the site category EC8-A are set to zero ($s_{EC8-A}=0$; $s_{EC8-B} \neq s_{EC8-C} \neq s_{EC8-D} \neq s_{EC8-E} \neq 0$);
- **Clust:** Site classification after the cluster analysis, where the coefficients of the *cluster #1* are set to zero ($s_{\#1}=0$; $s_{\#2} \neq s_{\#3} \neq \dots \neq s_{\#9} \neq 0$);
- **Ref:** Classification of the sites in two classes, the reference rock sites, after the analysis of the stations of cluster #1 and #6 (described in section 3.0), and the remaining sites ('others') without any subdivisions; the coefficient of the reference rock site class is set to zero ($s_{ref}=0$; $s_{oth} \neq 0$).

The first option (**EC8**) is the common way to account for site effects into GMMs when the $V_{S,30}$ is not available for the majority of the sites. The second option (**Clust**) is totally data-driven and we expect that

returns the lowest variability. The third option (**Ref**) mimics the GMMs proposed by Kotha et al. (2016) for Europe and Middle-East; in particular, the main difference is that the ‘zero’ level of the Kotha et al. (2016) model median prediction corresponds to the average of the δS_{2S} , with respect to all sites. Table 7 reports the number of records, events and station for GMMs calibration. The dataset of **EC8** and **Ref** is the same, while the calibration of **Clust** is performed on a subset including only the stations used for the cluster analysis (see section 2.0). However, the **Clust** subset is the 92% of the **EC8** dataset and the number of stations is the 70% of the total. Figure 24 shows the distribution of data among the site categories for each model: the records of the sites classified as EC8-B in **EC8** model are about the 60% of the data, while the percentage of EC8-D and E are almost negligible; the most represented categories for **Clust** model are the *cluster #1* (22%), #6 (17%), #7 (18%) and #9 (15%); finally, the percentage of records of reference rock sites in **Ref** model is about the 15% of the dataset.

Table 7. Number of records, events and stations in the datasets for the calibration of EC8, Clust and Ref.

Dataset	#Recs	#Events	#Stations
EC8/Ref	34821	456	460
Clust	32174	456	343

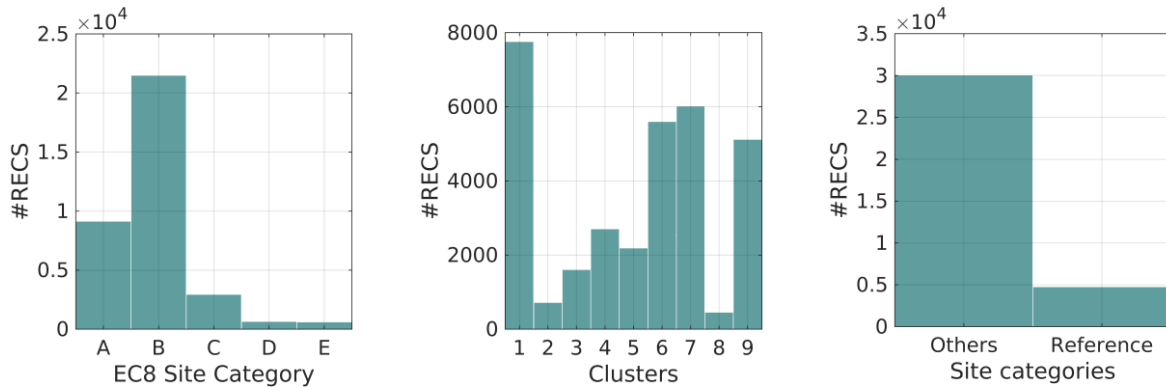


Figure 24. Histograms of data with respect to the GMMs site categories. Left: EC8; center: Clust; right: Ref.

In a first stage of the analysis, we perform a nonlinear regression without the site term F_S to obtain the reference magnitude M_{ref} and the pseudo-depth h . The coefficients a , b_1 , b_2 , c_1 , c_2 and c_3 , the site effect coefficients (fixed-effects) and the random-effects variabilities τ (between-event), ϕ_{S2S} (site-to-site) and ϕ_0 (event- and site- corrected residuals) are derived in a second stage by the calibration of a linear ordinary least-squares mixed-effect model. The calibration results of the three models for the geometric mean of

horizontal components of PGA and 69 ordinates of the acceleration spectra SA (5% damping), in the period range $T=0.04-2s$, are reported in the Appendix III. The coefficient for anelastic attenuation c_3 tends to assume positive values at longer periods and this is corrected setting c_3 to zero in the regression. Figure 25 reports the plot of the attenuation with distance at two different magnitudes of the three models (**EC8**, **Clust** and **Ref**), considering the predictions for the site class set to zero in each model (reference level). As expected the prediction for the reference sites of **Ref** and cluster #1 of **Clust** are remarkably lower than those obtained for EC8-A class of **EC8**. The reduction is almost independent on distance and is more evident at short periods.

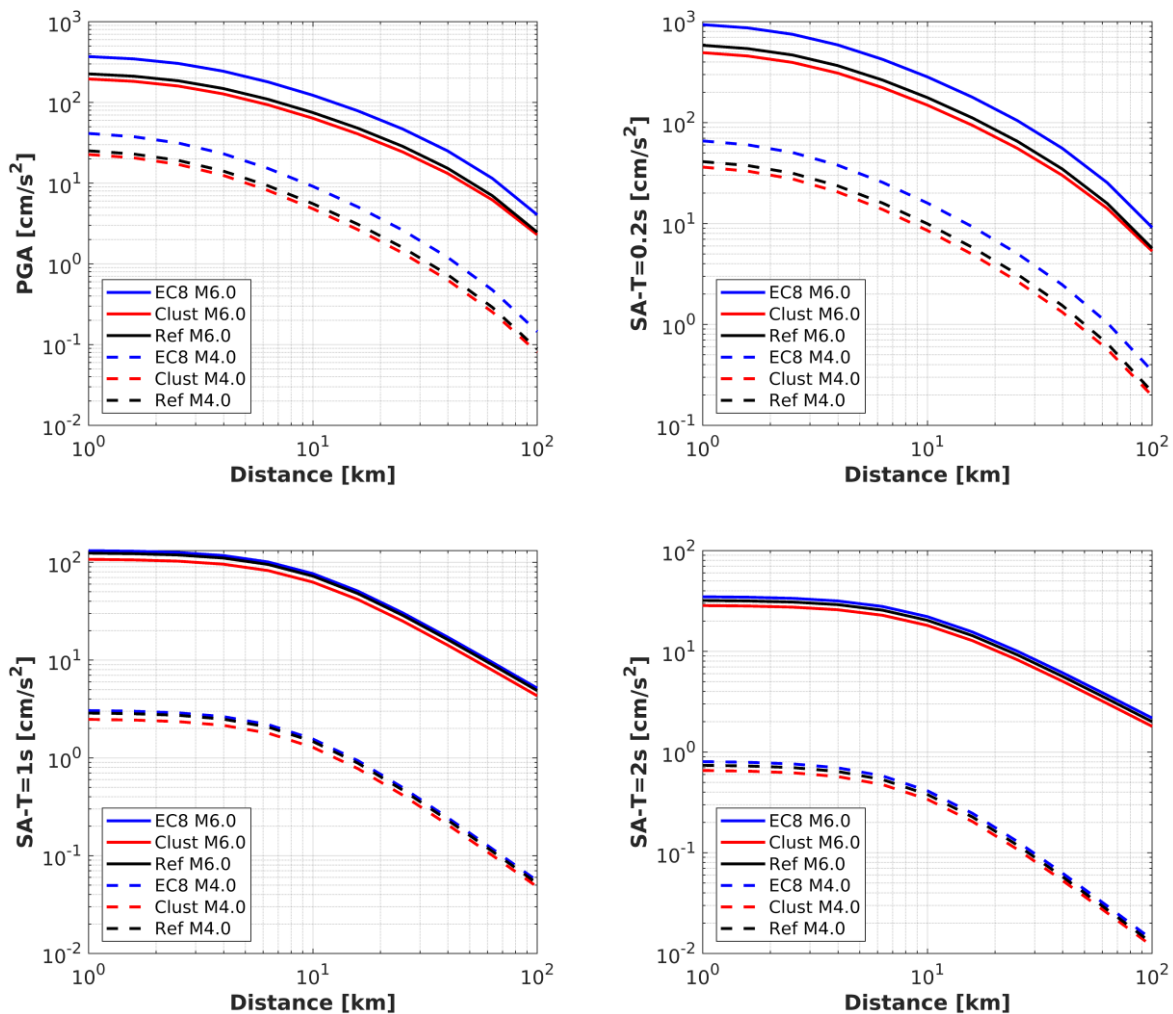



Figure 25. Predictions of **EC8**, **Clust** and **Ref** model for M4.0 and M6.0 as a function of Joyner-Boore distance.

	Research and Development Program on Seismic Ground Motion	Ref : SIGMA2-2019-D3-027/1
		Version : 1

In order to quantify this reduction, Table 8 shows the ΔY (%), which is the difference between the EC8-A predictions of model **EC8** and the reference predictions of the model **Ref**, normalized with respect to EC8-A predictions.

Since the magnitude F_M and distance F_R terms of the **EC8** and **Ref** models are very similar (see Appendix III), the values of ΔY are averaged over all distances and magnitudes and are reported for five intensity measures (PGA, SA at T=0.1, 0.2, 1 and 2s). Table 8 also reports the percentage reduction calculated by Felicetta et al. (2018) between the generic and the reference rock predictions of a GMMs calibrated with the same dataset of Bindi et al. (2011).

Table 8. Percentage reduction between the predictions of **EC8** for site A and **Ref** for the reference rock sites. The results of Felicetta et al. (2018) are derived from Figure 6 of the paper.

ΔY (%)	PGA	SA-T=0.1s	SA-T=0.2s	SA-T=1s	SA-T=2s
This study	39.0	44.1	37.7	5.7	8.1
Felicetta et al. (2018)	35.1	33.5	38.5	26.5	28.0

The reduction is the largest at spectral ordinate T=0.1s (44%) and is smaller at longest periods (T=1 and 2s). The results are quite similar to those obtained by Felicetta et al. (2018), except for long periods, where we find a smaller reduction (at T=1s 5.7% vs. 26.5%).

The site coefficients for **EC8** and **Clust** are shown in Figure 26. The classification of **EC8** model seems ineffective, especially for EC8-D sites, mainly because they are scarcely represented in the dataset. The trend of coefficients for the **Clust** model resembles the amplification functions of the same clusters, showed in Figure 10. Figure 27 shows the standard deviation components for the three proposed models.

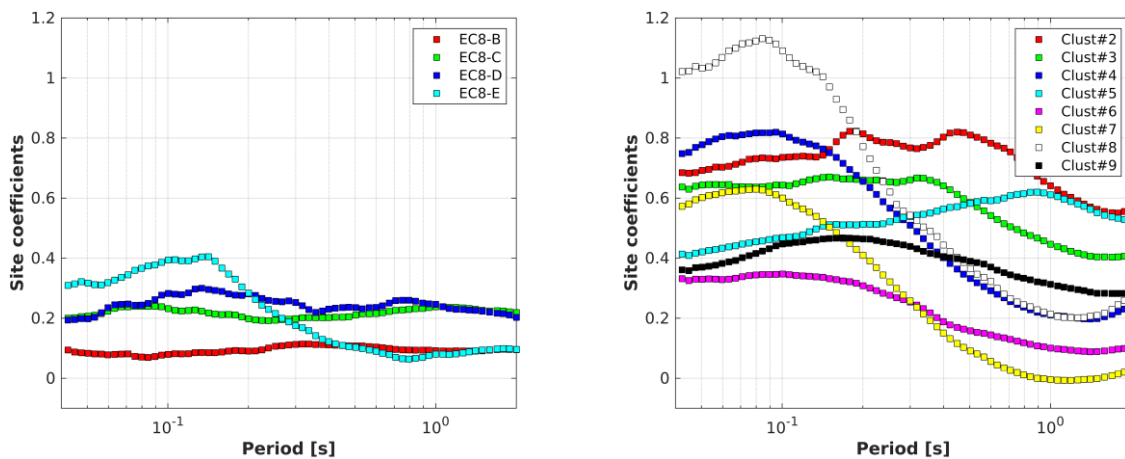


Figure 26. Site coefficients of model **EC8** (left) and **Clust** (right).

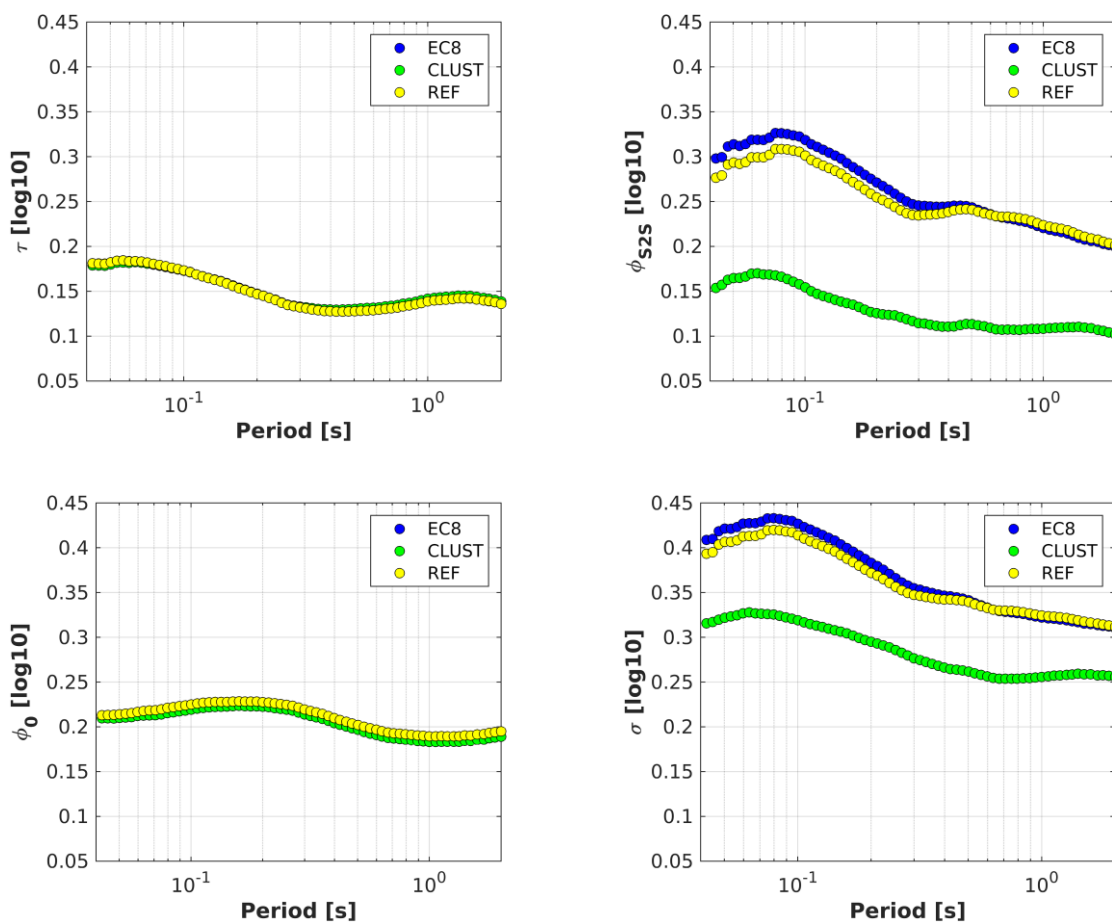



Figure 27. Standard deviations of **EC8**, **Clust** and **Ref** models. Top left: between-event term; top right: site-to-site term; bottom left: variability of the event- and site- corrected residuals; bottom right: total sigma.

	<p style="text-align: center;">Research and Development Program on Seismic Ground Motion</p>	<p>Ref : SIGMA2-2019-D3-027/1</p>
		<p>Version : 1</p>

As expected, the between-event term τ and the residual aleatory variability ϕ_0 are unaffected by the classification scheme adopted for calibrating the GMMs. The site-to-site variability ϕ_{S2S} of **Clust** model is, instead, significantly lower than those found for **EC8** and **Ref** models. This is not surprising since the **Clust** model is a data-driven approach, but the clusterization, at the moment, is not justified by any explanatory variable, and the aggregation of this study is not repeatable in a future model with different data. What is, instead, interesting is that the models **EC8** and **Ref** have very similar site-to-site variability: it means that the model with the EC8 classification, mainly based on geological proxies, has the same variability of another model without any classification (with the exception of the reference rock sites). As a matter of fact, most of the stations of this dataset are classified in EC8-B class on the basis of surface geology (Figure xx). However, the assignment of the site classes of the EC8 on the basis of geologic proxies is too rough, especially if inferred from large scale maps (e.g. 1:50.000). Recent studies (Felicetta et al. 2018; Forte et al. 2019) showed that, on the basis of in-situ surveys carried out within the same geological unit, V_s profiles may belong to more than one EC8 subsoil. As a result, the total sigma σ reflects same differences found in ϕ_{S2S} .


5. Conclusions

The main objective of this report is to define a robust strategy to identify seismic stations that can be considered as reference rock sites. This work is an update of the proposal of Felicetta et al. (2018).

To tackle this issue, in this study we propose seven proxies: four proxies are based on geophysical and seismological data ($\delta S2S_{EC8-A}$ of horizontal ground motion component, $V_{s,30}$, HVRS, HVNSR), whereas the remaining ones on geological and geomorphological features (outcropping rocks or stiff soils, flat topography and absence of interaction with structures). The proposed proxies are designed to be applied for qualified recording database (such as ESM flatfile, Lanzano et al., 2019) from which site information can be easily retrieved and seismological analysis performed.

First, we preselect the candidates reference sites on the base of the outcomes of the residual analysis carried out on the horizontal components of the ground motion. To reach this goal, we exploit a very large training dataset, composed by accelerometric and velocimetric waveforms, recorded in central Italy since 2008. This dataset includes more than 450 recording sites and more than 450 earthquakes in the magnitude range 3.2-6.5.

We estimate the site-to-site term, $\delta S2S_{EC8-A}$, with respect to the EC8-A class of the ITA10 model, assuming that this parameter gives a raw estimate of empirical amplification function of the station. Then,

	<p style="text-align: center;">Research and Development Program on Seismic Ground Motion</p>	<p>Ref : SIGMA2-2019-D3-027/1</p>
		<p>Version : 1</p>

we perform a cluster analysis, that allows to recognize 133 stations as candidates for reference rocks sites. Further efforts will be devoted to test the sensitivity of $\delta S2S$ proxies using different GMMs, that could differ in the predictions of rock sites.

In the second step, we introduce a weighting scheme to take into account the availability and the quality of the site information, as well as the fulfillment of the criteria associated to each proxy. We also introduce a hierarchical index, with the aim of taking into account the relevance of the proposed proxies in the description of the site effects. In particular, we assume that the most important site-effects indicators are GEO, VS30 and HV from noise measurements. The fulfillment of the criteria related to these parameters can be considered sufficient to identify of potential reference sites, also in absence of recordings.

For each candidate, we evaluate the proxies and assign the proper scores in order to obtain a final ranking. A total of 41 are recognized as reference stations: the majority of them are installed on rock sites, with flat topography, but this condition is not sufficient to guarantee the absence of amplifications, especially at high frequencies. Seismological analyses are necessary to exclude stations affected by possible resonances. The impact of these sites on the calibration of GMM is significant, leading to a maximum reduction of 44% at short periods with respect to the generic rock predictions (EC8-A).

This proposal of a weighting scheme has been successfully applied to a specific region and should be tested on other datasets, also related to different seismotectonic environments such as the stable continental regions, to evaluate their effectiveness to rank the reference rock stations.

6. Reference

Al Atik L, Abrahamson N, Bommer JJ, Scherbaum F, Cotton F, Kuehn N (2010). The variability of ground-motion prediction models and its components. *Seismological Research Letters*, 81(5), 794-801.

Anderson, J. G., and S. E. Hough (1984). A model for the shape of the Fourier amplitude spectrum of acceleration at high frequencies, *Bull. Seism. Soc. Am.* 74, 1969–1993.

Arias A (1970) A measure of earthquake intensity. In: Hansen RJ (Ed.) *Seismic Design for Nuclear Power Plants*, M.I.T. Press, 438–483

Bard PY, S Singh Bora, F. Hollender, A. Laurendeau, P. Traversa (2018). ARE THE STANDARD VS 30 -KAPPA HOST-TO-TARGET ADJUSTMENTS THE BEST WAY TO GET CONSISTENT HARD- ROCK GROUND MOTION PREDICTION?. *Best Practices in Physics-based Fault Rupture Models for Seismic Hazard Assessment of Nuclear Installations: issues and challenges towards full Seismic Risk Analysis*, May 2018, Cadarache France.

Bonnefoy-Claudet S, Köhler A, Cornou C, Wathelet M, Bard PY (2008) Effects of love waves on microtremor H/V ratio. *Bull Seismol Soc Am* 98(1):288–300

Bindi D, Pacor F, Luzi L, Puglia R, Massa M, Ameri G, Paolucci R (2011). Ground motion prediction equations derived from the Italian strong motion database. *Bulletin of Earthquake Engineering*, 9(6), 1899-1920. <http://dx.doi.org/10.1007/s10518-011-9313-z>

	Research and Development Program on Seismic Ground Motion	Ref : SIGMA2-2019-D3-027/1 Version : 1
---	--	---

Bindi D, Pacor F, Luzi L, Massa M, Ameri G. The Mw 6.3, 2009 L'Aquila earthquake: source, path and site effects from spectral analysis of strong motion data. *Geophys J Int* 2009;179(3):1573–9. <http://dx.doi.org/10.1111/j.1365-246X.2009.04392.x>.

Bindi, D., Picozzi, M., Spallarossa, D., Cotton, F., & Kotha, S. R. (2019). Impact of Magnitude Selection on Aleatory Variability Associated with Ground-Motion Prediction Equations: Part II—Analysis of the Between-Event Distribution in Central Italy. *Bulletin of the Seismological Society of America*, 109(1), 251-262.

Boncio P, Lavecchia G, Pace B (2004) Defining a model of 3D seismogenic sources for Seismic Hazard Assessment applications: the case of Central Apennines (Italy). *Journal of Seismology* 8(3):407-425

Borcherdt, R. D., and Glassmoyer, G. (1992). On the characteristics of local geology and their influence on ground motions generated by the Loma Prieta earthquake in the San Francisco Bay region, California, *Bull. Seismol. Soc. Am.*, 82, 603-641.

Borcherdt, R.D. (1994). Estimates of site-dependent response spectra for design (methodology and justification). *Earthquake Spectra* 10,617–654.

Bordoni P., F. Pacor, G. Cultrera, M. Massa, P. Casale, F. Cara, G. Di Giulio, D. Famiani, C. Ladina, M. Pischiutta, M. Quintiliani, G. Milana, A. Mercuri, C. Marcocci, V. Pessina, E. D'Alema, S. Lovati, C. Mascandola, M. D'Amico, C. Felicetta, L. Luzi, R. Puglia, A. Fodarella, S. Pucillo, R. Cogliano, G. Riccio, L. Zarrilli, L. Scarfi, R. Azzaro, S. Branca, S. Di Prima, G. Tusa, L. Zuccarello, M. Paratore, A. Scaltrito, D. Di Naccio, S. Amoroso, G. Di Giulio, L. Cantore, M. Vassallo, M. Cattaneo, M. Amanti, G. Conte, C. Cipolloni, G.M. Monti, B. Roberto, C. D'Ambrogio, M. D'Orefice, P. Di Manna, D. Fiorenza, R.M. Gafà, M. Roma, L. Vita. (2017) Le attività per la caratterizzazione dei siti della rete sismica nazionale dell'INGV. 36° Convegno GNGTS, Trieste 14 – 16 November 2017. (in Italian)

BSSC (2003). NEHRP Recommended Provisions for Seismic Regulations for New Buildings and Other Structures (Fema 450).

Boore D.M., Stewart J.P., Seyhan E., and Atkinson G.M (2014). NGA-West 2 equations for predicting PGA, PGV, and 5%-damped PSA for shallow crustal earthquakes. *Earthquake Spectra*, 30(3):1057–1085, Aug 2014. doi: 10.1193/070113EQS184M.

Burjanek J, Edwards B, Fah D. Empirical evidence of local seismic effects at sites with pronounced topography: a systematic approach. *Geophys J Int* 2014;197(1):608–19. <http://dx.doi.org/10.1093/gji/ggu014>.

Cacciuni A., Centamore E., Di Stefano R., Dramis F. (1995): Evoluzione morfotettonica della conca di Amatrice. *Studi Geol. Cam.*, vol. spec. 1995/2, 95-100 (in italian)

Castellaro S, Mulargia F, Rossi P.L (2008). Vs30: Proxy for Seismic Amplification? *Seismological Research Letters* 79 (4): 540–543. doi: <https://doi.org/10.1785/gssrl.79.4.540>.

Chiaraluce L, Di Stefano R, Tinti E, Scognamiglio L, Michele M, Casarotti E, Cattaneo M, De Gori P, Chiarabba C., Monachesi G, Lombardi A, Valoroso L, Latorre D, Marzorati S (2017) The 2016 Central Italy Seismic Sequence: A First Look at the Mainshocks, Aftershocks, and Source Models. *Seismological Research Letters* 88(3):757–771. doi:<https://doi.org/10.1785/0220160221>

Cara F., Cultrera G., Riccio G., Bordoni P., Bucci A., Famiani D., Mercuri A., Milana G., Pischiutta M., Amoroso S., Cantore L., Di Giulio G., Di Naccio D., Vassallo M., Cogliano R., Fodarella A., Pucillo S., D'Alema E., D'Amico M., Carannante S., Felicetta C., Franceschina G., Lanzano G., Lovati S., Luzi L., Mascandola C., Massa M., Pacor F., Piccarreda D., Puglia R., Boniolo G., Caielli G., Corsi A., De Franco R., Tento A., Bongiovanni G., Hailemichael S., Martini G., Paciello A., Peloso A., Poggi F., Verrubbi V., Gallipoli M.R., Stabile T.A., Mancini. M. (submitted). Temporary dense seismic network during the 2016 Central Italy seismic emergency for microzonation studies. *Scientific Data*

CEN (Comité Europé en de Normalisation) Eurocode 8: design of structures for earthquake resistance-Part 1: general rules, seismic actions and rules for buildings, Comité Européen de Normalisation Brussels 2004; May; <http://www.cen.eu/cenorm/homepage.htm> .

C. FELICETTA/ G. LANZANO/ F. PACOR- Methodology to identify reference rock sites- SIGMA2-2019-D3-027/1

	Research and Development Program on Seismic Ground Motion	Ref : SIGMA2-2019-D3-027/1 Version : 1
---	--	---

CS.LL.PP - DM 14 Gennaio 2008. Norme Tecniche per le Costruzioni 29. Gazzetta Ufficiale della Repubblica Italiana; 2008. (in Italian).

David A., Vassilvitskii S. (2007). K-means++: The Advantages of Careful Seeding. SODA '07: Proceedings of the Eighteenth Annual ACM-SIAM Symposium on Discrete Algorithms, pp. 1027–1035.

Di Bona M (2016) A local magnitude scale for crustal earthquakes in Italy. Bull Seism Soc Am 106:242–258.

Ditommaso R., Mucciarelli M., Gallipoli M.R., Ponzo F.C. (2010) Effect of a single vibrating building on free-field ground motion: numerical and experimental evidences. Bull Earthquake Eng 8:693–703 DOI 10.1007/s10518-009-9134-5

EmerTer Project (2017/2018): Report relativo all'Accordo ai sensi dell'art. 15 Legge 7 agosto 1990 n. 241, e dell'art.6 della Legge 24 febbraio 1992, n. 225 tra il Dipartimento della Protezione Civile e l'Istituto di Geologia Ambientale e Geoingegneria del Consiglio Nazionale delle Ricerche per il supporto alle attività della DICOMAC di Rieti e della Struttura di Missione (Prot. CNR IGAG n. 1484 del 17/05/2017), Prot. CNR IGAG n. 359 del 30/01/2018.

Felicetta C., Lanzano G., D'Amico M., Puglia R., Luzi L., Pacor F. (2018). Ground motion model for reference rock sites in Italy. Soil Dynamics and Earthquake Engineering, 110, 276-283, DOI: 10.1016/j.soildyn.2018.01.024.

Ferrari F, Lavecchia G, de Nardis R, Brozzetti F (2015) Fault geometry and active stress from earthquakes and field geology data analysis: the Colfiorito 1997 and L'Aquila 2009 Cases (Central Italy). Pure and Applied Geophysics 172(5):1079-1103, doi 10.1007/s00024-014-0931-7

Forte, G., Chioccarelli, E., De Falco, M., Cito, P., Santo, A., & Iervolino, I. (2019). Seismic soil classification of Italy based on surface geology and shear-wave velocity measurements. Soil Dynamics and Earthquake Engineering, 122, 79-93.

Gallipoli MR, Mucciarelli M, Castro RR, Monachesi G, Contri P. Structure, soil— structure response and effects of damage based on observations of horizontal-to-vertical spectral ratios of microtremors. Soil Dyn Earthq Eng 2004;24(6):487–95. <http://dx.doi.org/10.1016/j.soildyn.2003.11.009>.

Gorini A., Nicoletti M., Marsan P., Bianconi R., De Nardis R., Filippi L., Marcucci S., Palma F., Zambonelli E. (2010). The Italian strong motion network. Bull Earthquake Eng (2010) 8: 1075. <https://doi.org/10.1007/s10518-009-9141-6>

Herraiz M, Espinosa AF (1986) Coda waves: a review. Pure Appl Geophys 125(4):499–577. doi:10.1007/BF00879572

Konno K, Ohmachi T (1998) Ground-motion characteristics estimated from spectral ratio between horizontal and vertical components of microtremor. Bull Seismol Soc Am 88:228–241

Kotha, S. R., Cotton, F., & Bindi, D. (2018). A new approach to site classification: Mixed-effects Ground Motion Prediction Equation with spectral clustering of site amplification functions. Soil Dynamics and Earthquake Engineering, 110, 318-329.

Kotha, S. R., Bindi, D., & Cotton, F. (2016). Partially non-ergodic region specific GMPE for Europe and Middle-East. Bulletin of Earthquake Engineering, 14(4), 1245-1263.

Ktenidou, O. J., and Abrahamson, N. A. (2016). Empirical estimation of high-frequency ground motion on hard rock. Seismological Research Letters. 87(6):1465-1478, doi: 10.1785/0220160075

Ktenidou O.J., Abrahamson N.A., Drouet S., Cotton F. (2015) Understanding the physics of kappa (κ): insights from a downhole array, Geophysical Journal International, Volume 203, Issue 1, October, 2015, Pages 678–691, <https://doi.org/10.1093/gji/ggv315>

	Research and Development Program on Seismic Ground Motion	Ref : SIGMA2-2019-D3-027/1 Version : 1
---	--	---

Ktenidou O.J., Cotton F., Abrahamson N.A., Anderson J.G. (2014). Taxonomy of κ : A Review of Definitions and Estimation Approaches Targeted to Applications. *Seismological Research Letters* ; 85 (1): 135–146. doi: <https://doi.org/10.1785/0220130027>

Lanzano G., Luzi L., Pacor F., Felicetta C., Puglia R., Sgobba S., D'Amico M. (2019). A revised ground motion prediction model for shallow crustal earthquakes in Italy. *Bulletin of the Seismological Society of America* 109 (2): 525-540. <https://doi.org/10.1785/0120180210>

Lanzano G., Sgobba S., Luzi L., Puglia R., Pacor F., Felicetta C., D'Amico M., Cotton F., Bindi D. (2018). The pan-European Engineering Strong Motion (ESM) flatfile: compilation criteria and data statistics. *Bulletin of Earthquake Engineering*. <https://doi.org/10.1007/s10518-018-0480-z>

Lanzano G., D'Amico M., Felicetta C., Luzi L., Puglia R. (2017). Update of the single-station sigma analysis for the Italian strong-motion stations. *Bulletin of Earthquake Engineering* 15 (6), 2411-2428, DOI: 10.1007/s10518-016-9972-x.

Lermo J, Chávez-García FJ (1993) Site effect evaluation using spectral ratios with only one station. *Bull Seismol Soc Am* 83:1574–1594

Luzi, L., Bindi, D., Puglia, R., Pacor, F., & Oth, A. (2014). Single-station sigma for Italian strong-motion stations. *Bulletin of the Seismological Society of America*, 104(1), 467-483.

Luzi L., Pacor F., Puglia R., Lanzano G., Felicetta C., D'Amico M., Michelini A., Faenza L., Lauciani V., Iervolino I., Baltzopoulos G., Chioccarelli E. (2017). The Central Italy seismic sequence between August and December 2016: analysis of strong-motion observations. *Seismological Research Letters*, 88 (5), 1219-1231, DOI: 10.1785/0220170037

Luzi L, Pacor F, Puglia R (2019). Italian Accelerometric Archive v3.0. Istituto Nazionale di Geofisica e Vulcanologia, Dipartimento della Protezione Civile Nazionale. doi: 10.13127/itaca.3.0.

Luzi L., Pacor F., Lanzano G., Felicetta C., Puglia R., D'Amico M. (submitted). 2016-2017 Central Italy seismic sequence: strong-motion data, seismic hazard and design earthquakes for the seismic microzonation. *Bulletin of Earthquake Engineering*.

Marzorati S, Ladina C, Falcucci E, Gori S, Saroli M, Ameri G, Galadini F. Site effects “on the rock”: the case of Castelvechio Subequo (L’Aquila, central Italy). *Bull Earthq Eng* 2011;9:841–68. <http://dx.doi.org/10.1007/s10518-011-9263-5>.

Massa M, Barani S, Lovati S. Overview of topographic effects based on experimental observations: meaning, causes and possible interpretations. *Geophys J Int* 2014;197(3):1537–50. <http://dx.doi.org/10.1093/gji/ggt341>.

Nakamura Y (1989) A method for dynamic characteristics estimation of subsurface using microtremor on the ground surface. *QR Railw Tech Res Inst* 30:25–33

Pacor F, Paolucci R, Luzi L, Sabetta F, Spinelli A, Gorini A, Nicoletti M, Marcucci S, Filippi L, Dolce M. Overview of the Italian strong motion database ITACA 1.0. *Bull. Earthq Eng* 2011;9(6):1723–39. <http://dx.doi.org/10.1007/s10518-011-9327-6>.

F. Pacor F., Spallarossa D., Oth A., Luzi L., Puglia R., Cantore L., Mercuri A., D'Amico M., Bindi D. (2016). Spectral models for ground motion prediction in the L’Aquila region (Central Italy): Evidence for stress-drop dependence on magnitude and depth, *Geophys J Int* 204:697–718. <https://doi.org/10.1093/gji/ggv448>

	Research and Development Program on Seismic Ground Motion	Ref : SIGMA2-2019-D3-027/1 Version : 1
---	--	---

Pacor F., Felicetta C., Spallarossa D., Lanzano G., Luzi L., Milana G., Cultrera G., Di Giulio G., Cara F., Famiani D., Moscatelli M., Gaudiosi I., De Franco R., Gallipoli M.R., Pergalani F., Hailemichael S. & MZS Working Group. Amplification functions in the epicentral area of the 2016, Mw 6.0, Amatrice earthquake (Central Italy) using ground-motion records and geological-geophysical data. 7th International Conference on Earthquake Geotechnical Engineering, 17 – 20 June 2019

Paolucci R, Pacor F, Puglia R, Ameri G, Cauzzi C, Massa M (2011) Record processing in ITACA, the new Italian strong-motion database. In Akkar et al. (eds.), *Earthquake Data in Engineering Seismology*, chapter 8, geotechnical, geological and earthquake engineering series, vol 14, Springer

Paolucci R. Amplification of earthquake ground motion by steep topographic irregularities. *Earthq Eng Struct Dyn* 2002;31:1831–53.

Pischiutta M, Rovelli A, Vannoli P, Calderoni G. Recurrence of horizontal amplification at rock sites: a test using H/V based ground motion prediction equations. in: *Proceedings of the 4th IASPEI/IAEE International Symposium*, Santa Barbara (CA), August 23- 26; 2011.

Pondrelli S, Salimbeni S, Perfetti P (2016) Moment tensor solutions for the Amatrice 2016 seismic sequence. *Annals of Geophysics* 59. doi:http://dx.doi.org/10.4401/ag-7240

Porreca M, Minelli G, Ercoli M, Brobia A, Mancinelli P, Cruciani F, et al (2018) Seismic reflection profiles and subsurface geology of the area interested by the 2016–2017 earthquake sequence (Central Italy). *Tectonics* 37:1116–1137. <https://doi.org/10.1002/2017TC004915>

Priolo E., Pacor F., Spallarossa D., Milana G., Laurenzano G., Romano M.A., Felicetta C., Hailemichael S., Cara F., Di Giulio G., Ferretti G., Barnaba C., Lanzano G., Luzi L., D'Amico M., Puglia R., Scafidi D., Barani S., De Ferrari R., Cultrera G. (2019). Seismological analyses for the seismic microzonation of the 138 municipalities damaged by the 2016-2017 seismic sequence in Central Italy. *Bulletin of Earthquake Engineering*. <https://doi.org/10.1007/s10518-019-00652-x>

Puglia, R., Russo, E., Luzi, L., D'Amico, M., Felicetta, C., Pacor, F., & Lanzano, G. (2018). Strong-motion processing service: a tool to access and analyse earthquakes strong-motion waveforms. *Bulletin of Earthquake Engineering*, 16(7), 2641-2651.

Puglia R., Albarello D., Luzi L., Bindi D., Gallipoli M.R., Mucciarelli M., Naso G., Pacor F., Peronace E. (2015) On the Performances of Site Parameters for Soil Classification. In: Lollino G., Manconi A., Guzzetti F., Culshaw M., Bobrowsky P., Luino F. (eds) *Engineering Geology for Society and Territory - Volume 5*. Springer, Cham. DOI https://doi.org/10.1007/978-3-319-09048-1_219


Puglia R., Albarello D., Gorini A., Luzi L., Marcucci S., Pacor F. (2011a) Extensive characterization of Italian accelerometric stations from single-station ambient-vibration measurements. *Bull Earthquake Eng* (2011) 9:1821–1838 DOI 10.1007/s10518-011-9305-z

Rovelli A, Caserta A, Marra F, Ruggiero V. Can seismic waves be trapped inside an inactive fault zone? The case study of Nocera Umbra, Central Italy. *Bull Seismol Soc Am* 2002;92(6):2217–32.

Site Effects Assessment using Ambient Excitations (SESAME) European project (2005) Deliverable D23.12—Guidelines for the implementation of the H/V spectral ratio technique on ambient vibrations: measurements, processing and interpretation. <http://www.sesame-fp5.obs.ujf-grenoble.fr>. Accessed March 2010

Spallarossa D, Ferretti G, Scafidi D, Torino C, Pasta M (2014) Performance of the RSNI-Picker, *Seismol Research Letters* 85(6):1243-1254. doi: 10.1785/0220130136

C. FELICETTA/ G. LANZANO/ F. PACOR- Methodology to identify reference rock sites- SIGMA2-2019-D3-027/1

	<p style="text-align: center;">Research and Development Program on Seismic Ground Motion</p>	<p>Ref : SIGMA2-2019-D3-027/1</p>
		<p>Version : 1</p>

Stewart P, Fenves L, Seed B. Seismic soil-structure interaction in buildings. I: analytical methods. *J Geotech Geoenviron Eng* 1999;125(1):26–37. [http://dx.doi.org/10.1061/\(ASCE\)1090-0241\(1999\)125:1\(26\)](http://dx.doi.org/10.1061/(ASCE)1090-0241(1999)125:1(26)).


Stewart, J. P. (2000). Variations between foundation-level and free-field earthquake ground motions. *Earthquake Spectra* 16(2): 511-532.

Steidl HJ, Tumarkin AG, Archuleta RJ. What is a reference site? *Bull Seismol Soc Am* 1996;86(6):1733–48.

Stehly L., Campillo M., Shapiro N.M. (2006) A study of the seismic noise from its long-range correlation properties. *Journal of geophysical research*. vol. 111, B10306, doi:10.1029/2005JB004237, 2006

Tibshirani, R., Walther, G., & Hastie, T. (2001). Estimating the number of clusters in a data set via the gap statistic. *Journal of the Royal Statistical Society: Series B (Statistical Methodology)*, 63(2), 411-423.

Zhao John X, Irikura Kojiro, Zhang Jian, Fukushima Yoshimitsu, Somerville Paul G, Asano Akihiro, Ohno Yuki, Oouchi Taishi, Takahashi Toshimasa, Ogawa Hiroshi. An empirical site-classification method for strong-motion stations in Japan using h/v response spectral ratio. *Bull Seismol Soc Am* 2006;96(3):914–25. <http://dx.doi.org/10.1785/0120050124>.

	<p style="text-align: center;">Research and Development Program on Seismic Ground Motion</p>	<p>Ref : SIGMA2-2019-D3-027/1</p>
		<p>Version : 1</p>

APPENDIX I

Summary of the procedures used to compute H/V spectral ratio and high-frequency attenuation parameter kappa

HVNSR computation

To compute the H/V from noise (HVNSR) and estimate the fundamental frequencies, all the measurements were analyzed with the procedure proposed by Puglia et al. (2011), in order to obtain comparable results.

The procedure involves the application of a 1st order baseline correction and a 4th order acausal Butterworth band-pass filtering to each components. Each record is then subdivided in windows and the minimum expected f_0 is defined following the criteria recommended in the project SESAME (2005) and considering the lower frequency recordable by the instrument used to the measure. 1st order baseline correction and a 5% cosine taper was applied to each window and the Fourier spectra are calculated and smoothed through the Konno and Ohmachi (1998). The mean HVNSR curve is obtained averaging the single HVNSR curves within each time window, calculated as the ratio between the horizontal components (vector sum) and the vertical one.

HVSR-C and HVSR-S computation

H/V of earthquake records on coda (HVSR-C) and S-waves (HVSR-S) are computed considering strong-motion waveforms with magnitude larger than 3.0


The waveforms are manually processed using the web-tool implemented by Puglia et al. (2018) based on the procedure proposed by Paolucci et al. (2011), which includes the baseline correction and band-pass filtering with a 2nd order a-causal time-domain Butterworth filter.

The analysis consists in the extraction from the waveform of the S-wave phase and the signal coda. The preliminary S-time window is set in the range t_{S1} - t_{S2} , both evaluated on the base of the Arias intensity function (Eq. 1; Arias 1970) computed from the time-of-the-first-sample of the waveform (t_0):

$$I(t) = \frac{\pi}{2g} \int_{t_0}^t a^2(\tau) d\tau$$

where $a(t)$ is the acceleration at time t and g is the gravity acceleration.

t_{S1} and t_{S2} times are selected corresponding to the values I_1 and I_2 of the Arias intensity, normalized with respect to its maximum value, as reported in Table 1.

	Research and Development Program on Seismic Ground Motion	Ref : SIGMA2-2019-D3-027/1 Version : 1
---	--	---

The minimum length of the interval [tS1, tS2] is fixed to 5 s in order to have a resolution of the discrete Fourier transform above 0.2 Hz. However, tS1 and tS2 times can be manually modified after a visually inspection of waveforms; for instance, when the S-window includes surface waves, tS2 is manually reduced, in order to exclude this part of the signal. The coda window, instead, starts from twice after the S-wave travel time after the earthquake origin time (Herraiz and Espinosa 1986) and ends after 10 s.

Table 1. Range of epicentral distance and percentages of Aria Intensity used to compute the S time window.

Repi [km]	I1 [%]	I2 [%]
Repi < 25	5	95
25 <= Repi < 50	10	90
Repi >= 50	15	85

The S and coda windows were tapered along 5% of the window length using a cosine function and azimuthally projected on a ten-degree interval from 0 to 180. The horizontal and vertical Fourier spectra were smoothed through the Konno and Ohmachi (1998) algorithm (with $b = 40$). The H/V curve is calculated as the ratio between the vector sum of Fourier spectra of horizontal components and the spectrum of the vertical component.

KAPPA estimate

In cooperation with the University of Genoa, we implement the following procedure to estimate k : i) composition (vectorial sum) of the horizontal components of the S-waves Fourier spectra (described in Section 1); ii) evaluation of the signal to noise ratio (SNR) for each frequency in the range [0.5-40 Hz] and rejection of data with $SNR > 3$ for more than 65% of the spectral ordinates; iii) pre-computation of linear fit in lin-log scale for 10 frequency bands variable in the range 8-40 Hz; iv) computation of theoretical corner frequency using the Brune model v) visual selection of the best fitting on the spectral ordinates plotted both on lin-log scale and log-log scale (Figure 1).



Figure 1. Example of application of the tool adopted to estimate the k parameter: the horizontal Fourier spectra of a M 2.7 earthquake at IV.ATPI station is plotted in lin-log (left) and log-log (right) scale. The diamond pink is the theoretical corner frequency; the green line is the fitted model visually selected; the k values estimated in the other frequency band is also reported.

	Research and Development Program on Seismic Ground Motion	Ref : SIGMA2-2019-D3-027/1
		Version : 1

APPENDIX II

List of the candidate stations belonging to cluster #1 and the corresponding ranking

NET CODE	STA CODE	HOU	W_H	HVtype	HV	W_HV	HVRS	W_HVR	TOP	W_T	VS,30	W_Vs	GEO scale	EC8	W_GEO	W_CL#1	AV.PROXIES	SUM_W
IT	BGR	FF	0.5	HVNSR	F	2	F	1	slope ≤ 15°	0.5	A	1.5	5000	A	2	1	7	8.5
IT	MVB	FF	0.5	HVNSR	F	2	F	1	slope ≤ 15°	0.5	A	1.5	5000	A	2	0.75	7	8.25
IT	LSS	FF	0.5	HVNSR	F	2	F	1	slope > 15°	0.25	A	1.5	10000	A	2	1	6	8.25
IT	GRN	CAB	0.375	HVNSR	F	2	F	1	slope > 15°	0.25		1	5000	A	2	1	4	7.625
IV	SACS	FF	0.5	HVNSR	F	2	F	1	slope ≤ 15°	0.5		1	100000	A	1.5	1	6	7.5
3A	MZ102	FF	0.5	HVNSR	F	2	BB	0.5	slope ≤ 15°	0.5		1	5000	A	2	1	6	7.5
IV	POFI	FF	0.5	HVNSR	F	2	F	1	slope ≤ 15°	0.5		1	100000	A	1.5	0.75	6	7.25
IV	CAFI	FF	0.5	HVNSR	F	2	F	1	slope > 15°	0.25		1	100000	A	1.5	1	5	7.25
IV	FIAM	FF	0.5	HVNSR	F	2	F	1	slope > 15°	0.25		1	100000	A	1.5	1	5	7.25
IV	SACR		0.25	HVNSR	F	2	F	1	slope ≤ 15°	0.5		1	100000	A	1.5	1	5	7.25
IV	SGTA		0.25	HVNSR	F	2	F	1	slope ≤ 15°	0.5		1	100000	A	1.5	1	5	7.25
3A	MZ31	FF	0.5	HVNSR	F	2	F	1	slope ≤ 15°	0.5		1	5000	B	1	1	6	7
IT	CSO1	FF	0.5	HVNSR	F	2	F	1	slope > 15°	0.25		1	25000	A	1.5	0.75	5	7
IV	ATLO	FF	0.5	HVNSR	F	2		0.5	slope ≤ 15°	0.5		1	100000	A	1.5	1	5	7
IV	TRIV		0.25	HVNSR	F	2	F	1	slope ≤ 15°	0.5		1	100000	A	1.5	0.75	5	7
IT	FMG	NO-FF	0	HVNSR	F	2	F	1	slope > 15°	0.25	B	1.5	5000	B	1	1	5	6.75
IT	PAN	FF	0.5	HVSR-S	F	1	F	1	slope ≤ 15°	0.5		1	20000	A	1.5	1	6	6.5

C. FELICETTA/ G. LANZANO/ F. PACOR- Methodology to identify reference rock sites- SIGMA2-2019-D3-027/1

  	Research and Development Program on Seismic Ground Motion	Ref : SIGMA2-2019-D3-027/1
  		Version : 1

IT	SLO	FF	0.5	HVSR-C	BB	1	BB	0.5	slope $\leq 15^\circ$	0.5	1	10000	A	2	1	6	6.5
IV	ATVO	FF	0.5	HVNSR	F	2	BB	0.5	relief	0	1	100000	A	1.5	1	5	6.5
IT	MNF	HOU	0	HVNSR	F	2	F	1	slope $> 15^\circ$	0.25	1	50000	A	1.5	0.75	4	6.5
IV	RM03		0.25	HVSR-C	F	2	BB	0.5	slope $\leq 15^\circ$	0.5	1	100000	A	1.5	0.75	5	6.5
IT	PSC	FF	0.5	HVNSR	P	0	F	1	slope $> 15^\circ$	0.25	A	5000	A	2	1	5	6.25
IV	ATPI	FF	0.5	HVSR-S	F	1		0.5	slope $\leq 15^\circ$	0.5	1	100000	A	1.5	1	5	6
IV	GUAR	FF	0.5	HVSR-S	F	1		0.5	slope $\leq 15^\circ$	0.5	1	100000	A	1.5	1	5	6
IV	T1215		0.25	HVSR-S	F	1	F	1	slope $\leq 15^\circ$	0.5	1	100000	A	1.5	0.75	5	6
IV	CIGN	FF	0.5	HVSR-S	F	1		0.5	slope $\leq 15^\circ$	0.5	1	100000	A	1.5	0.75	5	5.75
IV	MNS		0.25	HVSR-C	BB	1	BB	0.5	slope $\leq 15^\circ$	0.5	1	100000	A	1.5	1	5	5.75
IV	ATVA		0.25	HVSR-S	F	1		0.5	slope $\leq 15^\circ$	0.5	1	100000	A	1.5	1	4	5.75
3A	MZ11	FF	0.5	HVNSR	P	0	BB	0.5	slope $\leq 15^\circ$	0.5	1	5000	A	2	0.75	5	5.25
XO	MN06		0.25	HVSR-S	F	1	F	1	slope $\leq 15^\circ$	0.5	1	100000	B	0.5	1	5	5.25
IV	T1299		0.25	HVSR-S	F	1	F	1	slope $\leq 15^\circ$	0.5	1	100000	B	0.5	1	5	5.25
IV	T1221		0.25	HVSR-S	F	1	F	1	slope $\leq 15^\circ$	0.5	1	100000	B	0.5	1	5	5.25
IV	PTQR	NO-FF	0	HVSR-S	F	1		0.5	slope $\leq 15^\circ$	0.5	1	100000	A	1.5	0.75	4	5.25
IT	BZZ	HOU	0.5	HVNSR	F	2	F	1	slope $\leq 15^\circ$	0.5	B	100000	C	0	1	5	5
IV	PIO1	NO-FF	0	HVNSR	P	0	F	1	slope $\leq 15^\circ$	0.5	1	100000	A	1.5	1	4	5
IV	GIUL	FF	0.5	HVSR-S	MP	0		0.5	slope $\leq 15^\circ$	0.5	1	100000	A	1.5	1	4	5
IV	PARC	FF	0.5	HVSR-S	P	0		0.5	slope $\leq 15^\circ$	0.5	1	100000	A	1.5	1	4	5
IV	TOLF	FF	0.5	HVSR-S	P	0		0.5	slope $\leq 15^\circ$	0.5	1	100000	A	1.5	1	4	5
IV	VVLD	FF	0.5	HVSR-S	MP	0		0.5	slope $\leq 15^\circ$	0.5	1	100000	A	1.5	1	4	5
IV	RM02		0.25	HVSR-S	F	1	F	1	slope $\leq 15^\circ$	0.5	1	100000	B	0.5	0.75	5	5
IV	GIGS	NO-FF	0	HVSR-S	F	1		0.5	slope $> 15^\circ$	0.25	1	100000	A	1.5	0.75	3	5

C. FELICETTA/ G. LANZANO/ F. PACOR- Methodology to identify reference rock sites- SIGMA2-2019-D3-027/1

	Research and Development Program on Seismic Ground Motion	Ref : SIGMA2-2019-D3-027/1
		Version : 1

IT	ANT	NO-FF	0	HVNSR	P	0	P	0	slope ≤ 15°	0.5	A	1.5	5000	A	2	0.75	4	4.75
IV	MIDA	FF	0.5	HVNSR	P	0	BB	0.5	slope > 15°	0.25	1	100000	A	1.5	1	4	4.75	
XO	CP06		0.25	HVSR-S	F	1	F	1	slope ≤ 15°	0.5	1	100000	C	0	1	4	4.75	
IV	T0105		0.25	HVSR-S	BB	0.5	F	1	slope ≤ 15°	0.5	1	100000	B	0.5	1	5	4.75	
IV	CESX	FF	0.5	HVNSR	P	0		0.5	slope > 15°	0.25	1	100000	A	1.5	1	3	4.75	
IV	CRE	FF	0.5	HVSR-S	P	0		0.5	slope > 15°	0.25	1	100000	A	1.5	1	3	4.75	
IV	LRP		0.25	HVSR-S	P	0		0.5	slope ≤ 15°	0.5	1	100000	A	1.5	1	3	4.75	
IT	STF	FF	0	HVNSR	P	0	F	1	slope ≤ 15°	0.5	B	0	5000	A	2	1	4	4.5
IT	SGSC	HOU	0.5	HVSR-S	P	0	F	1	slope ≤ 15°	0.5	1	100000	B	0.5	1	5	4.5	
IT	TRN1	NO-FF	0	HVSR-S	F	1	F	1	slope ≤ 15°	0.5	1	100000	D	0	1	4	4.5	
IV	ATTE	NO-FF	0	HVNSR	P	0	BB	0.5	slope ≤ 15°	0.5	1	100000	A	1.5	1	4	4.5	
IT	GLT	NO-FF	0	HVSR-S	F	1	F	1	slope ≤ 15°	0.5	1	100000	C	0	1	4	4.5	
IV	MTCE	NO-FF	0	HVSR-S	P	0		0.5	slope ≤ 15°	0.5	1	100000	A	1.5	1	3	4.5	
IT	PLS	CAB	0.375	HVNSR	P	0	F	1	slope ≤ 15°	0.5	1	50000	B	0.5	1	4	4.375	
IV	SRES	FF	0.5	HVSR-S	F	1		0.5	slope > 15°	0.25	1	100000	C	0	1	3	4.25	
IV	CAMP	NO-FF	0	HVNSR	P	0		0.5	slope > 15°	0.25	1	100000	A	1.5	1	2	4.25	
IV	SGG	NO-FF	0	HVNSR	P	0		0.5	slope > 15°	0.25	1	100000	A	1.5	1	2	4.25	
IT	SSO	FF	0.5	HVSR-S	P	0	BB	0.5	slope ≤ 15°	0.5	1	100000	B	0.5	1	5	4	
IV	RM22		0.25	HVSR-S	P	0	F	1	slope ≤ 15°	0.5	1	100000	B	0.5	0.75	4	4	
IV	ATFO	FF	0.5	HVNSR	P	0	F	1	relief	0	1	100000	B	0.5	0.75	4	3.75	
IT	SNM	NO-FF	0	HVNSR	P	0	F	1	slope ≤ 15°	0.5	1	100000	B	0.5	0.75	4	3.75	
XO	MN04		0.25	HVSR-S	MP	0	BB	0.5	slope ≤ 15°	0.5	1	100000	B	0.5	1	4	3.75	
XO	MN08		0.25	HVSR-S	P	0	BB	0.5	slope ≤ 15°	0.5	1	100000	B	0.5	1	4	3.75	
IV	PSB1		0.25	HVNSR	P	0	BB	0.5	slope ≤ 15°	0.5	1	100000	B	0.5	1	4	3.75	

C. FELICETTA/ G. LANZANO/ F. PACOR- Methodology to identify reference rock sites- SIGMA2-2019-D3-027/1

	Research and Development Program on Seismic Ground Motion	Ref : SIGMA2-2019-D3-027/1
		Version : 1

TV	SF14	0.25	HVSR-S	P	0	0.5	slope ≤ 15°	0.5	1	100000	B	0.5	1	3	3.75		
MN	AQU	NO-FF	0	HVNSR	MP	0	BB	0.5	slope ≤ 15°	0.5	1	100000	B	0.5	1	4	3.5
IV	RM11	0.25	HVSR-S	P	0	BB	0.5	slope ≤ 15°	0.5	1	100000	B	0.5	0.75	4	3.5	
IV	ARRO	0.25	HVSR-S	P	0	0.5	slope ≤ 15°	0.5	1	100000	B	0.5	0.75	3	3.5		
IV	RM09	0.25	HVSR-S	P	0	P	0	slope ≤ 15°	0.5	1	100000	B	0.5	1	3	3.25	
IV	T1222	0.25	HVSR-S	P	0	P	0	slope ≤ 15°	0.5	1	100000	B	0.5	1	3	3.25	

List of the candidate stations belonging to cluster #6 and the corresponding ranking

NET CODE	STA CODE	HOU	W_H	HVtype	HV	W_HV	HV RS	W_HVR	TOP	W_T	VS,30	W_Vs	GEO scale	EC8	W_GEO	W_CL#1	AV.PROXIES	SUM_W
IT	SNO	FF	0.5	HVNSR	F	2	F	1	slope ≤ 15°	0.5	1	10000	A	2	0.75	7	7.75	
IV	APEC	NO-FF	0	HVNSR	F	2	F	1	slope ≤ 15°	0.5	1	100000	A	1.5	0.75	6	6.75	
IV	SNAL	0.25	HVNSR	F	2	F	1	slope > 15°	0.25	1	100000	A	1.5	0.75	5	6.75		
IV	CAFR	FF	0.5	HVNSR	F	2	0.5	slope ≤ 15°	0.5	1	100000	A	1.5	0.5	6	6.5		
IT	ORC	NO-FF	0	HVSR-C	BB	1	BB	0.5	slope ≤ 15°	0.5	767	1.5	5000	A	2	0.75	7	6.25
IT	SDM	CAB	0.375	HVNSR	F	2	F	1	slope ≤ 15°	0.5	752	1.5	5000	C	0	0.75	6	6.125
3A	MZ25	0.25	HVNSR	F	2	0.5	slope ≤ 15°	0.5	1	5000	B	1	0.75	5	6			
IT	MMP1	FF	0.5	HVNSR	P	0	BB	0.5	slope ≤ 15°	0.5	800	1.5	5000	A	2	0.75	7	5.75
IT	CSC	NO-FF	0	HVNSR	F	2	F	1	relief	0	698	0	10000	A	2	0.75	5	5.75
IT	NRN	CAB	0.375	HVNSR	BB	1	BB	0.5	slope ≤ 15°	0.5	1	50000	A	1.5	0.75	6	5.625	
3A	MZ05	0.25	HVNSR	P	0	F	1	slope ≤ 15°	0.5	1	5000	A	2	0.75	5	5.5		
IV	CSP1	0.25	HVSR-S	F	1	0.5	slope ≤ 15°	0.5	1	100000	A	1.5	0.75	5	5.5			
IV	RM01	0.25	HVSR-C	BB	1	BB	0.5	slope ≤ 15°	0.5	1	A	1.5	0.75	6	5.5			

C. FELICETTA/ G. LANZANO/ F. PACOR- Methodology to identify reference rock sites- SIGMA2-2019-D3-027/1

	Research and Development Program on Seismic Ground Motion	Ref : SIGMA2-2019-D3-027/1
		Version : 1

IT	MSC	FF	0.5	HVNSR	F	2	BB	0.5	slope ≤ 15°	0.5	652	0	5000	B	1	0.75	7	5.25
IV	FDMO	FF	0.5	HVSR-S	F	1		0.5	slope > 15°	0.25		1	100000	A	1.5	0.5	5	5.25
IV	FOSV	NO-FF	0	HVSR-S	F	1	F	1	slope > 15°	0.25		1	100000	A	1.5	0.5	5	5.25
IT	SPD	NO-FF	0	HVNSR	F	2	F	1	slope > 15°	0.25		1	25000	B	0.5	0.5	5	5.25
IV	T0106		0.25	HVSR-C	BB	1	BB	0.5		0.25		1		A	1.5	0.75	5	5.25
IV	T1217		0.25	HVSR-S	F	1	F	1	slope ≤ 15°	0.5		1		B	0.5	0.75	6	5
IV	T1241		0.25	HVSR-S	F	1	F	1	slope ≤ 15°	0.5		1		B	0.5	0.75	6	5
IT	MTR	NO-FF	0	HVNSR	MP	0	BB	0.5	slope ≤ 15°	0.5	1024	1.5	5000	A	2	0.5	6	5
IV	VAGA		0.25	HVSR-C	BB	1	BB	0.5	slope > 15°	0.25		1	100000	A	1.5	0.5	5	5
IV	CERT	FF	0.5	HVSR-S	P	0		0.5	slope ≤ 15°	0.5		1	100000	A	1.5	0.75	5	4.75
IV	CERA		0.25	HVNSR	P	0	F	1	slope ≤ 15°	0.5		1	100000	A	1.5	0.5	5	4.75
3A	MZ29		0.25	HVNSR	BB	1	BB	0.5		0.25		1	5000	B	1	0.75	5	4.75
IV	SENI	FF	0.5	HVNSR	F	2	P	0	slope ≤ 15°	0.5	242	0	5000	B	1	0.5	6	4.5
IV	MA9	FF	0.5	HVSR-S	P	0		0.5	slope ≤ 15°	0.5		1	100000	A	1.5	0.5	5	4.5
IV	RM06		0.25	HVSR-S	BB	0.5	F	1	slope ≤ 15°	0.5		1		B	0.5	0.75	6	4.5
IV	RM08		0.25	HVSR-S	F	1	BB	0.5	slope ≤ 15°	0.5		1		B	0.5	0.75	6	4.5
IV	RM33	FF	0.5	HVSR-S	P	0	BB	0.5	slope > 15°	0.25		1	100000	A	1.5	0.75	5	4.5
IV	RNI2		0.25	HVNSR	P	0	BB	0.5	slope ≤ 15°	0.5		1	100000	A	1.5	0.75	5	4.5
IV	T0102		0.25	HVSR-S	F	1	BB	0.5	slope ≤ 15°	0.5		1		B	0.5	0.75	6	4.5
IV	T1212		0.25	HVSR-S	P	0	BB	0.5	slope ≤ 15°	0.5		1		A	1.5	0.75	5	4.5
IT	MCS	FF	0.5	HVNSR	MP	0	BB	0.5	slope ≤ 15°	0.5	568	0	5000	A	2	0.75	6	4.25
IT	MSCT	FF	0.5	HVSR-S	BB	0.5	BB	0.5	slope ≤ 15°	0.5		1		B	0.5	0.75	7	4.25
IV	T1256		0.25	HVSR-S	P	0	BB	0.5	slope ≤ 15°	0.5		1		A	1.5	0.5	5	4.25
IT	ACC	NO-FF	0	HVSR-S	P	0	BB	0.5	slope ≤ 15°	0.5		1		A	1.5	0.75	5	4.25

C. FELICETTA/ G. LANZANO/ F. PACOR- Methodology to identify reference rock sites- SIGMA2-2019-D3-027/1

	Research and Development Program on Seismic Ground Motion	Ref : SIGMA2-2019-D3-027/1
		Version : 1

IV	CAFE	FF	0.5	HVNSR	P	0	F	1	slope ≤ 15°	0.5	1	100000	B	0.5	0.5	6	4	
IV	ATPC	FF	0.5	HVSR-S	P	0	BB	0.5	relief	0	1	100000	A	1.5	0.5	5	4	
IT	CSS	FF	0.5	HVSR-S	P	0	BB	0.5	slope ≤ 15°	0.5	648	0	25000	A	1.5	0.75	6	3.75
IV	RM20		0.25	HVSR-S	P	0	F	1	slope ≤ 15°	0.5		1		B	0.5	0.5	5	3.75
IV	RM13		0.25	HVSR-C	P	0	P	0	slope ≤ 15°	0.5		1		A	1.5	0.5	4	3.75
IV	ATMC		0.25	HVSR-S	P	0		0.5	relief	0		1	100000	A	1.5	0.5	3	3.75
IV	RM21		0.25	HVSR-S	P	0	BB	0.5	slope ≤ 15°	0.5		1		B	0.5	0.75	5	3.5
IV	T1214		0.25	HVSR-S	P	0	BB	0.5	slope ≤ 15°	0.5		1		B	0.5	0.75	5	3.5
IT	CPS	FF	0.5	HVNSR	P	0	BB	0.5	slope ≤ 15°	0.5	732	0	5000	B	1	0.5	6	3
3A	MZ13		0.25	HVNSR	P	0		0.5	slope ≤ 15°	0.5	638	0	5000	B	1	0.75	4	3
XO	CP04		0.25	HVSR-S	MP	0		0.5	slope ≤ 15°	0.5		1		C	0	0.75	3	3
XO	CP05		0.25	HVSR-S	P	0	BB	0.5	slope ≤ 15°	0.5		1		C	0	0.75	4	3
IV	T1218		0.25	HVSR-S	P	0	P	0	slope ≤ 15°	0.5		1		B	0.5	0.75	4	3
IT	PRE	NO-FF	0	HVSR-S	P	0	BB	0.5		0.25		1		B	0.5	0.75	4	3
IT	SGPA	FF	0.5	HVSR-S	P	0	BB	0.5	slope ≤ 15°	0.5	378	0		B	0.5	0.75	6	2.75
3A	MZ08		0.25	HVNSR	P	0	BB	0.5	slope ≤ 15°	0.5	670	0	5000	B	1	0.5	5	2.75
IV	RM18		0.25	HVSR-S	P	0	P	0	slope ≤ 15°	0.5		1		B	0.5	0.5	4	2.75
IT	AQA	FF	0.5	HVNSR	P	0	BB	0.5	slope ≤ 15°	0.5	549	0	100000	B	0.5	0.5	6	2.5

C. FELICETTA/ G. LANZANO/ F. PACOR- Methodology to identify reference rock sites- SIGMA2-2019-D3-027/1

	Research and Development Program on Seismic Ground Motion	Ref : SIGMA2-2019-D3-027/1
		Version : 1

APPENDIX II

Calibration results of the three models for the geometric mean of horizontal components of PGA and 69 ordinates of the acceleration spectra SA (5% damping), in the period range $T=0.04-2s$.

REF MODEL

IM	a	b1	b2	c1	c2	c3	soth	Mh	h [km]	tau	phi_S2S	phi_0	sigma
0.000	2.536	0.580	0.220	0.162	-1.130	-8.077E-03	0.305	3.772	2.786	0.156	0.269	0.214	0.378
0.040	2.622	0.471	0.155	0.204	-1.124	-9.128E-03	0.336	3.912	2.915	0.180	0.276	0.214	0.393
0.042	2.628	0.467	0.156	0.204	-1.118	-9.167E-03	0.335	3.951	2.936	0.181	0.287	0.213	0.401
0.045	2.634	0.464	0.143	0.207	-1.114	-9.413E-03	0.330	3.921	2.932	0.181	0.289	0.213	0.402
0.047	2.634	0.458	0.134	0.210	-1.107	-9.464E-03	0.333	3.943	2.956	0.181	0.301	0.213	0.411
0.050	2.641	0.459	0.136	0.209	-1.101	-9.592E-03	0.335	3.936	2.963	0.182	0.304	0.214	0.414
0.053	2.642	0.459	0.136	0.207	-1.126	-9.810E-03	0.333	3.737	2.853	0.184	0.302	0.215	0.414
0.056	2.648	0.466	0.137	0.204	-1.122	-9.898E-03	0.338	3.696	2.786	0.184	0.304	0.215	0.416
0.060	2.639	0.472	0.144	0.199	-1.115	-1.001E-02	0.344	3.638	2.681	0.184	0.309	0.217	0.420
0.063	2.647	0.485	0.152	0.191	-1.106	-1.013E-02	0.349	3.592	2.608	0.184	0.309	0.218	0.420
0.067	2.651	0.494	0.161	0.186	-1.093	-1.031E-02	0.351	3.557	2.576	0.183	0.309	0.218	0.420
0.071	2.660	0.509	0.167	0.177	-1.083	-1.037E-02	0.353	3.520	2.589	0.182	0.312	0.219	0.422
0.075	2.661	0.521	0.176	0.171	-1.072	-1.043E-02	0.347	3.470	2.535	0.181	0.318	0.220	0.427
0.080	2.652	0.533	0.177	0.166	-1.058	-1.049E-02	0.347	3.404	2.436	0.179	0.318	0.221	0.427
0.084	2.639	0.546	0.187	0.160	-1.039	-1.064E-02	0.346	3.316	2.281	0.178	0.317	0.222	0.426

C. FELICETTA/ G. LANZANO/ F. PACOR- Methodology to identify reference rock sites- SIGMA2-2019-D3-027/1

	Research and Development Program on Seismic Ground Motion	Ref : SIGMA2-2019-D3-027/1
		Version : 1

0.089	2.641	0.558	0.198	0.153	-1.029	-1.062E-02	0.347	3.266	2.228	0.176	0.316	0.223	0.425
0.095	2.649	0.572	0.207	0.147	-1.023	-1.053E-02	0.349	3.231	2.197	0.175	0.314	0.224	0.424
0.100	2.656	0.584	0.215	0.141	-1.016	-1.040E-02	0.349	3.214	2.170	0.173	0.310	0.225	0.421
0.106	2.665	0.597	0.226	0.135	-1.009	-1.034E-02	0.347	3.180	2.104	0.172	0.305	0.226	0.417
0.112	2.681	0.614	0.238	0.128	-1.002	-1.023E-02	0.343	3.153	2.081	0.169	0.302	0.227	0.414
0.119	2.684	0.627	0.243	0.122	-0.994	-1.011E-02	0.341	3.122	2.033	0.167	0.300	0.227	0.411
0.126	2.691	0.642	0.251	0.117	-0.989	-9.942E-03	0.340	3.099	2.005	0.165	0.297	0.228	0.409
0.134	2.702	0.653	0.259	0.113	-0.990	-9.731E-03	0.336	3.088	2.002	0.163	0.294	0.228	0.406
0.142	2.717	0.663	0.267	0.111	-0.995	-9.507E-03	0.329	3.093	2.018	0.161	0.290	0.228	0.403
0.150	2.744	0.679	0.276	0.106	-1.002	-9.258E-03	0.323	3.096	2.042	0.159	0.286	0.228	0.399
0.159	2.772	0.694	0.290	0.101	-1.013	-8.928E-03	0.317	3.129	2.149	0.156	0.281	0.229	0.395
0.168	2.796	0.709	0.305	0.094	-1.020	-8.607E-03	0.310	3.170	2.264	0.154	0.277	0.228	0.391
0.178	2.813	0.721	0.317	0.090	-1.028	-8.285E-03	0.305	3.213	2.388	0.151	0.273	0.228	0.387
0.189	2.833	0.731	0.331	0.087	-1.041	-7.961E-03	0.299	3.242	2.536	0.149	0.268	0.228	0.382
0.200	2.851	0.737	0.336	0.087	-1.060	-7.595E-03	0.292	3.294	2.672	0.147	0.264	0.228	0.378
0.212	2.879	0.746	0.347	0.086	-1.081	-7.226E-03	0.284	3.355	2.842	0.145	0.261	0.227	0.375
0.224	2.910	0.758	0.362	0.084	-1.103	-6.825E-03	0.279	3.441	3.056	0.143	0.257	0.226	0.371
0.238	2.943	0.768	0.376	0.082	-1.131	-6.327E-03	0.273	3.547	3.340	0.140	0.252	0.225	0.366
0.252	2.987	0.782	0.391	0.078	-1.165	-5.803E-03	0.267	3.637	3.606	0.137	0.248	0.225	0.362
0.267	3.030	0.795	0.404	0.074	-1.199	-5.322E-03	0.257	3.718	3.857	0.135	0.245	0.223	0.358
0.282	3.068	0.804	0.412	0.074	-1.234	-4.839E-03	0.249	3.812	4.090	0.134	0.243	0.222	0.355
0.299	3.095	0.809	0.420	0.075	-1.267	-4.330E-03	0.242	3.908	4.321	0.132	0.242	0.220	0.352
0.317	3.125	0.817	0.432	0.075	-1.300	-3.800E-03	0.233	4.008	4.578	0.131	0.242	0.218	0.351

C. FELICETTA/ G. LANZANO/ F. PACOR- Methodology to identify reference rock sites- SIGMA2-2019-D3-027/1

	Research and Development Program on Seismic Ground Motion	Ref : SIGMA2-2019-D3-027/1
		Version : 1

0.336	3.143	0.821	0.440	0.077	-1.328	-3.343E-03	0.226	4.097	4.782	0.130	0.242	0.216	0.349
0.356	3.157	0.827	0.453	0.078	-1.355	-2.927E-03	0.219	4.164	4.920	0.129	0.242	0.215	0.348
0.377	3.166	0.829	0.462	0.081	-1.384	-2.448E-03	0.213	4.223	5.033	0.128	0.242	0.212	0.347
0.398	3.202	0.832	0.465	0.085	-1.430	-1.817E-03	0.205	4.330	5.298	0.128	0.243	0.210	0.346
0.422	3.252	0.836	0.466	0.087	-1.478	-1.188E-03	0.197	4.503	5.669	0.127	0.245	0.208	0.345
0.448	3.287	0.842	0.473	0.088	-1.517	-6.827E-04	0.189	4.607	5.962	0.127	0.245	0.206	0.345
0.474	3.305	0.846	0.478	0.091	-1.551	-2.235E-04	0.181	4.672	6.195	0.128	0.245	0.204	0.344
0.503	3.296	0.847	0.486	0.093	-1.566	0	0.175	4.702	6.364	0.128	0.244	0.202	0.342
0.532	3.265	0.846	0.489	0.098	-1.561	0	0.170	4.746	6.565	0.128	0.242	0.200	0.339
0.565	3.242	0.851	0.494	0.100	-1.558	0	0.163	4.793	6.774	0.129	0.240	0.198	0.337
0.599	3.224	0.854	0.501	0.103	-1.554	0	0.156	4.859	7.047	0.129	0.238	0.197	0.335
0.633	3.220	0.853	0.509	0.108	-1.555	0	0.149	4.968	7.556	0.130	0.236	0.195	0.333
0.671	3.198	0.855	0.519	0.111	-1.551	0	0.142	5.033	7.840	0.130	0.235	0.194	0.332
0.709	3.167	0.857	0.524	0.114	-1.544	0	0.135	5.074	8.021	0.131	0.235	0.193	0.331
0.752	3.131	0.861	0.527	0.117	-1.534	0	0.128	5.123	8.170	0.132	0.234	0.193	0.331
0.794	3.092	0.859	0.522	0.123	-1.519	0	0.124	5.194	8.432	0.133	0.233	0.192	0.330
0.840	3.046	0.856	0.516	0.130	-1.504	0	0.121	5.246	8.625	0.134	0.232	0.191	0.329
0.893	2.997	0.851	0.511	0.137	-1.490	0	0.122	5.275	8.774	0.136	0.230	0.190	0.328
0.943	2.933	0.840	0.506	0.148	-1.470	0	0.122	5.287	8.872	0.137	0.227	0.190	0.327
1.000	2.864	0.826	0.506	0.160	-1.453	0	0.120	5.271	8.859	0.139	0.225	0.189	0.325
1.064	2.800	0.814	0.508	0.169	-1.440	0	0.117	5.253	8.839	0.140	0.223	0.189	0.324
1.124	2.745	0.808	0.507	0.176	-1.438	0	0.113	5.210	8.824	0.140	0.222	0.190	0.324
1.190	2.692	0.801	0.506	0.182	-1.429	0	0.111	5.222	8.833	0.141	0.221	0.190	0.323

C. FELICETTA/ G. LANZANO/ F. PACOR- Methodology to identify reference rock sites- SIGMA2-2019-D3-027/1

	Research and Development Program on Seismic Ground Motion	Ref : SIGMA2-2019-D3-027/1
		Version : 1

1.266	2.631	0.790	0.506	0.190	-1.421	0	0.110	5.215	8.842	0.141	0.219	0.190	0.322
1.333	2.579	0.773	0.502	0.201	-1.409	0	0.111	5.254	9.038	0.142	0.217	0.190	0.321
1.408	2.582	0.747	0.487	0.217	-1.304	0	0.111	5.844	10.000	0.142	0.214	0.190	0.320
1.493	2.469	0.743	0.485	0.222	-1.394	0	0.113	5.256	9.269	0.142	0.212	0.190	0.318
1.587	2.456	0.716	0.464	0.240	-1.215	0	0.117	6.061	10.000	0.141	0.210	0.192	0.317
1.695	2.332	0.711	0.466	0.244	-1.358	0	0.122	5.292	9.118	0.140	0.209	0.192	0.316
1.786	2.296	0.691	0.459	0.255	-1.366	0	0.125	5.280	9.410	0.139	0.207	0.193	0.315
1.887	2.224	0.681	0.458	0.262	-1.356	0	0.127	5.269	9.143	0.138	0.205	0.194	0.314
2.000	2.167	0.669	0.451	0.270	-1.361	0	0.131	5.231	9.028	0.136	0.203	0.195	0.313

CLUST MODEL

IM	a	b1	b2	c1	c2	c3	s#2	s#3	s#4	s#5	s#6	s#7	s#8	s#9	Mh	h [km]	tau	phi_S2S	phi_0	sigma
0.000	2.468	0.564	0.211	0.170	-1.172	-7.382E-03	0.736	0.630	0.713	0.465	0.304	0.506	0.954	0.406	3.772	2.786	0.154	0.122	0.209	0.287
0.040	2.556	0.457	0.150	0.212	-1.164	-8.502E-03	0.678	0.626	0.728	0.407	0.328	0.554	1.003	0.354	3.912	2.915	0.178	0.152	0.210	0.315
0.042	2.562	0.454	0.150	0.211	-1.158	-8.551E-03	0.683	0.636	0.747	0.414	0.333	0.572	1.019	0.361	3.951	2.936	0.179	0.154	0.210	0.316
0.045	2.569	0.451	0.136	0.214	-1.156	-8.755E-03	0.681	0.629	0.750	0.410	0.327	0.578	1.019	0.358	3.921	2.932	0.179	0.157	0.210	0.317
0.047	2.570	0.445	0.127	0.217	-1.150	-8.764E-03	0.683	0.638	0.767	0.417	0.332	0.593	1.036	0.368	3.943	2.956	0.179	0.163	0.209	0.320
0.050	2.576	0.444	0.131	0.216	-1.145	-8.881E-03	0.690	0.642	0.776	0.422	0.332	0.600	1.029	0.370	3.936	2.963	0.180	0.165	0.210	0.322
0.053	2.570	0.443	0.132	0.216	-1.170	-9.101E-03	0.693	0.644	0.786	0.426	0.333	0.606	1.033	0.373	3.737	2.853	0.182	0.165	0.210	0.323
0.056	2.581	0.450	0.132	0.212	-1.166	-9.211E-03	0.701	0.644	0.795	0.430	0.332	0.610	1.047	0.377	3.696	2.786	0.182	0.166	0.211	0.325
0.060	2.578	0.458	0.140	0.207	-1.158	-9.312E-03	0.701	0.643	0.803	0.434	0.331	0.616	1.065	0.383	3.638	2.681	0.182	0.170	0.212	0.327
0.063	2.586	0.469	0.146	0.200	-1.152	-9.417E-03	0.704	0.644	0.807	0.438	0.332	0.620	1.087	0.388	3.592	2.608	0.183	0.170	0.213	0.328

C. FELICETTA/ G. LANZANO/ F. PACOR- Methodology to identify reference rock sites- SIGMA2-2019-D3-027/1

	Research and Development Program on Seismic Ground Motion	Ref : SIGMA2-2019-D3-027/1
		Version : 1

0.067	2.592	0.480	0.154	0.194	-1.139	-9.567E-03	0.711	0.637	0.806	0.442	0.335	0.622	1.097	0.393	3.557	2.576	0.182	0.169	0.213	0.327
0.071	2.599	0.492	0.164	0.186	-1.130	-9.607E-03	0.718	0.637	0.809	0.447	0.340	0.625	1.112	0.402	3.520	2.589	0.181	0.169	0.213	0.326
0.075	2.603	0.507	0.169	0.178	-1.121	-9.658E-03	0.728	0.637	0.813	0.451	0.343	0.627	1.114	0.409	3.470	2.535	0.180	0.168	0.214	0.326
0.080	2.597	0.519	0.171	0.173	-1.110	-9.696E-03	0.730	0.636	0.816	0.455	0.346	0.628	1.121	0.416	3.404	2.436	0.178	0.166	0.215	0.325
0.084	2.583	0.531	0.180	0.168	-1.093	-9.842E-03	0.732	0.636	0.816	0.457	0.347	0.625	1.128	0.424	3.316	2.281	0.177	0.164	0.216	0.324
0.089	2.586	0.542	0.190	0.162	-1.086	-9.813E-03	0.730	0.639	0.816	0.462	0.347	0.618	1.123	0.432	3.266	2.228	0.176	0.161	0.217	0.322
0.095	2.594	0.553	0.198	0.157	-1.083	-9.701E-03	0.729	0.643	0.818	0.466	0.348	0.610	1.110	0.442	3.231	2.197	0.174	0.158	0.218	0.321
0.100	2.601	0.564	0.206	0.152	-1.078	-9.579E-03	0.734	0.642	0.812	0.469	0.349	0.599	1.088	0.448	3.214	2.170	0.173	0.154	0.219	0.319
0.106	2.608	0.576	0.216	0.146	-1.069	-9.534E-03	0.735	0.641	0.801	0.470	0.346	0.585	1.065	0.450	3.180	2.104	0.171	0.150	0.220	0.317
0.112	2.621	0.593	0.227	0.139	-1.063	-9.423E-03	0.737	0.647	0.792	0.472	0.344	0.574	1.046	0.453	3.153	2.081	0.169	0.147	0.221	0.315
0.119	2.623	0.606	0.231	0.134	-1.054	-9.325E-03	0.739	0.653	0.785	0.478	0.342	0.563	1.036	0.455	3.122	2.033	0.167	0.145	0.222	0.313
0.126	2.629	0.622	0.240	0.127	-1.048	-9.173E-03	0.738	0.661	0.780	0.488	0.341	0.553	1.026	0.459	3.099	2.005	0.165	0.143	0.222	0.312
0.134	2.636	0.632	0.248	0.124	-1.048	-8.973E-03	0.735	0.664	0.773	0.497	0.339	0.538	1.019	0.460	3.088	2.002	0.163	0.141	0.222	0.310
0.142	2.645	0.645	0.256	0.121	-1.047	-8.773E-03	0.742	0.668	0.763	0.507	0.337	0.521	1.002	0.464	3.093	2.018	0.162	0.138	0.223	0.308
0.150	2.666	0.662	0.266	0.115	-1.051	-8.536E-03	0.760	0.670	0.750	0.512	0.332	0.502	0.969	0.466	3.096	2.042	0.159	0.137	0.223	0.307
0.159	2.687	0.676	0.281	0.110	-1.058	-8.220E-03	0.787	0.667	0.735	0.512	0.329	0.485	0.927	0.467	3.129	2.149	0.157	0.135	0.224	0.305
0.168	2.707	0.690	0.296	0.104	-1.063	-7.901E-03	0.808	0.663	0.715	0.511	0.325	0.467	0.893	0.467	3.170	2.264	0.154	0.133	0.223	0.302
0.178	2.722	0.702	0.308	0.100	-1.071	-7.590E-03	0.821	0.663	0.694	0.512	0.323	0.449	0.858	0.467	3.213	2.388	0.152	0.130	0.223	0.299
0.189	2.741	0.712	0.321	0.097	-1.082	-7.290E-03	0.822	0.662	0.675	0.511	0.317	0.429	0.819	0.466	3.242	2.536	0.150	0.127	0.223	0.297
0.200	2.761	0.719	0.326	0.097	-1.099	-6.947E-03	0.813	0.660	0.655	0.513	0.309	0.409	0.771	0.464	3.294	2.672	0.147	0.126	0.223	0.295
0.212	2.790	0.731	0.337	0.095	-1.117	-6.589E-03	0.801	0.659	0.635	0.513	0.301	0.391	0.731	0.464	3.355	2.842	0.145	0.124	0.222	0.293
0.224	2.823	0.743	0.350	0.092	-1.138	-6.187E-03	0.791	0.660	0.612	0.513	0.293	0.368	0.692	0.459	3.441	3.056	0.143	0.124	0.221	0.291
0.238	2.858	0.752	0.364	0.091	-1.164	-5.696E-03	0.786	0.658	0.588	0.515	0.284	0.344	0.655	0.455	3.547	3.340	0.141	0.123	0.220	0.289

C. FELICETTA/ G. LANZANO/ F. PACOR- Methodology to identify reference rock sites- SIGMA2-2019-D3-027/1

	Research and Development Program on Seismic Ground Motion	Ref : SIGMA2-2019-D3-027/1
		Version : 1

0.252	2.902	0.767	0.379	0.086	-1.195	-5.206E-03	0.785	0.654	0.567	0.522	0.277	0.322	0.621	0.452	3.637	3.606	0.138	0.121	0.219	0.286
0.267	2.942	0.781	0.392	0.082	-1.226	-4.751E-03	0.781	0.652	0.547	0.529	0.268	0.300	0.579	0.448	3.718	3.857	0.135	0.119	0.218	0.283
0.282	2.977	0.790	0.399	0.081	-1.258	-4.293E-03	0.773	0.656	0.528	0.536	0.262	0.278	0.557	0.445	3.812	4.090	0.134	0.117	0.216	0.280
0.299	3.002	0.797	0.407	0.082	-1.287	-3.807E-03	0.767	0.661	0.510	0.538	0.255	0.258	0.542	0.440	3.908	4.321	0.133	0.115	0.214	0.277
0.317	3.033	0.806	0.420	0.081	-1.318	-3.296E-03	0.764	0.667	0.489	0.542	0.244	0.236	0.525	0.432	4.008	4.578	0.132	0.114	0.212	0.275
0.336	3.056	0.812	0.427	0.082	-1.346	-2.847E-03	0.768	0.666	0.464	0.546	0.233	0.214	0.503	0.423	4.097	4.782	0.131	0.113	0.211	0.273
0.356	3.073	0.818	0.441	0.083	-1.371	-2.446E-03	0.774	0.659	0.440	0.550	0.219	0.192	0.488	0.416	4.164	4.920	0.130	0.111	0.209	0.270
0.377	3.089	0.822	0.449	0.085	-1.401	-1.985E-03	0.786	0.652	0.420	0.557	0.204	0.171	0.470	0.412	4.223	5.033	0.130	0.111	0.207	0.268
0.398	3.129	0.826	0.453	0.088	-1.446	-1.362E-03	0.801	0.641	0.401	0.563	0.189	0.150	0.442	0.405	4.330	5.298	0.130	0.111	0.204	0.266
0.422	3.180	0.832	0.454	0.090	-1.493	-7.317E-04	0.814	0.627	0.381	0.569	0.179	0.131	0.420	0.401	4.503	5.669	0.130	0.111	0.202	0.265
0.448	3.217	0.842	0.462	0.089	-1.532	-2.431E-04	0.816	0.612	0.362	0.572	0.171	0.115	0.401	0.398	4.607	5.962	0.130	0.112	0.200	0.264
0.474	3.218	0.847	0.469	0.090	-1.549	0	0.815	0.596	0.344	0.576	0.164	0.101	0.382	0.394	4.672	6.195	0.130	0.114	0.198	0.263
0.503	3.190	0.849	0.478	0.093	-1.545	0	0.806	0.582	0.328	0.581	0.158	0.087	0.359	0.388	4.702	6.364	0.130	0.113	0.197	0.262
0.532	3.159	0.849	0.483	0.097	-1.539	0	0.798	0.566	0.312	0.585	0.152	0.076	0.337	0.382	4.746	6.565	0.131	0.112	0.194	0.260
0.565	3.138	0.856	0.489	0.098	-1.536	0	0.789	0.551	0.298	0.588	0.148	0.065	0.325	0.376	4.793	6.774	0.132	0.111	0.193	0.258
0.599	3.124	0.862	0.496	0.099	-1.534	0	0.777	0.535	0.283	0.586	0.141	0.049	0.308	0.365	4.859	7.047	0.132	0.109	0.191	0.257
0.633	3.121	0.862	0.504	0.104	-1.535	0	0.768	0.519	0.269	0.587	0.134	0.036	0.283	0.353	4.968	7.556	0.132	0.108	0.189	0.255
0.671	3.100	0.866	0.513	0.106	-1.531	0	0.759	0.504	0.256	0.593	0.130	0.024	0.260	0.344	5.033	7.840	0.133	0.107	0.188	0.254
0.709	3.071	0.870	0.517	0.109	-1.525	0	0.746	0.492	0.241	0.599	0.124	0.015	0.243	0.335	5.074	8.021	0.134	0.108	0.187	0.254
0.752	3.037	0.876	0.520	0.110	-1.516	0	0.725	0.481	0.230	0.603	0.117	0.006	0.229	0.327	5.123	8.170	0.135	0.107	0.186	0.254
0.794	2.999	0.875	0.517	0.116	-1.501	0	0.702	0.469	0.219	0.604	0.111	-0.002	0.217	0.322	5.194	8.432	0.136	0.107	0.186	0.254
0.840	2.958	0.874	0.512	0.122	-1.487	0	0.680	0.458	0.209	0.608	0.105	-0.010	0.208	0.315	5.246	8.625	0.137	0.108	0.185	0.254
0.893	2.914	0.871	0.507	0.129	-1.474	0	0.663	0.449	0.200	0.607	0.099	-0.016	0.197	0.308	5.275	8.774	0.138	0.108	0.184	0.255

C. FELICETTA/ G. LANZANO/ F. PACOR- Methodology to identify reference rock sites- SIGMA2-2019-D3-027/1

	Research and Development Program on Seismic Ground Motion	Ref : SIGMA2-2019-D3-027/1
		Version : 1

0.943	2.854	0.860	0.503	0.139	-1.454	0	0.645	0.439	0.194	0.604	0.095	-0.018	0.188	0.305	5.287	8.872	0.140	0.108	0.184	0.255
1.000	2.788	0.846	0.504	0.151	-1.437	0	0.630	0.427	0.189	0.597	0.090	-0.021	0.179	0.299	5.271	8.859	0.142	0.108	0.183	0.256
1.064	2.724	0.834	0.505	0.161	-1.424	0	0.616	0.418	0.186	0.591	0.087	-0.023	0.170	0.293	5.253	8.839	0.143	0.109	0.183	0.257
1.124	2.670	0.829	0.505	0.167	-1.422	0	0.602	0.411	0.183	0.582	0.086	-0.024	0.167	0.289	5.210	8.824	0.143	0.109	0.183	0.257
1.190	2.619	0.824	0.504	0.172	-1.415	0	0.591	0.403	0.181	0.575	0.083	-0.025	0.167	0.285	5.222	8.833	0.144	0.109	0.183	0.258
1.266	2.562	0.814	0.504	0.179	-1.409	0	0.580	0.397	0.178	0.566	0.081	-0.023	0.167	0.281	5.215	8.842	0.144	0.110	0.184	0.258
1.333	2.513	0.798	0.499	0.189	-1.397	0	0.569	0.391	0.175	0.559	0.079	-0.022	0.167	0.277	5.254	9.038	0.145	0.110	0.184	0.259
1.408	2.517	0.772	0.484	0.206	-1.298	0	0.558	0.384	0.173	0.546	0.076	-0.023	0.167	0.271	5.844	10.000	0.145	0.110	0.185	0.259
1.493	2.409	0.767	0.480	0.211	-1.382	0	0.551	0.383	0.175	0.537	0.078	-0.019	0.173	0.269	5.256	9.269	0.145	0.110	0.184	0.259
1.587	2.396	0.740	0.461	0.229	-1.211	0	0.544	0.382	0.180	0.528	0.079	-0.015	0.178	0.267	6.061	10.000	0.144	0.109	0.186	0.259
1.695	2.273	0.734	0.462	0.234	-1.346	0	0.540	0.384	0.192	0.524	0.084	-0.008	0.196	0.268	5.292	9.118	0.143	0.107	0.186	0.258
1.786	2.237	0.714	0.456	0.246	-1.355	0	0.539	0.385	0.201	0.520	0.087	-0.002	0.211	0.269	5.280	9.410	0.142	0.106	0.187	0.258
1.887	2.165	0.703	0.455	0.253	-1.344	0	0.545	0.389	0.210	0.516	0.090	0.005	0.229	0.270	5.269	9.143	0.141	0.104	0.188	0.257
2.000	2.109	0.691	0.447	0.261	-1.350	0	0.555	0.391	0.219	0.510	0.092	0.012	0.244	0.270	5.231	9.028	0.139	0.102	0.189	0.256

EC8 MODEL

IM	a	b1	b2	c1	c2	c3	sB	sC	sD	sE	Mh	h [km]	tau	phi_S2S	phi_0	sigma
0.000	2.728	0.580	0.220	0.162	-1.130	-8.069E-03	0.080	0.220	0.243	0.306	3.772	2.786	0.156	0.277	0.214	0.383
0.040	2.828	0.471	0.155	0.203	-1.124	-9.132E-03	0.100	0.196	0.193	0.295	3.912	2.915	0.180	0.288	0.214	0.401
0.042	2.837	0.467	0.156	0.203	-1.118	-9.169E-03	0.095	0.201	0.193	0.309	3.951	2.936	0.181	0.298	0.213	0.409
0.045	2.843	0.464	0.143	0.207	-1.114	-9.414E-03	0.088	0.202	0.194	0.314	3.921	2.932	0.181	0.300	0.213	0.410
0.047	2.847	0.459	0.134	0.210	-1.107	-9.464E-03	0.086	0.206	0.198	0.321	3.943	2.956	0.181	0.311	0.213	0.419
0.050	2.858	0.459	0.136	0.209	-1.101	-9.591E-03	0.084	0.207	0.197	0.316	3.936	2.963	0.182	0.314	0.214	0.422

C. FELICETTA/ G. LANZANO/ F. PACOR- Methodology to identify reference rock sites- SIGMA2-2019-D3-027/1

	Research and Development Program on Seismic Ground Motion	Ref : SIGMA2-2019-D3-027/1
		Version : 1

0.053	2.858	0.459	0.135	0.207	-1.126	-9.808E-03	0.083	0.210	0.202	0.311	3.737	2.853	0.184	0.312	0.215	0.421
0.056	2.869	0.466	0.136	0.204	-1.122	-9.895E-03	0.082	0.216	0.217	0.310	3.696	2.786	0.184	0.314	0.215	0.423
0.060	2.866	0.472	0.144	0.199	-1.115	-1.001E-02	0.079	0.223	0.234	0.318	3.638	2.681	0.184	0.319	0.217	0.427
0.063	2.876	0.485	0.152	0.191	-1.107	-1.013E-02	0.081	0.232	0.244	0.327	3.592	2.608	0.184	0.319	0.218	0.428
0.067	2.881	0.494	0.161	0.186	-1.094	-1.030E-02	0.082	0.238	0.246	0.335	3.557	2.576	0.183	0.319	0.218	0.428
0.071	2.892	0.509	0.167	0.177	-1.083	-1.037E-02	0.082	0.237	0.247	0.344	3.520	2.589	0.182	0.321	0.219	0.429
0.075	2.894	0.521	0.175	0.171	-1.072	-1.042E-02	0.074	0.239	0.242	0.359	3.470	2.535	0.181	0.326	0.220	0.433
0.080	2.887	0.533	0.177	0.166	-1.058	-1.048E-02	0.071	0.239	0.243	0.366	3.404	2.436	0.179	0.326	0.221	0.433
0.084	2.874	0.546	0.187	0.160	-1.040	-1.064E-02	0.070	0.240	0.249	0.374	3.316	2.281	0.178	0.325	0.222	0.432
0.089	2.874	0.558	0.198	0.153	-1.030	-1.062E-02	0.073	0.239	0.261	0.377	3.266	2.228	0.176	0.324	0.223	0.431
0.095	2.880	0.572	0.207	0.147	-1.023	-1.052E-02	0.077	0.237	0.276	0.385	3.231	2.197	0.175	0.323	0.224	0.430
0.100	2.885	0.584	0.215	0.141	-1.017	-1.040E-02	0.080	0.231	0.282	0.393	3.214	2.170	0.173	0.319	0.225	0.427
0.106	2.891	0.597	0.226	0.135	-1.009	-1.033E-02	0.082	0.226	0.280	0.395	3.180	2.104	0.172	0.314	0.226	0.423
0.112	2.904	0.614	0.238	0.128	-1.003	-1.022E-02	0.082	0.224	0.278	0.391	3.153	2.081	0.169	0.311	0.227	0.420
0.119	2.905	0.627	0.242	0.122	-0.995	-1.010E-02	0.082	0.225	0.284	0.391	3.122	2.033	0.167	0.308	0.227	0.417
0.126	2.908	0.642	0.250	0.117	-0.989	-9.934E-03	0.086	0.227	0.297	0.397	3.099	2.005	0.165	0.305	0.228	0.414
0.134	2.914	0.653	0.259	0.113	-0.991	-9.722E-03	0.086	0.223	0.299	0.404	3.088	2.002	0.163	0.301	0.228	0.411
0.142	2.925	0.663	0.266	0.111	-0.995	-9.499E-03	0.086	0.217	0.295	0.404	3.093	2.018	0.161	0.298	0.228	0.408
0.150	2.946	0.679	0.276	0.106	-1.003	-9.249E-03	0.086	0.213	0.292	0.390	3.096	2.042	0.159	0.293	0.228	0.404
0.159	2.968	0.694	0.290	0.101	-1.014	-8.920E-03	0.088	0.212	0.289	0.366	3.129	2.149	0.156	0.288	0.229	0.400
0.168	2.985	0.709	0.305	0.094	-1.021	-8.599E-03	0.091	0.212	0.280	0.347	3.170	2.264	0.154	0.284	0.228	0.396
0.178	2.996	0.721	0.317	0.090	-1.029	-8.276E-03	0.093	0.211	0.276	0.330	3.213	2.388	0.152	0.280	0.228	0.392
0.189	3.011	0.731	0.331	0.087	-1.042	-7.953E-03	0.092	0.204	0.275	0.304	3.242	2.536	0.149	0.275	0.228	0.388

C. FELICETTA/ G. LANZANO/ F. PACOR- Methodology to identify reference rock sites- SIGMA2-2019-D3-027/1

	Research and Development Program on Seismic Ground Motion	Ref : SIGMA2-2019-D3-027/1
		Version : 1

0.200	3.025	0.737	0.336	0.087	-1.061	-7.587E-03	0.091	0.198	0.281	0.284	3.294	2.672	0.147	0.271	0.228	0.383
0.212	3.046	0.746	0.347	0.086	-1.082	-7.219E-03	0.092	0.194	0.276	0.262	3.355	2.842	0.145	0.267	0.227	0.380
0.224	3.070	0.759	0.362	0.084	-1.103	-6.818E-03	0.095	0.193	0.266	0.243	3.441	3.056	0.143	0.263	0.226	0.375
0.238	3.094	0.768	0.376	0.082	-1.131	-6.320E-03	0.101	0.191	0.260	0.230	3.547	3.340	0.140	0.259	0.225	0.371
0.252	3.128	0.782	0.391	0.078	-1.165	-5.797E-03	0.107	0.194	0.256	0.216	3.637	3.606	0.137	0.254	0.225	0.366
0.267	3.161	0.795	0.404	0.074	-1.199	-5.317E-03	0.109	0.196	0.255	0.200	3.718	3.857	0.135	0.250	0.223	0.362
0.282	3.191	0.804	0.412	0.074	-1.235	-4.834E-03	0.111	0.197	0.258	0.188	3.812	4.090	0.134	0.247	0.222	0.358
0.299	3.210	0.809	0.420	0.075	-1.267	-4.325E-03	0.113	0.199	0.252	0.175	3.908	4.321	0.132	0.246	0.220	0.355
0.317	3.231	0.817	0.432	0.075	-1.301	-3.796E-03	0.115	0.202	0.242	0.169	4.008	4.578	0.131	0.245	0.218	0.353
0.336	3.243	0.822	0.440	0.077	-1.329	-3.340E-03	0.115	0.202	0.229	0.159	4.097	4.782	0.130	0.245	0.216	0.351
0.356	3.251	0.827	0.453	0.078	-1.355	-2.924E-03	0.113	0.201	0.219	0.142	4.164	4.920	0.129	0.244	0.215	0.350
0.377	3.256	0.829	0.462	0.081	-1.385	-2.446E-03	0.113	0.202	0.224	0.130	4.223	5.033	0.128	0.244	0.212	0.348
0.398	3.285	0.832	0.465	0.084	-1.431	-1.815E-03	0.112	0.202	0.230	0.123	4.330	5.298	0.128	0.245	0.210	0.347
0.422	3.328	0.836	0.466	0.087	-1.478	-1.185E-03	0.111	0.203	0.234	0.116	4.503	5.669	0.127	0.245	0.208	0.346
0.448	3.356	0.842	0.473	0.088	-1.518	-6.804E-04	0.111	0.203	0.235	0.111	4.607	5.962	0.127	0.245	0.206	0.345
0.474	3.368	0.846	0.478	0.090	-1.552	-2.213E-04	0.110	0.205	0.237	0.106	4.672	6.195	0.128	0.245	0.204	0.343
0.503	3.353	0.847	0.486	0.093	-1.567	0	0.109	0.210	0.235	0.104	4.702	6.364	0.128	0.244	0.202	0.341
0.532	3.318	0.846	0.489	0.098	-1.561	0	0.109	0.214	0.228	0.097	4.746	6.565	0.128	0.241	0.200	0.338
0.565	3.291	0.851	0.494	0.100	-1.558	0	0.107	0.213	0.230	0.090	4.793	6.774	0.129	0.238	0.198	0.336
0.599	3.268	0.854	0.501	0.103	-1.555	0	0.105	0.213	0.229	0.084	4.859	7.047	0.129	0.236	0.197	0.333
0.633	3.258	0.853	0.509	0.108	-1.555	0	0.102	0.214	0.230	0.074	4.968	7.556	0.130	0.234	0.195	0.331
0.671	3.232	0.856	0.519	0.111	-1.551	0	0.100	0.218	0.238	0.067	5.033	7.840	0.130	0.232	0.194	0.329
0.709	3.196	0.857	0.524	0.114	-1.544	0	0.097	0.221	0.244	0.057	5.074	8.021	0.131	0.231	0.193	0.329

C. FELICETTA/ G. LANZANO/ F. PACOR- Methodology to identify reference rock sites- SIGMA2-2019-D3-027/1

	Research and Development Program on Seismic Ground Motion	Ref : SIGMA2-2019-D3-027/1
		Version : 1

0.752	3.156	0.861	0.526	0.117	-1.534	0	0.095	0.222	0.244	0.051	5.123	8.170	0.132	0.230	0.193	0.328
0.794	3.113	0.859	0.522	0.123	-1.519	0	0.094	0.223	0.240	0.047	5.194	8.432	0.133	0.229	0.192	0.327
0.840	3.066	0.856	0.516	0.130	-1.504	0	0.093	0.225	0.235	0.048	5.246	8.625	0.134	0.227	0.191	0.326
0.893	3.017	0.852	0.511	0.137	-1.490	0	0.093	0.225	0.227	0.049	5.275	8.774	0.136	0.225	0.190	0.325
0.943	2.954	0.840	0.506	0.148	-1.471	0	0.093	0.227	0.224	0.054	5.287	8.872	0.137	0.223	0.190	0.323
1.000	2.884	0.826	0.506	0.160	-1.454	0	0.091	0.229	0.221	0.058	5.271	8.859	0.139	0.221	0.189	0.322
1.064	2.818	0.815	0.507	0.169	-1.440	0	0.090	0.229	0.213	0.057	5.253	8.839	0.140	0.219	0.189	0.321
1.124	2.761	0.809	0.507	0.176	-1.438	0	0.090	0.227	0.206	0.056	5.210	8.824	0.140	0.217	0.190	0.321
1.190	2.705	0.802	0.506	0.182	-1.429	0	0.090	0.227	0.204	0.058	5.222	8.833	0.141	0.216	0.190	0.320
1.266	2.644	0.790	0.506	0.190	-1.421	0	0.090	0.226	0.203	0.061	5.215	8.842	0.141	0.214	0.190	0.319
1.333	2.593	0.774	0.502	0.201	-1.409	0	0.089	0.223	0.201	0.064	5.254	9.038	0.142	0.212	0.190	0.318
1.408	2.597	0.747	0.487	0.217	-1.304	0	0.088	0.219	0.195	0.064	5.844	10.000	0.142	0.210	0.190	0.317
1.493	2.485	0.743	0.485	0.222	-1.394	0	0.091	0.217	0.197	0.070	5.256	9.269	0.142	0.208	0.190	0.316
1.587	2.474	0.716	0.464	0.239	-1.215	0	0.092	0.214	0.191	0.068	6.061	10.000	0.141	0.206	0.192	0.315
1.695	2.352	0.711	0.466	0.243	-1.358	0	0.095	0.217	0.192	0.075	5.292	9.118	0.140	0.205	0.192	0.314
1.786	2.319	0.692	0.459	0.255	-1.367	0	0.095	0.216	0.190	0.077	5.280	9.410	0.139	0.203	0.193	0.313
1.887	2.249	0.681	0.458	0.262	-1.356	0	0.095	0.214	0.189	0.078	5.269	9.143	0.138	0.202	0.194	0.312
2.000	2.197	0.669	0.451	0.270	-1.362	0	0.094	0.212	0.183	0.078	5.231	9.028	0.136	0.200	0.195	0.311

C. FELICETTA/ G. LANZANO/ F. PACOR- Methodology to identify reference rock sites- SIGMA2-2019-D3-027/1